# ASSESSMENT OF GROUNDWATER-SURFACE WATER MIXING ZONE TRANSIENTS: BIRMINGHAM-RIVER TAME STUDY

**by**

Derek John Conran

Submitted in part fulfilment

of the requirements for an

**MSc in Hydrogeology**

September 2006

School of Earth Sciences

University of Birmingham

# Table of Contents

# List of Figures

# List of Tables

# Appendices

Appendices 1, 2, 3, 4, 6 and 7 have been included with the hard copy bound with this thesis. All other appendices may be found on CD ROM, a copy of which has been included with this thesis.

1. Temporal and spatial variation in Chloride Concentration.
2. Temporal and spatial variation in Nitrate Concentration.
3. Numerical Modeling.
4. Representative values of the Hazen Coefficient ( Fetter, 1994).
5. Calibration of Transducer for Slug Test Conversions.
6. Hydrographs from Water Orton and Bescot Flow Stations.
7. Rainfall Data from Sollihull Meteorological Station.
8. Temporal Head Variation in MDP's from refined study area.
9. Calculation of effective hydraulic conductivity $K_{effective}$.
10. Baseflow data from profile 8 and 11.
11. River Bed Elevations and Survey.
12. All falling head selected data and graphs.
13. All temporal and spatial chemical sampling data carried out during case study.

# Chapter 1 Introduction

## 1.1 Project Outline

The mixing zone between surface water and groundwater bodies has been identified as having a great potential for the attenuation of the contaminants crossing through the zone. The importance of the mixing zone or 'hyporheic zone' has recently been reiterated by the passing of EU legislation, which requires that nearly all inland and coastal waters must achieve good status by 2015. This legislation has been introduced through The Water Framework Directive and as a result of its imposition, it is now of great economic interest to quantify the natural attenuation potential of the hyporheic zone beneath surface water bodies.

The definition of the mixing zone varies, usually depending upon the discipline from which the area is being approached. Most commonly this variation in defining the mixing zone comes from ecologic, hydraulic or hydrogeologic studies. Nevertheless, it is fundamentally agreed by all disciplines that the concentration and realignment of groundwater flow lines within highly permeable river bed sediments results in mixing of the aquifer water with river water which normally have different geochemical signatures (Environment Agency., 2005).

One of the major factors controlling the natural attenuation potential of the hyporheic zone is the depth to which it extends below the surface water body. It is thus of fundamental importance to evaluate the temporal and spatial variability of the mixing zone extent and understand the hydraulic properties controlling it before the long-term natural attenuation potential of this distinctive zone can be estimated. Because of this fundamental requirement, this study focuses on the evaluation of the extent of the hyporheic zone in a river bed environment, an evaluation of

its contaminant attenuation potential and an assessment of the hydraulic properties which control the extent of the zone. Because both surface-water and groundwater bodies have different chemical signatures in the study area, it can be demonstrated that by analysing multiple sample horizons concentrations of chloride and dissolved organic matter (DOM) beneath the river bed at different locations in the river, an estimate of hyporheic zone thickness could be made. This can then be compared to river and river bed hydraulic data to explain the temporal and spatial variability of hyporheic zone thickness seen. Organic and inorganic degradation rates can be assessed by the combined use of geochemical profiles of nitrate, chloride, fluorescent excitation, emission and intensity wavelengths of DOM dissolved oxygen (DO) and sulphate.

The area of study is the River Tame in the North Birmingham region, UK. Previous work carried out in this region includes research which focuses on evaluating contaminant mass flux through the river bed and seepage zones and quantifying the temporal and spatial variation of biodegradation rates in the hyporheic zone and contaminant mass flux entering the river (Ellis, 2003) (Wilcox, 2005) (McLachlan, 2004).

## 1.2 Aims and Objectives

The aim of this research is to examine the relationship between physical hydraulic properties, base flow rates and observed chemical gradients to delineate the mixing zone, to explain the reasons for its temporal and spatial variability in thickness and to qualitatively examine its temporal and spatial contaminant degradation potential. The objectives of the study are as follows:

1. Delineate the extent of the mixing zone under distinct defining criteria at 2 cross channel profiles with different hydraulic properties.

2. Examine the contrasting inorganic concentration gradients between 2 cross channel profiles and establish whether inorganic determinand attenuation is occurring in hyporheic waters
3. Assess the temporally varying hyporheic zone extent and the temporal contaminant degradation potential.
4. Identify whether inorganic attenuation can be linked to inorganic reduction.
5. Examine the use of fluorescence as a hyporheic delineation tool.
6. Examine the relationship between hyporheic zone thickness, base-flow and hyporheic response to increased base-flow rates.

## 1.3 Case-study layout

To meet the aims and objectives of the study a 150m stretch of the river has been selected for a more in depth survey. River bed surveying has been carried out on a longer stretch of river in which sediment type and hydrologic conditions were assessed. The recognition of suitably contrasting flow and river bed conditions at a particular area lead to the refinement of the study area.

For an evaluation of hydraulic properties in the river bed, nests of mini drive point piezometers (MDP's) have been installed at 3 cross channel profiles, and single horizon MDP's have been installed at 5 other cross channel profiles. Slug tests were carried out on these piezometers to estimate hydraulic conductivity variation of the river bed sediments with depth. Head gradients were frequently measured to comprehend their temporal and spatial

variability. From this data, an estimate of temporally varying base flow in the study reach has been calculated.

Multi-Level chemical sampling piezometers (ML piezometers) have been installed at 3 cross-section profiles to identify the temporal and spatial variability of chemical gradients in the stream bed and data obtained has been correlated with river flow data and hydraulic data to explain the temporal and spatial variability of chemical gradients. In all, 4 rounds of chemical sampling have been carried out. Temporally varying organic fractions are examined along with inorganic concentration gradients with an aim of assessing the temporally varying contaminant attenuation potential.

# Chapter 2 Background Research

## 2.1Groundwater Surface water Interactions

The interaction between groundwater and surface water bodies can be viewed as potentially occurring on a variety of scales. Three scenarios of mixing are commonly seen. If the pressure head in the aquifer beneath the surface water body is higher than the stage of the surface water body, then the surface water body will receive inflow from the aquifer. Thus, the river is gaining. This scenario is commonly seen in low land rivers and streams. If the stage in the surface water body is higher that the pressure head in the underlying aquifer the river will loose water to the aquifer, this is referred to as a 'loosing river'. A third scenario may occur if the stage in the river and the head in the aquifer are equal, this will generate its own hyporheic zone thickness depending on other hydraulic conditions. In cases in which there is no head difference, irregularities in river bed form and the pressure distribution caused by river flow will give rise to infiltration of river water through sections of the upper river bed sediments (intergravel flow) and hence a mixing zone, (Ellis, 2003). This is often the case also if the surface water body is receiving water from the underlying aquifer, hence the occurrence of a mixing zone between the surface and groundwater bodies is usually going to occur, regardless of which mechanism the surface and groundwater bodies are interacting.

In the case of a river channel, it has been found by (Woessner, 2000) that groundwater flow to the river channel is dependent on:

1. The distribution and magnitude of hydraulic conductivities within the river channel, the associated flood plain sediments and the underlying bedrock.
2. The relation of river stage to the adjacent groundwater gradients.
3. The geometry and position of the river channel within the fluvial plain.

Hence, even on a local scale, or cross channel scale, the magnitude of groundwater flow to the river channel can be highly variable due to the natural variation of the factors it depends on.

## 2.2 Hyporheic Zone

The hyporheic zone is the area beneath and adjacent to streams and rivers where surface and groundwater mix. A number of more specific definitions exist, and as the majority of the current literature is presented by ecologists, most definitions are drawn from ecological criteria. The term hyporheic zone itself is an ecological term referring to the zone around a stream in which fauna characteristic of the hyporheic zone (the hyporheos) are distributed and live. To the hydrogeological community the hyporheic zone is part of the groundwater system, which is subsurface water that occurs beneath the water table in soils or geological formations that are fully saturated (Ellis, 2003). (Figure 2.2.1) presents a conceptualization of the hyporheic zone of a river system.

Figure 2.2.1, Conceptual Model of River Channel System and hyporheic zone.

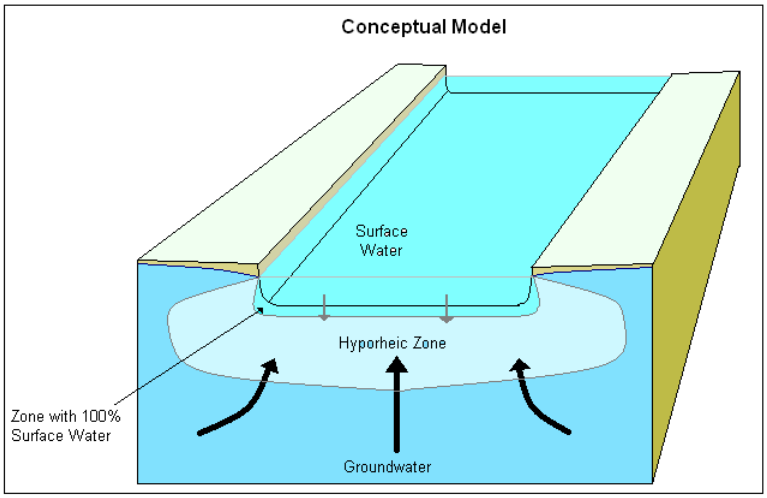


The chemical composition of the hyporheic zone varies with depth and is an environment in which aerobic and anaerobic microbial processes occur. Because of this and the higher concentration of nutrients present in the zone in comparison to the underlying purely aquifer water, it has been recognized that a greater potential exists for the attenuation of contaminants passing from the aquifer to the river channel.

## 2.3 Delineation of the Hyporheic Zone

Methods for determining the presence and extent of the hyporheic zone have been demonstrated in past studies and vary greatly in the quantity and quality of data recovered. Also, it must be recognized that the different methods are often closely linked to the academic discipline for which the zone is being delineated. These usually comprise hydrologic, hydrogeologic or ecologic identities, in which the definition and extent of the hyporheic zone may vary dramatically. For the purpose of this study an adaptation of a stream tracer delineation technique has been used in which artificially high levels of chloride are naturally present in the river water due to sewage treatment works discharges (STW's).

### 2.3.1 Delineation based on Tracer Tests

Tracer experiments are valuable tools for analysing the transport characteristics of streams and their interaction with shallow groundwater (Harvey et al., 1996). Tracers can either be artificially injected into the stream or if sufficient background contaminant concentrations exist within the stream, it has been shown that these can be used as an alternative. Most common experiments involve the injection of a conservative tracer either into the river bed or into the stream/river bed. A conservative tracer such as Sodium Chloride (NaCl) can be used as it will not be biologically, chemically or physically altered as it moves through the system. Tracer tests are usually designed to characterise the physical transport properties of a stream. (Harvey et al., 1996) identified 4 basic transport processes which act upon a tracer mass which moves down stream.

1. Advection, the rate at which the tracer mass moves down stream.
2. Dispersion, which accounts for the mixing process in the stream that causes the tracer body to spread.
3. Groundwater inflow to the channel, which serves to increase the rate of flow and to dilute the tracer.
4. Storage zone exchange, which describes the movement of solute between the active channel and stagnant or slow moving zones in the stream or in the sub-surface.

By observing the tracer concentration history at some point downstream of the injection point, an evaluation can be made of the coupled system which consists of a system of flowing water in the stream channel and a system of storage zones at the margins of the stream channel or in the subsurface that contains slowly moving or immobile water, (Harvey et al., 1996). By quantifying the lag times of solutes in the storage zones, a conceptualisation of the hyporheic zone flow path

can be made and when this is correlated with the hydraulic properties of the alluvial sediment, the depth to which the hyporheic zone can be estimated.

Tracers may also be placed below the sediment surface to identify zones of upwelling and zones of down dwelling water (EA, 2005). If groundwater up-welling is occurring, the tracer will be detected in the stream immediately above the stream bed. In zones of down dwelling, stream water and tracer either go unobserved or reappear in the stream at some distance downstream where up-welling conditions exist, (EA, 2005).

Natural solute tracers can be used when the groundwater and surface-water are known to vary significantly in variables such as chloride and other conservative major ions. (Hill and Lymburner, 1998) used a chemical mixing equation using differences in background stream and groundwater chloride concentrations as well as well as injections of chloride to stream flow to delineate the hyporheic zone of two head water streams in Southern Ontario Canada. They found that good agreement exists between the two methods which confirmed that the extent of the stream-groundwater exchanges can be successfully estimated using background conservative ions as a tracer method. It can generally be stated that if the measured conservative variables level is definitively not that of groundwater or surface water but rather in between, then a degree of connectivity between surface water and groundwater exists.

Water temperature is sometimes used effectively as a natural tracer in hyporheic studies. As groundwater temperatures are relatively constant in comparison to surface water temperatures which vary seasonally and diurnally, temperature gradient will be seen through the surface water groundwater mixing zone. As the hyporheic temperature profile is dependent on the direction of groundwater flow, the difference between groundwater and surface water temperature and the flux of water, an analysis of the gradient can lead to an assessment of hyporheic zone extent.

In this study the hyporheic zone was delineated based in a definition that the zone contains some proportion of surface-water. This is a common definition used by hydrologeologists and allows for an easy delineation method to be used based on the natural tracer method and a two component chemical mixing equation (Hill and Lymburner, 1998).

$$\% \text{ stream water} = (Cp - Cg)/(Cs-Cg) \times 100$$

Cp = Chloride concentration in the pore water
Cg = Chloride concentration in the groundwater
Cs = Chloride concentration in the stream water

## 2.3.2 Delineation based on other methods.

### 2.3.2.1 Geophysics

(Acworth and Dasey, 2003) used a combination of borehole logging, borehole electrical tomography, and cross-creek electrical imaging to map the hyporheic zone around a tidal creek in New South Wales, Australia. The use of electrical conductivity imaging on a cross creek scale allowed for the delineation of a mixing zone in which saline waters from the creek mixed with fresh water in the underlying aquifer. As saline water has a higher conductivity than fresh water, resistivity imaging maps allowed for an assessment to be made of the geometry and heterogeneity of the hyporheic zone extent. It can be seen in (Figure 2.3.1.1) that an asymmetrical hyporheic zone was identified which extended to a depth of 10m at some locations within the creek. The highly asymmetrical shape demonstrates the sensitivity the zone has to local scale heterogeneity of hydraulic properties.

Figure 2.3.1.1, Asymmetric hyporheic zone of tidal creek delineated using electrical imagery techniques

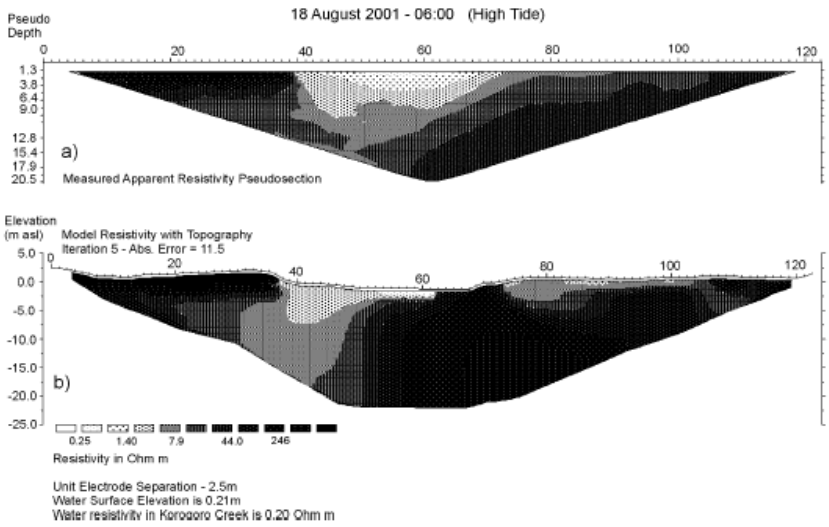


Adapted from Acworth and Dasey, 2003)

### 2.3.2.2 Hyporheic Invertebrate mapping

Based entirely on an ecologic definition, an assessment of invertebrate samples drawn from hyporheic wells can lead to a delineation of the hyporheic zone. As invertebrates can be classed into different groups; those that only live in groundwater, those that can only survive in a mixture of surface or groundwater and those that may be found in surface water, hyporheic delineation is feasible. In one case, invertebrate mapping on particular fauna (meio and macro-invertebrate fauna) in alluvial aquifers reported the presence of taxa characteristic of the hyporheic zone as deep as 1m beneath the streambed and up to a few hundred meters from the channe1 (EA, 2000). This conflicted an earlier theory which suggested that the hyporheos fauna were only part time residents in the hyporheic zone, hence hyporheic invertebrate mapping could now be used as a delineation tool.

In a study carried out by (Malard et al, 2003) on the longitudinal patterns of invertebrates in the hyporheic zone of a glacial river, it was found that the spatial variability in taxanomic richness

was best explained by temperature, the influence of groundwater and the amount of organic matter. As all these variables have measurable values that can be associated with either groundwater surface water or hyporheic water, the use of invertebrate mapping has been proven to be appropriate in the delineation of the hyporheic zone.

#### 2.3.2.3 Piezometric Head

The flux of water into or out of the stream bed is a function of the difference in hydraulic head between surface and subsurface water. Thus a measure of hydraulic head difference allows for the determination of the possible movement of water into or out of the river bed. (Ellis et al., 2004) used predominantly a network of riverbed drive-point piezometers to estimate baseflow and associated contaminant/solute flux from groundwater to surface-water. Although head gradients can give a first impression of the likely shape of the mixing zone, their measurement does not aid in the quantification of the extent of the hyporheic zone. To achieve this, other methods such as chemical gradients within the river bed have to be used in conjunction with head data.

## 2.4 Natural Attenuation

Studies have been carried out investigating how the size and biogeochemical function of the hyporheic zone differ in streams and how these differences may influence attenuation of contaminants as well as stream ecosystems. It has been proposed that the importance of hyporheic zone processes to a stream and hyporheic chemical environment is determined by the proportion of stream water that passes through the hyporheic zone and the rate of sediment biochemical processes. Knowledge of the dimensions of the hyporheic zone and the proportion

of stream and groundwater present at various locations within this zone provides an essential template for the analysis of solute chemistry (Hill and Lymburner, 1998).

The degredation of organic contaminants in the mixing zone owes its occurrence partly to the dense microbial community which is known to exist in the hyporheic zone. These microbes which thrive in the chemical environments created by surface water and groundwater mixing, act as catalysts to oxidise organic contaminants through a complex chain of events. The biodegradation process involves the transfer of electrons ($e^-$) from the organic contaminant to some electron acceptor. Per say, the organic contaminant is being oxidised while the electron acceptor is being reduced. The order in which electron acceptors or oxidization agents are used for redox reactions is as follows.

1. Aerobic Respiration
2. Denitrification
3. Mn(IV) reduction
4. Nitrate reduction
5. Fe(III) reduction
6. Sulphate reduction
7. Methanogenesis

By monitoring the rate at which these species are being depleted in the mixing zone, an indication of the rate at which organic fractions including contaminants are being oxidised can be estimated.

A useful system of quantifying the rate at which reactive species such as $NO_3$, $SO_4$, and D.O. are being depleted is by comparing background chloride concentrations to reactive species concentrations. As the percentage of surface and groundwater at any depth horizon can be calculated based on chloride concentrations, the equivalent reactive species concentrations can also be calculated for a hypothetical situation in which no depletion was occurring, for a given

percentage of surface water at a particular depth horizon. By comparing these hypothetical concentrations to those observed, a quantification of the degree of depletion of each species can be calculated. This method can only be applied to environments in which the surface water and groundwater have fixed concentrations, however in environments which have varying groundwater and surface water concentrations such as that seen in the River Tame, the method can be used to give a qualitative overview of determinand depletion.

## 2.5 Fluorescence Spectroscopy

The analysis of fluorescent properties of dissolved organic material (DOM) in river, aquifer or hyporheic waters provides a bank of data which can be used to identify organic fingerprints of both surface and groundwater and can also be used to identify the rates of degredation of organic contaminants within the microbial hyporheic zone. DOM has distinctive spectrophotometric properties in terms of both absorption and fluorescence. Recent advances in fluorescent spectrophotometry permit the rapid (~1 min) detection of fluorescent DOM at a wide range of both excitation and emission wavelengths to produce an excitation-emission matrix or EEM (Baker and Inverarity, 2004). Fluorescence spectroscopy also provides an excellent tool to source dissolved organic matter fractions, and to monitor and understand dissolved organic matter transformations in aquatic systems. DOM can be either anthropogenic or naturally present in the water body. Some is created in-situ through microbial activity, which may provide an independent source of organic matter (Hudson et al., 2005). The identification of DOM type is possible as all organic molecules absorb and emit energy at different wavelengths and intensities. Organic matter fluorescence occurs when a loosely held electron in an atom or molecule is excited to a higher energy level by the absorption of energy e.g. a photon, and fluorescence

occurs when energy is lost as light as the electron returns to its original energy level (ground state). Some energy is transferred to the surrounding molecules from the "excited" electron, prior to emission, so the energy of the emitted photon is lower that the excited energy (the Stoke's shift). The wavelength at which absorption (excitation) and emission occur allows for the identification of molecule type (Hudson et al., 2005). The intensity of the emission allows for the quantification of the DOM present. Concentrations can be determined based on calibration of fluorescence against total organic carbon (TOC).

The most commonly studied fluorescent organic compounds of natural waters include humic substances and amino acids in proteins and peptides. Humic substances are derived from the breakdown of plant matter by biological and chemical processes in aquatic environments. These substances can be sub-divided into three categories, chemically defined by solubility at different pH.

- Humic Acids which are insoluble in aqueous solutions at Ph lower than 2
- Fulvic acids which are soluble in water under all Ph conditions
- Humines which are insoluble in water under any Ph condition.

The presence of amino acids is indicative of the presence of proteins and peptides. Three notable amino acids fluoresce, (tryptophan, tyrosine and phenylalanine). Debate continues about the origin of protein-like fluorescence, however there is clear evidence for a bacterial origin (Hudson et al., 2005). Thus, is indicative of biodegradation of organic substances.

The fluorescent properties of water samples can be efficiently inspected using excitation emission matrix fluorescence spectroscopy (EEMS) which is a state-of-the-art technique used. The principle of EEMS is that excitation, emission, and fluorescence intensity can be scanned over a range of wavelengths synchronously and plotted on a single chart, developing a "map" of

optical space. The production of a 3-D plot of fluorescence excitation wavelength, emission wavelength and intensity allows the visualisation of a range of fluorophores (compounds that absorb and re-emit light) in a given sample, in their relative positions in optical space. (Hudson et al., 2005). (Figure 2.5.1) illustrates typical EEM fluorescent peaks of humic and amino acids.

Figure 2.5.1, Typical EEM's of (a) humic acid standard 12.5ppm, (b) fulvic acid standard 12.5ppm, (c) amino acid (tryptophan) standard 0.1ppm and (d) amino acid (tyrosine) standard 0.2ppm.

(a) (b)

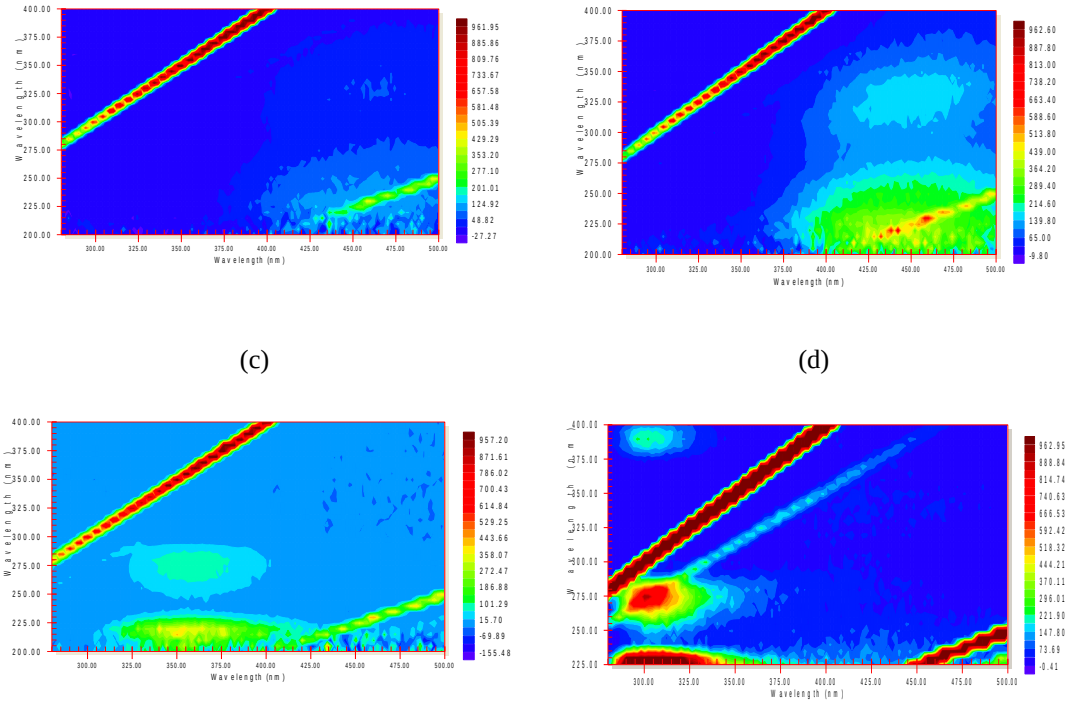


(c) (d)

Adapted from Hudson et al., 2005

For an urban river environment such as that seen in North Birmingham it is important to note that groundwater has relatively low concentrations of organic matter when compared to river water. This is due to the high concentrations of humic-like matter present in river water due to untreated and treated sewage discharge and the high degree of microbial activity associated with

it. (Figure 2.5.2) illustrates the typical EEM's of sewage effluent diluted to different proportions. River water EEM's from the River Tame show similar fluorescent patterns to those seen in (Figure 2.5.2).

Figure 2.5.2, Typical EEM scans of marine, river, sewage and treated sewage

a.) Typical marine EEM

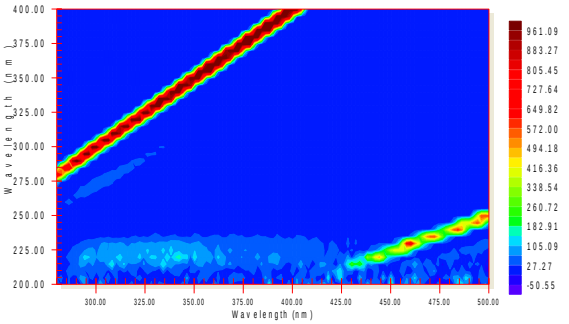


b.) Typical river EEM

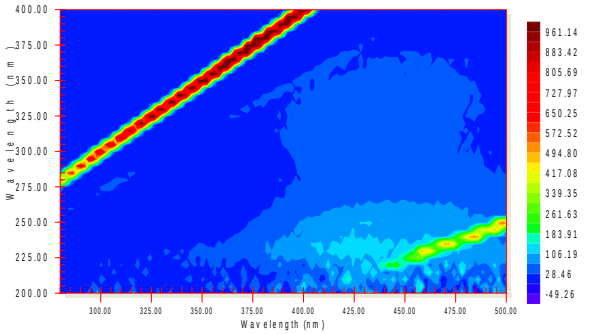


c.) Typical untreated sewage EEM

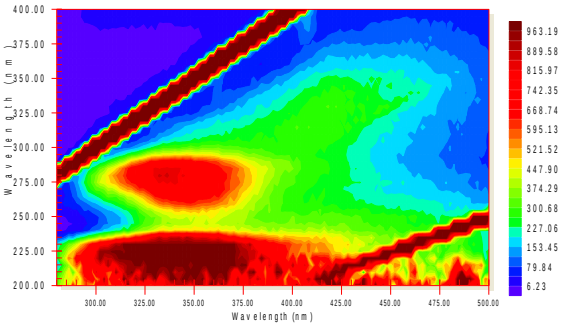


d). Typical treated sewage effluent EEM

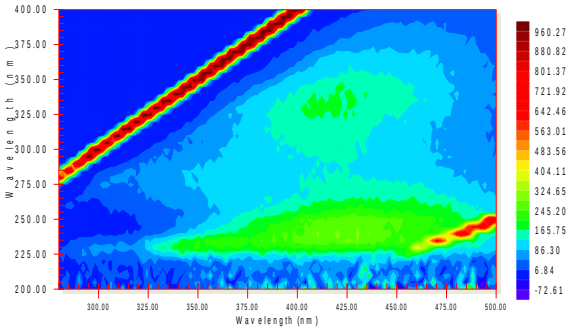


Adapted from Hudson et al., 2005

The degree of microbial activity at any particular depth horizon below the river bed can be quantified by dividing the intensity of the amino acid peak (Peak T) by the intensity of the humic-like matter peak (Peak A) Figure 2.5.3, thus giving a relative proportion of microbial activity. The higher the ratio value, the greater the degree of microbial activity and hence the

greater the likelihood organic contaminant degredation occurrence. (Figure 2.5.30) illustrates the location of different organics fractions in EEM optical space and the names which have been applied to different peaks.

Figure 2.5.3, EEM showing the positions of peaks, C, A, T and B

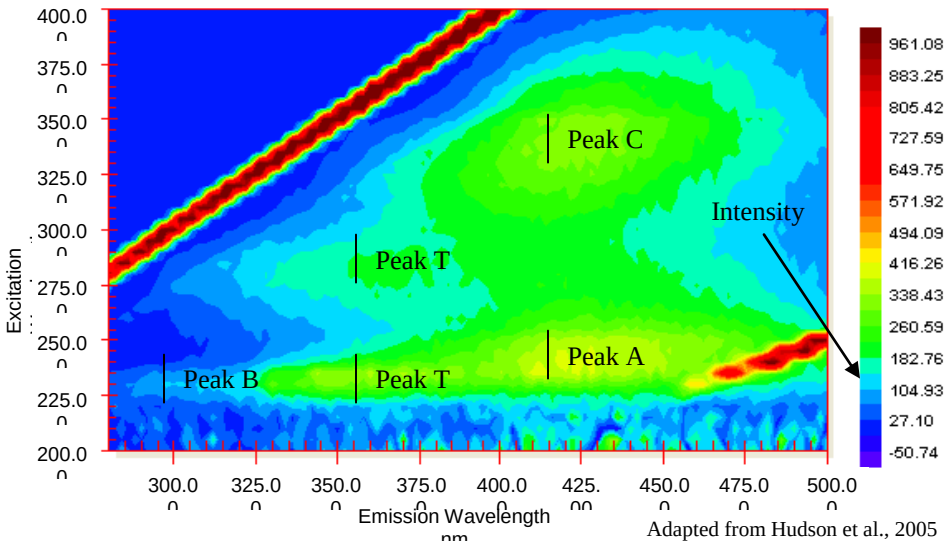


Peak C = Humic-like Matter
Peak A = Humic-like Matter
Peak T = Tryptophan
Peak B = Tyrosine

Natural fluorescence of organic matter has been used for two purposes in the current study.

1. To identify organic fingerprints of both surface and groundwater and to evaluate the use of fluorescence as a hyporheic delineation tool.
2. To correlate depleted concentrations of inorganic determinands to increased microbial activity horizons to assess the reasons for inorganic determinand depletion.

# Chapter 3 Characterisation of the Study Area

The study has been carried out on a 600m stretch of the River Tame in the North Birmingham Region. The broader area is continuously being subjected to case studies because of the known contaminant plumes which are present in the underlying aquifer which are known to be discharging through base flow and seepage to the river Tame. The area is thus ideal for qualitative and quantative research of contamination degredation and hyporheic zone studies.

## 3.1 Regional and local Setting

### 3.1.1 Regional Setting

The River Tame flows through the industrial city of Birmingham, UK which has a population of over one million. The Tame drains a 450 $km^2$ catchment of which urbanisation covers an area of some 250 $km^2$. The Tame flows in an easterly direction through North Birmingham and drains to the River Trent which in turn drains to the North Sea. Historically, Birmingham has been a focal point of heavy industry since the industrial revolution. The historic lack of legalisation to control the industrial expansion and urbanisation, and the overloading of sanitary systems, (sewage and industrial effluent were often discharged untreated) led to the deterioration of the groundwater, surface water and soils. The River Tame supported no fish life by 1918 and by 1945 virtually no aquatic life prevailed. (Ellis, 2003).

### 3.1.2 Study Location

The study site is located roughly 2 miles north of Smethwick and 1.5 miles west of Erdington and is situated between the Holford industrial Estate and the M6 motorway. The study area has been selected to host a series of hyporheic zone control experiments over the coming years in

which dipole-dipole experiments are proposed. Initially the site consisted of a 600m stretch of river between Elliot Way which crosses the river to the west and Gavin Way to the east.

At a later date the study area was refined to a 150m stretch within this initial study area, (Figure 3.1.2). The refined study area was selected because of contrasting hydraulic conditions that were seen within. The river bed to the western end of the refined section consisted of a shallow gravel zone with relatively high hydraulic conductivity values. River flow rates in this section were also relatively high. In contrast, the river bed to the eastern border of the study section close to Gavin Way consisted predominantly sands and silts. The river stage was generally higher than that close to the western border and the flow rate was much slower.

Figure 3.1.2, Map of Initial study Section and Refined study section

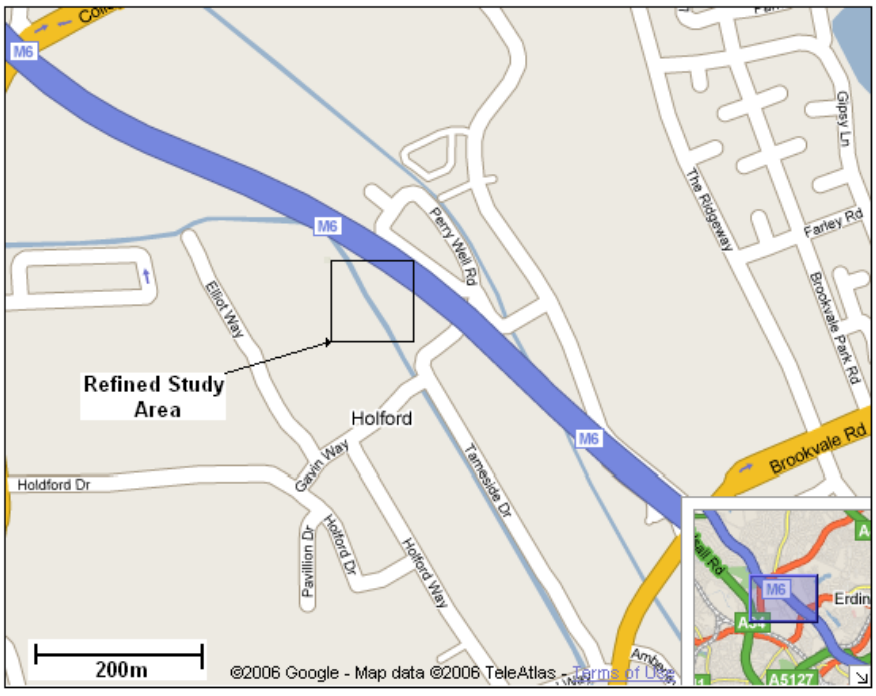


It was found that the refined site provided sufficiently contrasting hydraulic conditions for an assessment of the different hyporheic zone hydraulics and chemical fluxes, which in turn lead to the completion of the main aim of the project.

## 3.2Regional Geology

### 3.2.1 Post Carboniferous Geological History

The geology of the Birmingham region comprises mainly of a series of post Permian sedimentary sequences which have been deposited in a series of east-west extensional graben and half graben basins. Birmingham itself and its surroundings are located within the Knowle Basin which is bordered to the west by the Eastern Boundary Fault, to the east by the Western Boundary Fault and to the North-West by the Birmingham Fault, (Figure 3.2.1). Within this basin a thick sequence of Triassic and later Jurassic rocks were deposited over time. The Sherwood Sandstone Group was deposited in fluvial environments with in the extensional graben and a thinner succession was deposited on adjacent highs Powell et al. (2000). These sedimentary deposits are generally overlain by the Mercia Mudstone Group which were deposited in fluvial and lacustrine environments. The end of the Triassic saw a major transgression of sea-level which resulted in a thin sequence of limestones and mudstones to be deposited over the Triassic sediments. These in turn are overlain by the marine Jurassic rocks, glacial and post-glacial drift deposits recent fluvial deposits and due to urbanisation, small sections of made ground.

Figure 3.2.1, Regional Geological Setting of the Study Area

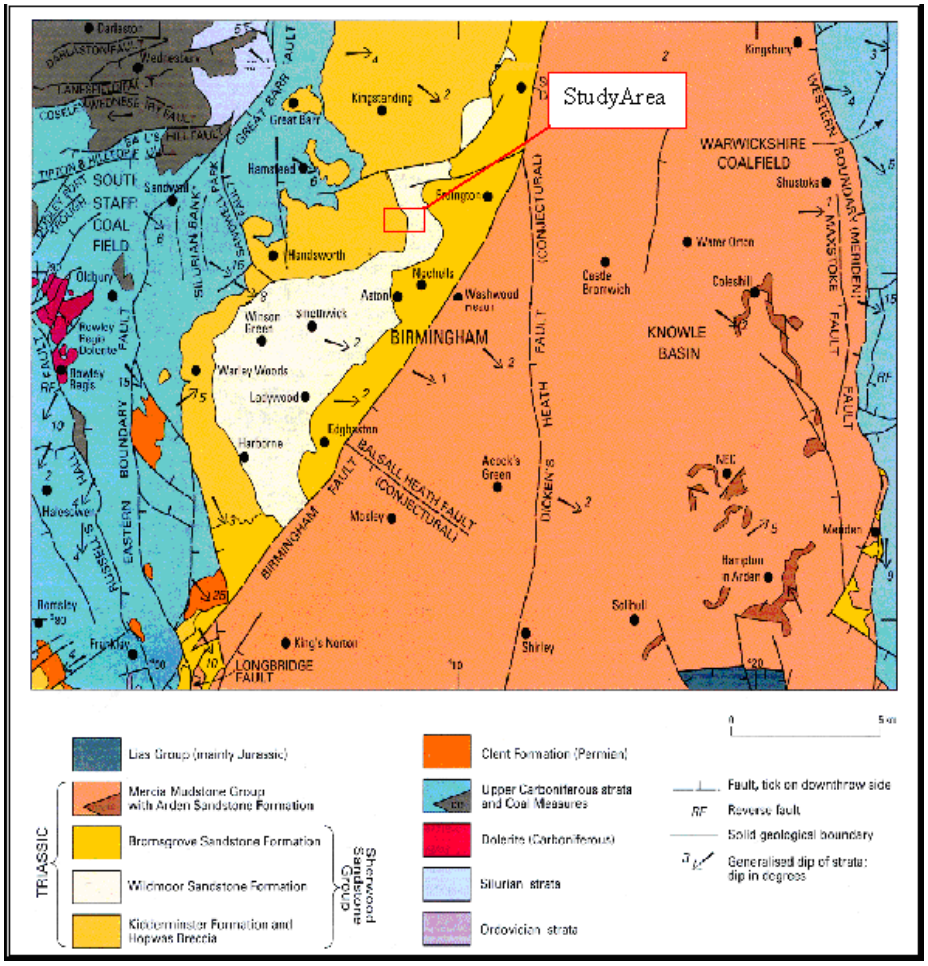


## 3.2.2 Post Permian Sequences and Formations

The Triassic sediments have been divided up into 4 different groups based on sub-era in which they were deposited (Figure 3.2.2). The Sherwood Sandstone, comprising the Kidderminster, Wildmoor Sandstone and Bromsgrove formations has a thickness on the general range 100-150m although it achieves 200m in places, (Ford and Tellam, 1993). A brief description of the groups and formations of the Triassic sediments and other eras are summarised in (Figure 3.2.2).

Figure 3.2.2, Post Pre-Permian Lithological description of Group Formations.

| Era | Group | Formation | Description |
|---|---|---|---|
| Quaternary | | Quaternary | Consist of Glacial deposits, glaciolacustrine deposits, interglacial deposits, till and sandy till, made ground and recent fluvial deposits. |
| | | | |
| Jurrasic | Lias Group | Blue Lias Formation | Mudstone with locally intercalated siltstone and limestone. (Wilmcote Limestone Member).The Upper Saltford Shale Member consists of fissile and blocky mudstone with sparse thin limestone beds. |
| | | | |
| Triassic | Penarth Group | Lilstock Formation | Grey green calcareous mudstone with sparse limestone beds. Gradual boundary with the underlying Westbury Formation. |
| | | Westbury Formation | Consists of dark-grey, fissile mudstone with silty laminae and thin beds of limestone and siltstone. Rests with a sharp base on the Blue Anchor Formation. |
| | | | |
| | Mercia Mudstone Group | Blue Ancor Fm. And Twyning Mudstone Formation | Consists of pale, green-grey, blocky mudstone and thin beds of siltstone with dolomite concretions. |
| | | Eldersfield Mudstone Fm. and unconformable Arden Blue Ancor Fm. And | Consists of red-brown, locally gypsiferous mudstone with thin, green-grey siltstones. The Arden Sandstone Formation is generally between 0m and 10m in thickness. Consists of pale, green-grey, blocky mudstone and thin beds of siltstone |
| | | | |
| | Sherwood Sandstone Group | Bromsgrove Formation | Consists of red-brown, micaceous, calcareous sandstone with pebble conglomerate lenses and sub-ordinate mudstone. The formation ranges in thickness from 84m to 180m. |
| | | Wildmoor Sandstone Fm. | Consists of orange red fine-grained, micaceous, soft sandstone and subordinate thin beds of red-brown and green-grey mudstone. A maximum thickness of 120m has been proven in boreholes to the North-East of the Birmingham fault. |
| | | Kidderminster Formation | Consists of pebbly conglomerates, pebbly sands. Crossbedded sandstone with sparse thin mudstone beds. Ranges in thickness from 45 to 120m. Formation rests disconformably on the Hopwas Breccia. |
| | | | |
| | | Hopwas Breccia Fm. | Red-brown sandstone, pebbley in part, with minor mudstone. The formation has been found to be up to 10m thick. |

## 3.3 Local geology and Drift deposits

### 3.3.1 Local Geology

The overall study is underlain by the Kidderminster Formation. This is the predominant outcrop in the study region. (Figure 3.3.1.1), (Figure 3.3.1.2). To the north east of the River Tame the Wildmoor Sandstone can be seen to outcrop which is then followed by the Bromsgrove Sandstone Formation. Formations of the Mercia Mudstone Group are not seen to outcrop close to the study area but are seen to outcrop both to the east and west within a 1.5 km radius.

Figure 3.3.1.1, Regional Geology of the Knowle Basin with Study Area location

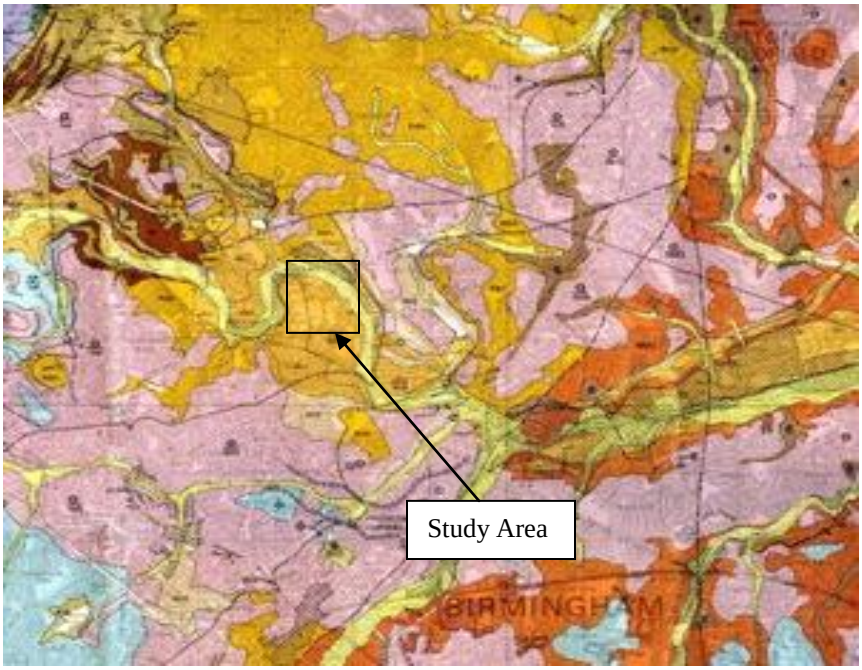


- Kidderminster Formation
- Wildmoor Sandstone Formation
- Bromsgrove Sandstone Formation
- Drift Deposits
- Mercia Mudstone Group
- Mercia Mudstone Group

Figure 3.3.1.2 Local geology of study section

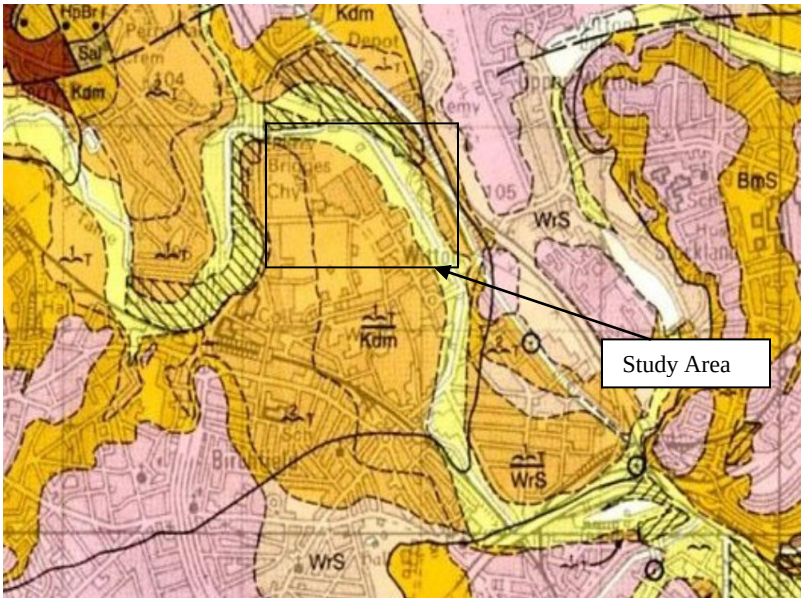


## 3.3.2 Regional and Local Drift Deposits

The superficial drift deposits in the region comprise of till and sandy till, glaciofluvial deposits (sand and gravel) and glaciolacustrine deposits (mostly laminated clay, silt and sand). (Powell et al., 2000). The deposits have a complex distribution reflecting the glacial and post-glacial history of the Pleistocene and recent times. (Ellis, 2003). Three phases of Pleistocene glacial advance and retreat are recognised in the English Midlands. Associated sediments were initially laid down upon a topography determined by the underlying Triassic Sandstone (Greswell, 1992). The buried landscape of the Triassic is substantially different to that which we see today and would have included several buried valley systems which now contain a sand and gravel fill.

Glacial drift deposits vary greatly based on the mechanism by which they were deposited however four main divisions based on lithlology have been identified. (Knipe et al., 1993).

1. The first comprises Glacial till deposits which have been laid down beneath the ice sheets and retreating glaciers. The till consists of red, orange-brown, brown and yellow clay and sandy clay. Un-bedded drift comprises rock debris and a sandy clay matrix. Rock clasts generally comprise of red-brown quartzite pebbles and quartz and sandstone reworked from the conglomerates of the Triassic Kidderminster Formation.
2. Glacio-lacustrine deposits formed by the movement of ice up river valleys and the trapping of lakes between the ice and the surrounding high ground. The unit comprises clay, silt, fine-grained silt and peat.
3. Glacio-fluvial deposits which formed from melt waters flowing from beneath the glaciers. (Ellis, 2003). These deposits consisted of poorly sorted red, orange and yellow sand, clayey sand, pebble sand, and gravel. These deposits are present at the surface over much of the central and east of the Birmingham district
4. Inter glacial deposits comprising humic clays, silt and peat. The humic clays consist of finely comminuted organic detritus, woody peat and humic fine- to medium-grained sand with coarse organic debris. (Powell et al. 2000)

Glacio-fluvial deposits of sand, clayey sand and gravely sand are known to be present in the sediment filled paliovalleys of the Proto-Tame. These along with glacio-lacustrine and interglacial deposits have been proven in boreholes to be up to 36m thick within the palaeovalley. Away from the valleys the deposits generally range in thickness from 5m to 19m.

Post-glacial deposits in the district are generally the product of erosion and deposition during the latter stages of the last glaciation, (Devensian) (Powell et al. 2000). Alluvial

deposits of sands, gravels and clays are found on the valley bottom of the Tame water course as well as two additional stages of river terrace deposition which have been identified to predate the recent alluvium.

Made ground deposits are extensive in the Tame Valley with large amounts of material having been deposited on otherwise marshy ground for urbanisation purposes as well as for flood defense and the diverting of water courses. Made ground consists of mine spoil, sand and gravel mixtures, often with substantial quantities of ash, slag and rubble.

## 3.4 River Bed Deposits

(Ellis, 2003) took cores of the riverbed sediments in the River Tame. Cores generally penetrated up to 0.5m into the river bed. It was found that they typically consisted of a top 10cm layer of coarse gravel with cobbles, underlain by mixed sands and gravel. The finest material present was classed as fine sand and more than 60% of the samples were classed as gravels. Core samples and shallow digging has been carried out in the current study site of the Tame in which sediments range from coarse gravel and sand to organic rich silt deposits. Most commonly, red sands and silt sands were found below the gravel and silt deposits and represented the lower hydraulic conductivity values in the alluvial deposits.

## 3.5 Regional Hydrogeology

The principle groundwater bearing unit in the region is the Triassic sandstone aquifer which is both confined and unconfined at different locations of the Birmingham Region. The base of the aquifer if believed to extend to the eroded surface of the Carboniferous. The main

hydrogeological units are bounded by major faults, and the most significant unconfined Triassic Sandstone Aquifer is bound to the Northern by an anticline and to the southern, by a series of faults. To the east of the region the Mercia mudstone group is overlying the Triassic Sandstone. The Mercia Mudstone is considered to effectively be impermeable. The group is said to have a hydraulic conductivity of at most about 0.001 m $day^{-1}$ and often much lower. This mudstone group thus confines the underlying sandstone aquifer in the eastern section. To the west the Aquifer is bound by the Carboniferous coal measures which do support some water abstraction, but not to the extent of the Triassic Sandstone.

Most of the district lies within the Trent River basin in which the River Tame and its tributaries are the primary focus of natural discharge in the region with flows in a north and south direction towards the river, (Ellis, 2003). The Birmingham Fault which runs in a NW-SE direction through the region (Figure 3.2.1) has faulted Mercia Mudstone group against Triassic Sandstone. The fault is a low permeability feature and results in a significant drop in piezometric head across the boundary.

A simple conceptual model of ground water flow has been developed by ( Greswell, 1992) (Figure 3.5.1). Water enters the system as recharge, flows down gradient in an easterly direction and discharges to water courses in areas of low relief where the groundwater head is at or above surface water elevation. The Birmingham fault to the east then acts as a boundary to groundwater flow and the Mercia mudstone create confining conditions (Greswell, 1992)

Figure 3.5.1, Conceptual Section of the Birmingham Aquifer (after Greswell, 1992 and Jackson, 1981).

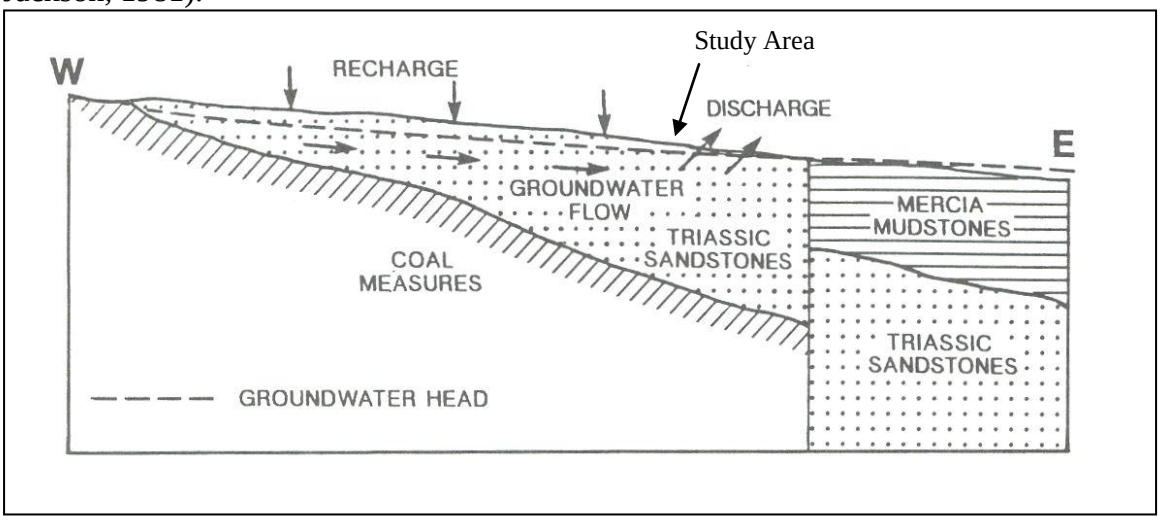


The glacial Quaternary deposits are lithologically heterogeneous with rapid lateral and vertical changes in character. The rate and amount of infiltration of precipitation is controlled by the thickness and type of geological drift covering the Triassic Sandstone. The influence of drift deposits on flow to the river may also be significant in that some drift deposits have higher horizontal hydraulic conductivity values than vertical. This results in recharge only penetrating the upper drift layers and then moving horizontally to a river without ever entering the aquifer.

Water abstractions from the Birmingham aquifer were substantial up until the 1960's. Prior to this time, a heavy industrial use of groundwater lead to a drawdown of the water table. Abstraction rates peaked in the industrial era at 60 $Mld^{-1}$ during the 1950's. After the 1960's, abstraction rates declined substantially with a consequent rise in water table. This rebound is predicted to have had an adverse effect on engineered structures in the region in which foundations and excavated structures have been subjected to flooding, contaminants from previously unsaturated waist have been mobilised. By 1989 the much reduced levels

of abstraction had resulted in a recovery of water table levels by as much as 20m in large areas of central Birmingham.

The Triassic Sandstones are in general relatively low-permeability/high storativity aquifers: typical permeability and specific yield are of the order of 1m $day^{-1}$ and 0.1 respectively. (Ford and Tellam, 1992) The hydraulic properties of the different formations of the Triassic Sandstone have been obtained from pump tests carried out in previous studies in the region and the following hydraulic conductivity and porosity values have been referenced from (Ellis, 2003).

| | $K_{Horizontal}$ m/d | $K_{Vertical}$ m/d | Porosity |
|---|---|---|---|
| Kidderminster Formation | 3.5 | 2.7 | 0.29 |
| Wildmoor Formation | 1 | 0.83 | 0.27 |
| Bromsgrove Formation | 0.93 | 0.53 | 0.28 |

Recharge is complex and has a high spatial variability in the urban catchment. Values have been significantly reduced by urbanisation although it is thought that the system is augmented to such a degree by mains water and drainage system leakage that overall amounts of recharge are similar to pre-urbanisation. (Ford and Tellam, 1993) This has generated recharge that is much more localised than in an equivalent non-urban area. As well as this, the distribution of precipitation across the area is not uniform with average annual rainfall of 800mm in the south-west and only 650mm in the north-east (Ellis, 2003). Urbanisation has also caused runoff to be higher than a non-urban area.

## 3.6 Local Hydrogeology

On a scale relative to the study area the River Tame is gaining throughout the full section. This is evident from head measurements carried out in MDP's installed in the river bed during field work and a numerical model constructed by (Ellis, 2003). (Figure 3.6.1), illustrates the conceptualisation generated in Mod Flow of the groundwater flow direction in the region surrounding the study area. The model, which was constructed in 2003 is assumed to be accurate to recent times as all current abstractions are believed to have been included. It can clearly be seen that the general hydraulic gradient in the area is in an easterly direction causing a general movement of groundwater to the east. However, in close proximity to the river channel, head gradients to the north-west of the river are sloping in a south-westerly direction. Also it should be noted that a much steeper hydraulic head gradient exists to the north- west of the river possibly generation higher groundwater flux rates through the river bank and seepage faces of the northern bank (Figure 3.6.2). However, little evidence was seen in the field to support such a claim. At two locations of the study reach, artificial barriers in the form of sheet piles have been used on the northern bank for infrastructural stability purposes. The upstream piling is located at the sharp bend in the river close to the M6 motorway. The downstream piling is located under Gavin Way Bridge. It has been taken into account that these structures could possibly obscure shallow groundwater flow paths to the river and the areas have thus been avoided for more concentrated field work studies. River bed sediments do not appear to present a barrier to groundwater movement from the aquifer.

Figure 3.6.1, Numerical Conceptualisation of groundwater flow direction in study area

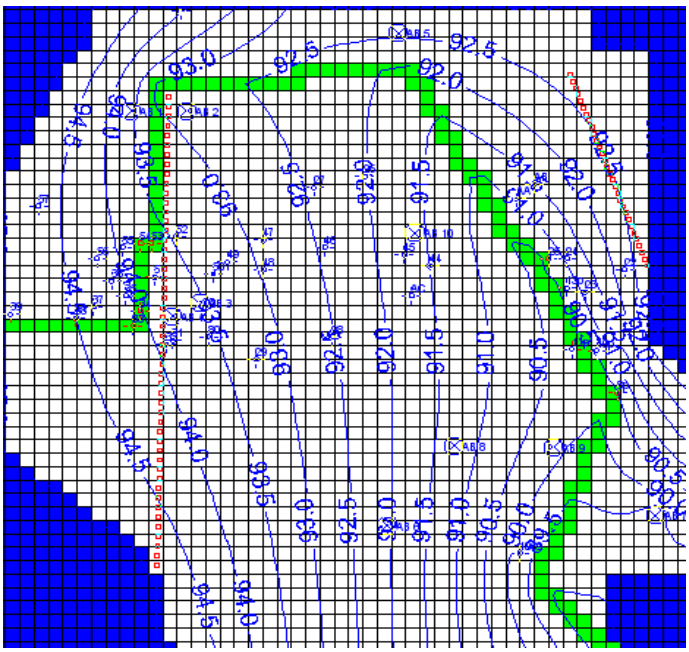

Adapted from Ellis, 2003

Figure 3.6.2, Cross-section of conceptualised hydraulic head passing through the River Tame in a N-S direction.

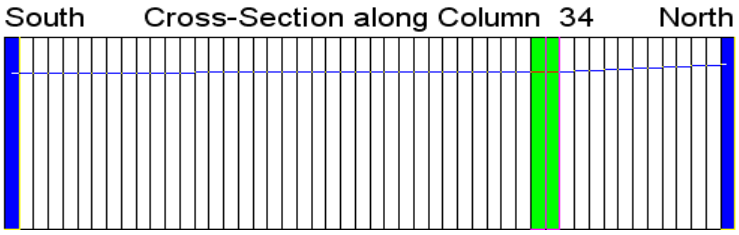


Adapted from Ellis, 2003

## 3.7 Hydrology

Previous surveys carried out by (Ellis, 2003) reveal that the river Tame is typically 8-12 m wide, 0.2-2 m deep with average dry weather flow velocities of 0.1-0.8 $ms^{-1}$. This is with little exception of the study area in which the current field work was carried out, in which a maximum river width of 11.2m was recorded and a minimum width of 7.6m. Flow data from Water Orton flow stations down stream of the study reach suggest average summer dry flow rates in the region 0.25-0.35$ms^{-1}$. Peak river flow rates of 10.5 $ms^{-1}$ (Water Orton) occurred during the first round of sampling of this project.

The river has been extensively modified from its original form as a meandering braded system on a broad flood plain. In the study section, flood defense banks have been constructed throughout the full length of river. At least one known major sewerage line has been installed beneath the river in which it is likely that made ground constituted at least a portion of the back fill material. The remainder of the riverbed is believed to be unaltered from its natural state. Weed growth within the channel has been abundant throughout the course of the project.

The diurnal flow rate variation of the river is significant and is evident from hydrographs from both Water Orton and Bescot gauging station. This variation can be attributed to sewage discharges from sewage treatment works plants. Sewage effluent contributes significantly to the dry weather flow of the river, with 55% of flow at the Lea Marston Lakes attributed to sewage discharge (Ellis, 2003).

## 3.8 Contamination

The completion of the main aim of this study is based on the fact that groundwater and surface-water have distinct chemical signatures. Of most importance are chloride concentration differences as it has a conservative nature in the system. Chloride concentrations do indeed vary between surface and groundwater bodies in the region as well as other inorganics such as nitrate and sulphate. Generally it can be seen that chloride concentrations are higher in the river than in the groundwater, where as the opposite is generally the case for both nitrate and sulphate.

A study carried out by (Ford and Tellam, 1993) found that water quality of abstraction wells in the city of Birmingham indicated that the aquifer is polluted, though not excessively so, with only $NO_3$ and Ba concentrations regularly exceeding EC Maximum Admissible Concentrations levels. The highest salinity, sulphate, chloride, sodium, boron and total heavy metal concentrations in the Birmingham aquifer are associated with metal-working sites and are from point sources. Hence, a considerable degree of heterogeneity in groundwater quality on a small scale can generally be seen. Nitrate concentrations in groundwater do not vary as much with depth as some other species which reflects a long history of supply and a wide range of sources. Numerous diffuse and point sources of different groundwater contaminants occur across Birmingham including industrial waist and processing chemicals, sewage, road de-icing salts, urea, domestic waists, fertilisers, construction wastes, historic animal waste, human burial and wet cleaning processes ( Ellis, 2003). The recent rise in water levels in the aquifer due to closure of industry has increased the vulnerability of groundwater and in some cases, has mobilised previous immobile contaminants. This along with chemical loading of rainfall in the urban setting has caused groundwater to be severely affected by pollution even in areas where Quaternary deposits and unsaturated zones are of greatest thickness (20-40 m).

Major ion analysis from groundwater samples from a number of pumped boreholes in the Birmingham region have been analysed by (Ford and Tellam, 1993). It was found that the majority of unconfined aquifer groundwater samples have Ca and $HCO_3$ as the dominant ions and are oxygenated ($O_2$ from less than 2 ml $l^{-1}$ to 10mg $l^{-1}$) with platinum electrode $E_H$ in the range 300-350 mV. Despite the almost ubiquitous presence of pollution in the aquifer system, it is only $NO_3$ amongst the major ions which frequently exceeds the EC (MAC) values (set at 50 mg $l^{-1}$ $NO_3$) (Ford and Tellam, 1993). This proves to be without exception on the current study site in which groundwater concentrations of nitrate exceeded the (MAC) in 37.5% of groundwater sample locations below the river bed in the study area.

Borehole samples taken from pumped boreholes in the Tame Valley from the Kidderminster Sandstone formation by (Ford and Tellam, 1992) and showed a broad range of $SO_4$, Cl and $NO_3$ concentrations. (Figure 3.8.1) shows some of the concentrations observed. This again reflects the high degree of heterogeneity in groundwater quality on a relatively local scale.

Figure 3.8.1, Observed groundwater concentrations in the Tame Valley

| Site | $SO_4$,mg $l^{-1}$ | Cl mg $l^{-1}$ | $NO_3$ mg $l^{-1}$ |
|---|---|---|---|
| 1 | 74.9 | 50.0 | 18.4 |
| 2 | 125.1 | 54.8 | 34.7 |
| 3 | 149.0 | 43.9 | 34.7 |
| 4 | 84.1 | 32.5 | 43.4 |
| 6 | 133.9 | 58.0 | 50.9 |
| 7 | 114.1 | 41.1 | 59.8 |
| 8 | 139.1 | 55.4 | 46.5 |
| 9 | 132.7 | 59.2 | 61.1 |

Adapted from (Ford and Tellam, 1992)

The distribution of organic contaminant within the aquifer differs from that of the inorganics with organic pollutants being very localised to specific industrial users and absent at depth in the

system. This reflects the specificity of use of the organic chemicals and the relatively short time for which they have been available for use (Ford and Tellam, 1992). The principle organic contaminants detected in the groundwater are chlorinated solvents which could be directly related to metal work or dry cleaning industries (Ellis, 2003). Chlorinated VOCs were widely encountered in groundwater discharging as base-flow to surface water in the Tame conurbation and impacting surface-water quality, (Shepherd et al., 2005).

## 3.9 Local Water Quality

The study reach has been conceptualised as having three distinctive chemical horizons from which samples have been retrieved. These are the river, groundwater and mixing zone between the two. The latter has a concentration gradient between the surface water and groundwater dependant on degradation rates and mixing processes occurring within, hence has been sampled at selected horizons for interpretation. Of all 22 samples believed to have been taken from 100%groundwater, the following concentrations were seen.

| Determinand | Lowest Concentration ($mgl^{-1}$) | Highest Concentration ($mgl^{-1}$) |
|---|---|---|
| Cl | 60 | 80 |
| $NO_3$ | 11.44 | 79.2 |
| $SO_4$ | 144 | 319 |

All determinands have higher upper concentration values than those observed by (Ford and Tellam, 1992) and this is believed to be because of the contrasting depths from which samples were retrieved. The samples retrieved in the current study were all from shallow groundwater sources while those observed by (Ford and Tellam, 1992) were all from deeper abstraction sampling boreholes. It was found in a survey of shallow wells at a particular industrial site and tunnel inflow waters below central Birmingham that the shallow waters can have very high concentrations of most determinands. High $Cl^-$ values of groundwater are potentially ascribed to

anthropogenic inputs, e.g., road salt, metal finishing wastes or water treatment (Shepherd et al., 2005).

A trilinear plot (Figure 3.9.1) of surface water major ion quality and various groundwater compositions observed in the Birmingham region by (Shepherd et al., 2005) shows that higher concentrations of chloride and sodium were found in the shallow groundwater. Higher chloride concentrations in groundwaters abstracted from the Tame Valley, compared to the rest of the aquifer, may have resulted from the inflow of surface water into the aquifer during periods of peak historical abstraction (Shepherd et al. 2005).

Figure 3.9.1, Trilinear diagram showing proportional concentrations ($mgl^{-1}$) of major ions in Birmingham groundwaters, river bed waters and surface water adapted from (Shepherd et al. 2005)

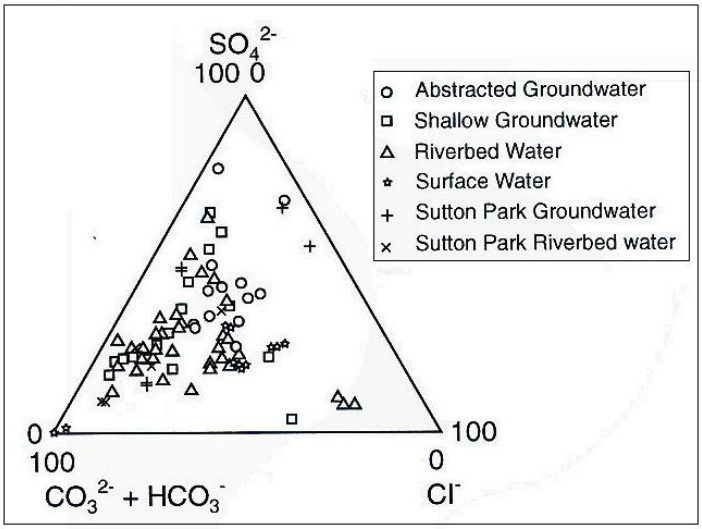

Surface water quality has been monitored throughout the course of this study. A total of 9 samples were retrieves and the following variations of concentrations were see

| Determinand | Lowest Concentration | Highest Concentration |
|---|---|---|
| Cl | 144 mg $l^{-1}$ | 171 mg $l^{-1}$ |
| $NO_3$ | 14.96 mg $l^{-1}$ | 41.36 mg $l^{-1}$ |
| $SO_4$ | 130 mg $l^{-1}$ | 166 mg $l^{-1}$ |

The variation in Cl concentration is believed to be as a result of diurnal fluctuations in sewage effluent discharge which is clearly evident from river hydrographs. The variation in $NO_3$ and $SO_4$ concentration could possibly be as a result of fluctuating base-flow discharges caused by temporally variable hydraulic conditions within the river.

# Chapter 4 Field Work and Methodology

## 4.1 Introduction

The full 600m project area was surveyed using leveling equipment, to acquire river bed and bank elevation data and two river bed samples were taken for visual analysis at 50m intervals throughout the section. From both sediment inspection and elevation data a more refined site was chosen for hyporheic zone monitoring and delineation. The refined site initially consisted of two cross channel profiles which were separated by a distance of 150m. At a later date an extra cross section profile was examined between the two original profiles at a distance of 50m down stream from the furthest upstream initial profile. However chemical sampling from this profile did not prove productive due to low K sediments.

Fieldwork Design:

The aims of the fieldwork and monitoring network applied to the study area are as follows:

- Survey the full study section and identify river bed gradients and elevation above ordinary datum (sea-level).
- To identify the hydraulic gradients below the river bed and evaluate its variation vertically, horizontally and temporally.
- Obtain hydraulic conductivity (K) estimates from both grain size analysis and slug tests.
- Identify likely zones in which contrasting hyporheic zone thicknesses may be seen, based on hydraulic gradients, (K) estimates and river bed sediment typing and river water flow environments.

- Carry out multiple horizon sampling in these pre-identified zones and correlate chemical gradients and identified variables, both spatially and temporally.

## 4.2 Site Survey

A survey of the full site was carried out to acquire absolute bed and river bank elevations. Initially, the full study stretch was divided up into 50m sections and named profiles were located at the start and end of the study section and at 50m intervals between. In all, this amounted to a total of 13 profiles (Figure 4.2.1). The survey was carried out by setting up the scope at profile one and taking elevation readings at the Southern and Northern flood defense banks, the edge of both river banks and at one meter intervals from the southern bank across the river bed. It was then necessary to forward scope to the next profile to identify the elevation difference between the two profiles before the procedure carried out at profile one was repeated. The full study area was surveyed in this manner which allowed for an overall physical characterisation of the reach in terms of river bed gradients and variation in river width. By averaging the river bed elevations at each profile and subtracting its elevation from the average elevation of the closest profile upstream, the elevation difference can be identified. Thus, by dividing this elevation change by the distance between the two profiles, the connecting river bed gradient can be calculated.

Figure 4.2.1, Profile Locations of study reach

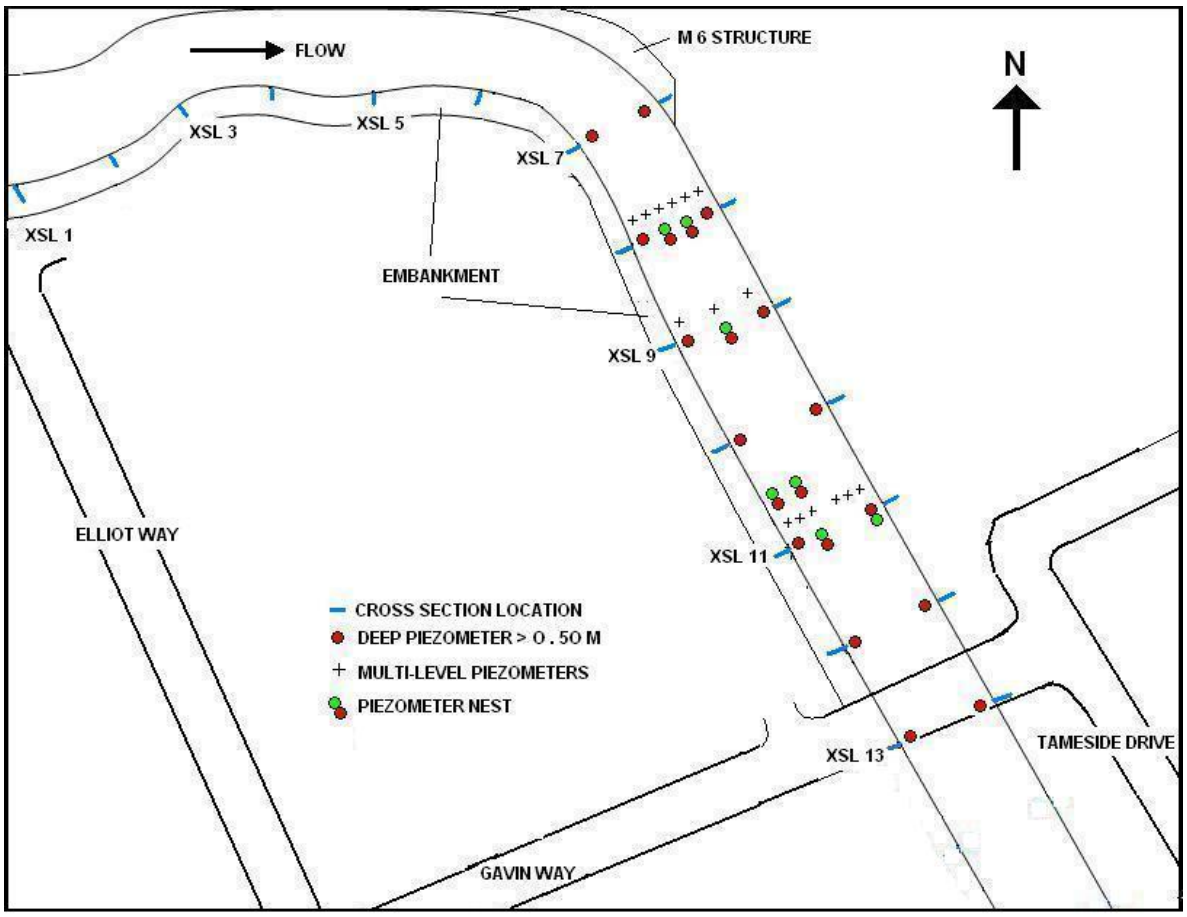


## 4.3 Grain Size Analysis

Samples retrieved from each profile were analysed visually and a selection of samples were analysed by sieve analysis. The hydraulic conductivity of unconsolidated sediments is directly related to the packing of the particles and the void spaces between them which are a function of the grain size distribution (Ellis, 2003). The grain size distribution of individual samples has been obtained by firstly drying the samples in a fan extractor at a temperature of 150$^{o}$C for 24 hours. Once all moisture has been expelled, the samples are passed through a set of increasingly

smaller sieves. By measuring the weight retained in each sieve, the cumulative percentage passing each sieve (or percentage finer) can be calculated. This can then be graphed against sieve size to obtain a grain size distribution.

The grain size distribution of the sample is related to the degree to which the unconsolidated sediment is sorted. An increase in standard deviation indicated a more poorly sorted sediment and less permeable sample. The degree of sorting of a sediment can be represented by the ratio of the grain size that is 60% finer by weight to the grain size that is 10% finer by weight. This is termed the uniformity coefficient (Cu).

$Cu=d60/d10$

If the uniformity coefficient is less than 4 the sediment is thought to be well sorted and if the coefficient is greater than 6 it is poorly sorted and hence will have a lower permeability. The Hazen Method (Hazen, 1911) can be applied to the grain size distribution curve of a sample to estimate the hydraulic conductivity of the sediment. If the grain size of the sample that is 10% finer by weight is between 0.1 and 3.0 mm.

$K=C(d10)^2$

K = hydraulic conductivity (cm/s)

d10 = grain size that is 10% finer (cm)

C coefficient based on sorting see Appendix 4

## 4.4 Refined site selection and River Bed Mapping

The refining of the initial 600m study area down to 150m stretch of river was based on river bed gradients identified from the initial site survey, river bed sediment inspection and river water flow rates. The refined site was to contain two contrasting hydraulic environments in which contrasting hyporheic zone thicknesses may be seen. (Figure 4.4.1) shows the contrasting flow environments at profiles 8 and 11. To meet the aims of the fieldwork, profiles 8 and 11 (Figure 4.2.1) were selected for a more in depth survey based on two factors.

1. Profile 8 has a steep river bed gradient over which river water flows rapidly and has a relatively low depth of water. Sediment type has a higher gravel content and in general, higher hydraulic conductivity values
2. Profile 11 has a shallow river bed gradient and slow moving deep water. The hydraulic conductivity of the bed sediments was on average lower than those at profile 8 and the river bed sediments contained less gravel and a more silt.

Figure 4.4.1, Contrasting flow environments at profiles 8 and 11.

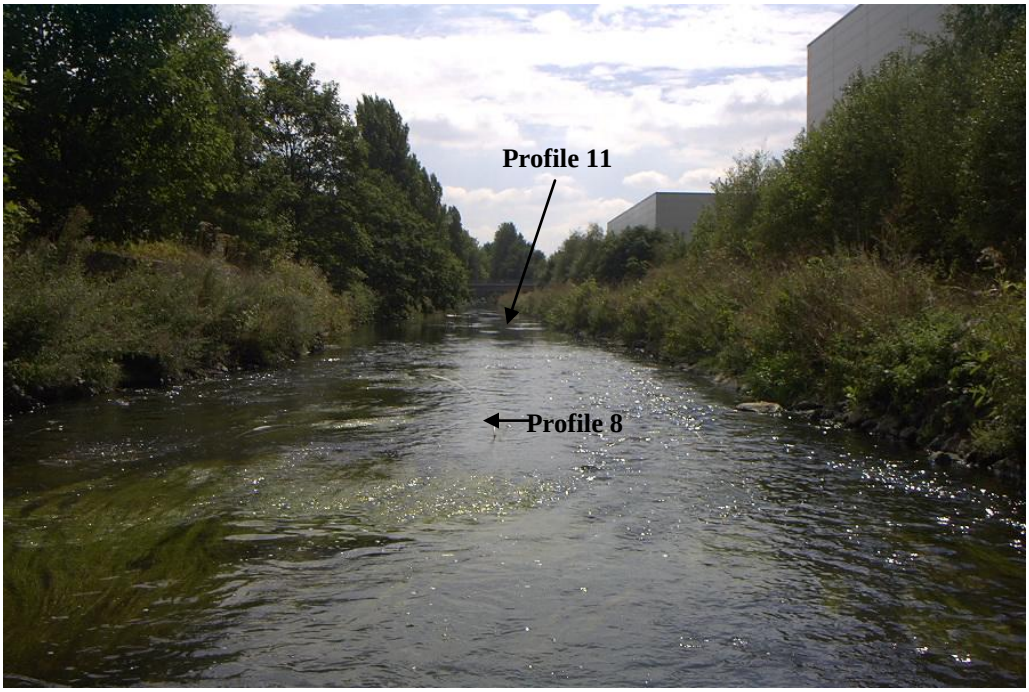


Once the refined sites had been selected, a river bed mapping exercise was carried out in which sediments types were mapped out in grid format for a distance of 6-13m upstream and downstream of the selected cross-channel profile location. This survey was carried out at both profiles 8 and 11. The survey involved a light excavation of the river bed sediments with a shovel followed by a description of colour, sediment type, percentage of different sediment type present and the grain shape and size. Care had to be taken so that sediment bed forms would not be interrupted beyond reason. The sediment was then assigned a number and was mapped on a pre-constructed grid. This process was repeated in 1m intervals across the river and in 2m intervals upstream. On completion of the grid, numbers were joined up in a conceptually feasible manned in order to get a general overview of the river bed in that location. At profile 11 sediment samples were then retrieved from each of the distinguishable units for sieve analysis.

## 4.5 Mini Drive Point Piezometer Construction and Installation

To identify the hydraulic gradients between the shallow aquifer and the river, mini drive point piezometers (MDP's) were constructed and installed at selected profiles in the study section. The MDP's were constructed using high density polyethylene tubing (HDPE), stainless steel bolts, washers, wire and 100 micron nylon mesh. The HDPE tubing which has an internal diameter of 10mm and ED of 13mm was first cut to the required length and a stainless steel bolt with 3 washers attached was screwed into one of the open ends. The area immediately above the bolt was then drilled with a 4mm drill bit to cover a length of 10cm of tubing. Drill holes were placed 1 cm apart longitudinally and 4 holes were drilled around the tube for each 1cm mark. The drilled section of the tube was then wrapped in 1 layer of the 100 micron nylon mesh and secured by stainless steel wire. The 100 micron nylon mesh acts as a screen to prevent clogging of the open section and the use of stainless steel wire, bolts and washers ensured no metals were introduced during sample extraction, (Figure 4.5.1). The installation of the piezometers required a hollow 2m steel pole and a fence driver! The piezometers were placed within the pole to the extent that the washers and bolt head were only protruding. As the radius of the washer was larger than that of the inner pole, the piezometer would not slip during installation via the post driver. Once the steel pole had been driver to the required depth, it was retreated using grasping stillages. With the driving pole remover the sediment around the piezometer were allowed to collapse naturally leaving the piezometers firmly in place. The HDPE tube was then sealed with a rubber cork to prevent algae growth within the tube and contamination of the shallow aquifer.

Figure 4.5.1, MDP base-section construction

A total of 25 MDP's were installed between profile 7 and profile 13. Profile 12 had previous installed piezometers from (Ellis, 2003), however due to possible clogging and old age, head measurements were not possible. Due to slight inaccuracies in the installation methodologies all piezometers were installed to slightly different depths, however three main installation depths were generally accomplished.

- 7 piezometers installed to a depth of 0.3m
- 6 piezometers installed to a depth of 0.5m
- 12 piezometers installed to a depth of 0.6-0.8m

(Figure 4.5.2) illustrates the location of installed MDP piezometers and the depths to which they were driven.

Figure 4.5.2, Location of Installed and depths of MDP's and multi-level samplers

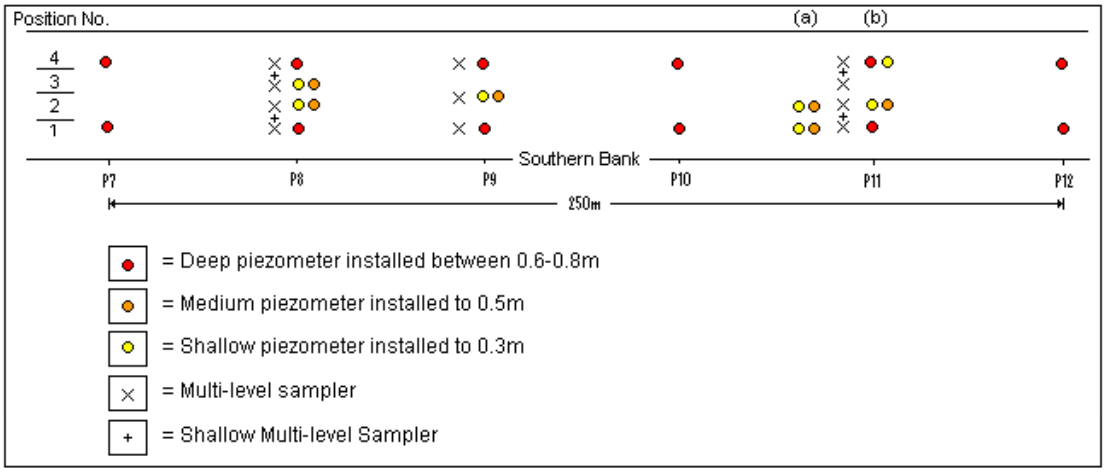


## 4.6 Multi-level Piezometer construction and installation

For the purpose of chemical sampling at different horizons below the river bed, multi-level piezometers were constructed and installed at three profile locations of the study area. Initially 8 multi-level piezometers were constructed and 4 installed at both profile 8 and 11. At a later stage 3 more multi-levels were installed at profile 9 to further characterise the chemical gradients beneath the river bed between the two existing sites, however due to installation into low permeability strata, very few samples could be retrieved. All piezometers installed at this time sampled at 10cm intervals between the surface of the river bed and to depths of approximately 60cm below the river bed.

After 2 rounds of chemical analysis which revealed a likely upper boundary of the hyporheic mixing zone between 0-0.2m below the river bed, it was decided that a more refined sampling instrument in the top 0.25m of the river bed would prove advantageous in hyporheic delineation. Hence, a further 4 multi-levels were constructed, each with 5 sampling points at 5cm intervals.

As well as allowing for the precise location of the upper boundary to be located, it allowed for a more detailed hyporheic concentration gradient to be assessed crossing the likely hyporheic-surface water interface.

The construction of multi-levels piezometers required the use of stainless steel rods, 3 mm external diameter (HDPE) tubing, 100 micron nylon mesh, stainless steel wire, stainless steel nuts and washers, brass screws and string. The stainless steel rods were initially cut to the required length and both ends were filed down for safety and for ease of tapping one end. By tapping one end of the steel rod a nut could be attached and by smoothing the end of the rod over which the nut had just been placed with hammer blows, the nut could not be removed. 3 stainless steel washers were then put on the open section of the rod and allowed to slide down until they were held securely in place by the nut. The rod was then marked in 10cm intervals from the open end to the base and 3 grooves were cut into the steel closely above each 10cm marking.

The HDPE tubing was prepared by cutting each length 15cm shorter than the previous, the longest being 200cm in length and the shortest being 125cm. Because the separation distance on the rod was 10cm apart this allowed for easy identification of tube sample depth from the surface once installed. The longest tube above the river bed corresponding to the deepest sampling point, and the shortest representing the shallowest with a tube length difference of 5cm between each consecutive tube. One end of the cut tube was then wrapped in 100 micron nylon mesh and secured using stainless steel wire, (Figure 4.6.1). This was repeated for each tube. To attach the tubes to the stainless steel rod, stainless steel wire was wrapped around the Teflon tubing and wound into the cut grooves on the steel rod. This prevented the tube from slipping while installing.

Once the (HDPE) tubes were attached to the steel rod, brass screws were inserted in the open section and of the tubes to prevent algae growth and cross contamination of sample horizons. (Figure 4.6.2) shows the completed design of a multi-level sampler.

Figure 4.6.1, HDPE tubing wrapped in 100 micron nylon mesh and secured with stainless steel wire

Figure 4.6.2, Completed design of multi-level piezometer

To install the ML piezometers, a length of string was attached to the steel rod (Figure 4.6.2) and threaded through the top of the installation pole. By tensioning the string during installation, the multi-level piezometer was prevented from slipping out of the drive pole. This was a problem that was encountered during the first 3 attempts of multi-level installation hence installation technique was readjusted to that discussed above. Due to slight inaccuracies in installation methodologies installation depths varied slightly however sampling horizons were generally located 10cm apart between the river bed and 60cm below.

The same construction and installation process was repeated for the more refined ML piezometers, again with 5cm separation lengths between tubes and the longest tube corresponding to the deepest sampling point. However in this case, sample horizons were located 5cm apart between the river bed and 25cm below.

## 4.7 Head Measurements in MDP's

To measure the hydraulic head gradient between the shallow aquifer and the river, the MDP's were used. A narrow dip-meter was initially used in the piezometers, however repeat analysis revealed a large degree of error in head measurement for any one piezometer. This occurred piezometers in which water beads were present in the tube above the hydraulic head position causing a complete circuit in the dipmeter and a falsely registered head position. To overcome this problem, head values were manually measured with a measuring tape from the top of each piezometer to the visible head position in the tubing, (Figure 4.7.1). This was possible because of the relatively transparent nature of the HTPE tubing. However, it is believed that this method can only be used in relatively newly installed piezometers as attempts to measure head in

piezometers installed by (Ellis, 2003) proved somewhat difficult due to the growth of algae on the outside of the tube and general decay of the tube material.

To measure the head, the rubber bung was first removed and the head was allowed to stabilise for 10 minutes. Because the top elevation of each piezometer had been leveled in to MASL, the absolute head level for each piezometer could be calculated. The same procedure was followed for measurement of river level at each piezometer allowing for the calculation of river stage (from piezometer length above river bed) and hydraulic gradient using installation depths.

Figure 4.7.1, Visual inspection of HDPE MDP to locate aquifer head position.

## 4.8 Hydraulic Gradient Estimates

The calculation of hydraulic gradients between the river and the groundwater has been carried out to:

1. Identify the direction of water movement below the river bed (Gaining or Loosing).
2. Use calculated gradients to estimate temporally varying groundwater discharges to the river.

Gradients (i) were calculated as follows:

$$i = \frac{h_2 - h_1}{L}$$

i = hydraulic gradient

$h_1$ = river stage

$h_2$ = water level in piezometer

L = Depth of open section of piezometer in river bed

In most cases it was found that the aquifer was discharging to the river, the rate at which this was occurring was calculated using the 1-dimensional Darcian flow equation

q = ki

q = specific discharge ($md^{-1}$)

k = hydraulic conductivity of river bed material ($md^{-1}$)

i = hydraulic gradient

A schematic representation of the variables is presented in (Figure 4.8.2)

Figure 4.8.2, Gaining river with measured variables

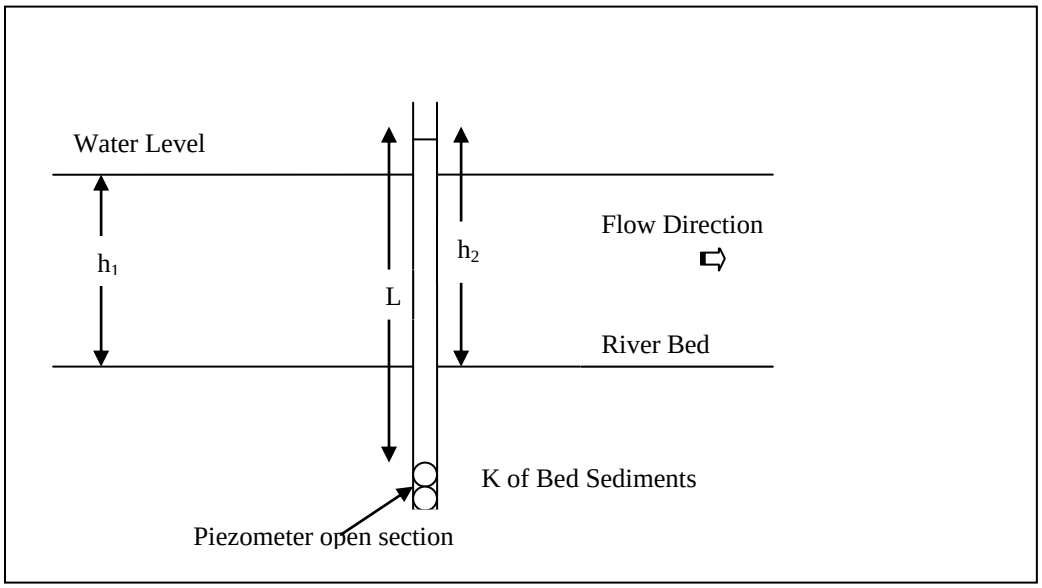


The discharge per unit length of channel can be calculated by multiplying the specific discharge by the width of river bed for which it is believed to be representable. In a typical river cross-section in which two MDP's have been installed, the specific discharge calculated from the MDP closest to the southern bank would be multiplied by the width of river bed between the southern bank and half way between the southern most MDP and the northern most MDP. The same calculation is applied to the MDP closest to the northern bank. The sum of these two products will give an estimate of discharge across the river for 1m length of river. This value can then be multiplied by the longitudinal length to which the value is believed to be applicable. It must be assumed that the river width is constant for such a calculation to be carried out.

## 4.9 Hydraulic Conductivity Estimations (Slug Tests)

Falling head tests were carried out on all MDP's to obtain an estimate of hydraulic conductivity values of the river bed sediments across 3 broad depth horizons. These values could then be used in Darcian flow calculations.

Tests were carried out using a pressure transducer and data logging device which was set to record an output voltage every second. The pressure transducer was connected to a plastic tube with an outer diameter of 0.6cm. This allowed it to be inserted into the piezometer and extended to the base. The head in the piezometer was then aloud to re-equilibrate before a slug of water was added to the piezometer which extended to the top. The transducer tube was held in the same position and the head in the piezometer was aloud to drop to its original value. This was usually between 1mm and 13mm above the stage of the river. Once falling head tests were carried out on the required number of piezometers, the data logger was stopped using "Green Line Software" and voltage and time values downloaded, (Figure 4.9.1).

Figure 4.9.1, Insertion of 0.6cm tube into MDP for falling head test

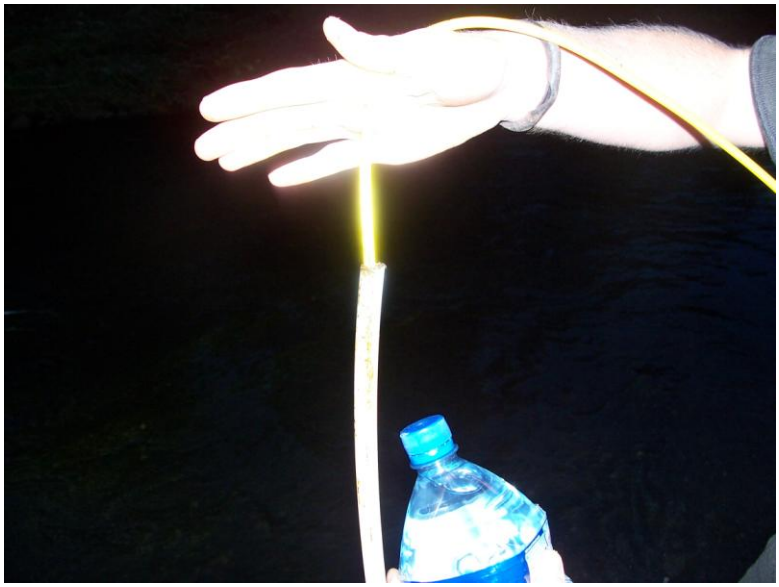

A graph of voltage verses time is automatically produced which can be converted into (xls.) format for further modification.

To convert transducer voltage measurements to equivalent depths, an initial calibration of the transducer was carried out. This involved submersing the transducer tube in a known depth of water for 30 seconds and averaging the voltage readings (taken every second) to get a single voltage value corresponding to a particular depth of water. After 30 seconds the transducer tube was lowered to another known depth and again, left for 30 seconds and voltage values averaged. This process was carried out between 0.05m and 1.50m of water in steps of 0.05m, resulting in a total of 30 averaged voltage measurements being made. Once representative voltage values for each depth have been obtained by averaging all the voltage readings for each depth, a graph of voltage verses depth (depth on the y axis) (Appendix 5) will produce a straight line of the form:

$y = mx + c$, where

y = Depth (m)
m = Slope of line
x = Voltage
c = constant

Hence for any known voltage, a corresponding depth can be calculated. Once all data has been converted to equivalent depths, the data of interest was isolated (for a particular falling head test), the water level before the slug of water was added is then subtracted from each value of the test to get the additional head of water during the test. A graph of H/Ho verses time is then produced with H/Ho on a logarithmic scale and an exponential trend line is fitted to the data. The value H/Ho refers to the ratio of the head at any particular time to the head at the start of the test. From the trend line an exponential equation is produced of the form:

$y = ae^{-bx}$

The values of hydraulic conductivity can then be estimated using a variant of the Hvorslev method. Ellis (2003)

$$K = \frac{r^2 Ln(Le/R)}{2LeT_o}$$

K = hydraulic conductivity cm $s^{-1}$

r = radius of well casing (0.5 cm)

R= radius of well screen (0.65 cm)

Le =length of well screen (10 cm)

$T_0$ =Time for water level to fall to 37% of the initial level

Where $T_0$ can be calculated from the equation of the exponential trend line of the falling head test as follows:

$$T_0 = \frac{(Log(0.37/a))}{-b}$$

Values of Hydraulic Conductivity calculated varied significantly across the study area reflecting the large degree of heterogeneity of the fluvial sediments.

## 4.10 Core Sampling

Core samples were taken from profile 11 to assess the variation of river bed sediment type with depth. The method of retrieval required the use of a solid steel core pipe into which a narrower diameter plastic tubing could be placed and a metal cap which could be placed at one end of the tube and struck with a sledge hammer, thus preventing damage to the core installer. The plastic tubing first had to be cut down to an appropriate size as to fit inside the coring pipe. The steel

cap was then placed on top, and the coring pipe was driven into the river bed at the required location. Once driven to the required depth, the coring pipe was remover and the internal plastic tubing withdrawn. The plastic tube was then sealed at both ends and labeled for way-up position identification.

Attempts were also carried out at profile 8 to retrieve sediment cores however, due to the highly unconsolidated nature of the bed sediment material (high gravel percentage), sediments could not be abstracted effectively and attempts were abandoned. In total two cores were retrieved, both from profile 11.

## 4.11 Geochemical Sampling

Sampling multi-level piezometers required the use of scaffolding as a work bench, a peristaltic pump, a car battery, multiple tube connectors and fittings, flow through cells, dissolved oxygen, Ph, redox, temperature and conductivity probes, and 30ml sample vials. The variables measurable on site were carried out in the field due to their unstable nature and so that instant feed back could be received on the fluxes which were being encountered.

At any one multi-level installation, each of the sampling tubes were connected to the inlet of the peristaltic pump in turn. The sample would pass through the pump without making contact with and mechanical parts and then through to the flow-through cells. Dissolved oxygen, pH, redox, temperature and conductivity were measured in the cells and the sample could then be collected at the outlet of the last flow-through cell. Generally, 4 flow-through cells were used for the samples taken from sample horizons that were 10cm apart and 1 or 2 cells used for those that were 5cm apart. Once samples had been retrieved from any individual tube, the brass screw was reinserted to prevent cross contamination. The plastic bottles containing the samples were

immediately transferred to a cool-box containing ice packs and placed in a refrigerator at 4$^{o}$C upon returning from the field. This helped maintain stability of the more reactive determinands for which analysis was to be carried out.

Figure 4.11.1 (a), (b), (c) and (d), Geochemical sampling using peristaltic pump and flow through cells.

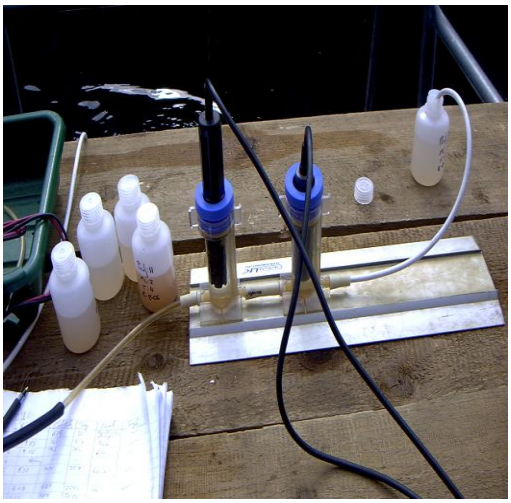

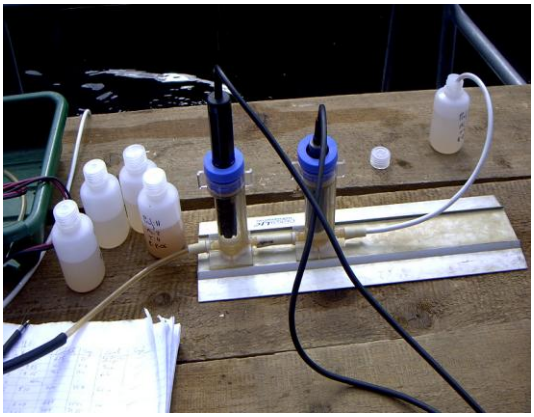

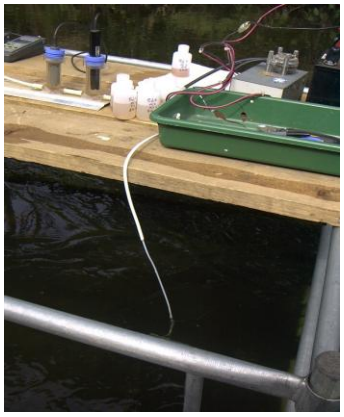

## 4.12 Sampling Time Series

A time series of sampling has been carried out at both profile 11 and profile 8, both at depths of 0.4m below the river bed. This time series was carried out to assess the sensitivity of the prolonged pumping and increasing sample volume extracted on the quality of sample analysis and its variation over time.

The time series analysis has been carried out by pumping a particular horizon continuously for 1 hour and collecting individual samples and pre-conceived time intervals. While samples were not being taken, the volume of water extracted was collected in a separate container. This container was then marked in such a way that the volume of water extracted between each sample could be identified. Samples were retrieved at the following time intervals:

0 minutes since start of pumping – Sample 1
2 minutes since start of pumping – Sample 2
6 minutes since start of pumping – Sample 3
10 minutes since start of pumping – Sample 4
14 minutes since start of pumping – Sample 5
22 minutes since start of pumping – Sample 6
30 minutes since start of pumping – Sample 7
40 minutes since start of pumping – Sample 8
60 minutes since start of pumping – Sample 9

Prior to the time series being carried out, all horizons for that multi-level were sampled to construct a concentration gradient below the river bed for that time. Hence, a total of 15 samples were retrieved for each time series with each sample was analysed for D.O., conductivity, temperature, chloride, nitrate, fluorescence, and one of the time series sample sets was also analysed for sulphate. This allowed for the sensitivity of each analytical component to increased volume extracted to be assessed.

## 4.13 Geochemical Analysis

The use of chemical probes for the analysis of D.O., conductivity, temperature, pH and redox allowed for a rapid feedback of environmental chemical conditions to be obtained. A Hanna D.O. probe was used in conjunction with a flow-through cell to measure the D.O. concentration below the river bed. The probe had to be calibrated prior to measurements being made at the start of every day. This involved topping up the probe with membrane solution and calibrating the probe to a preset atmospheric oxygen concentration. Measurements of D.O. were taken in parts per million (ppm).

The conductivity meter was calibrated by selecting a particular conductivity value in mμ on the probe and then inserting it into a pre made solution made of common salt and water to an exact concentration. Three solutions were used for calibration all which had different conductivity values.

Similar methods were followed for calibration of the pH meter with 2 different solutions of known pH value were used, however due to probe calibration problems, Ph readings had to be disregarded. The redox and temperature probes did not require calibration.

### 4.13.1 Major Ions

The analysis of major ions was carried out using an optical photometry technique which involver the use of a Palintest Photometer 5000, (Figure 4.13.1.1). The technique is based on a reagent being added to a portion of the sample and allowed to react with the determinand being analysed for. This forms a cloudy or colored solution, the degree of ‘cloudiness’ is proportional to the concentration of the determinand. Light is passed through a sample containing no reagent initially to represent 100% clarity. On that setting, light is then passed through the cloudy or

colored reacted sample and the drop in optical intensity passing through the sample is recorded. This value can then be used to identify determinant concentration from pre-calibrated tables. Repeat analyses have been carried out on the same sample for all determinands being analysed for.

Figure 4.13.1.1, Major ion analysis using a Palintest Photometer 5000, and the cloudy chloride solution.

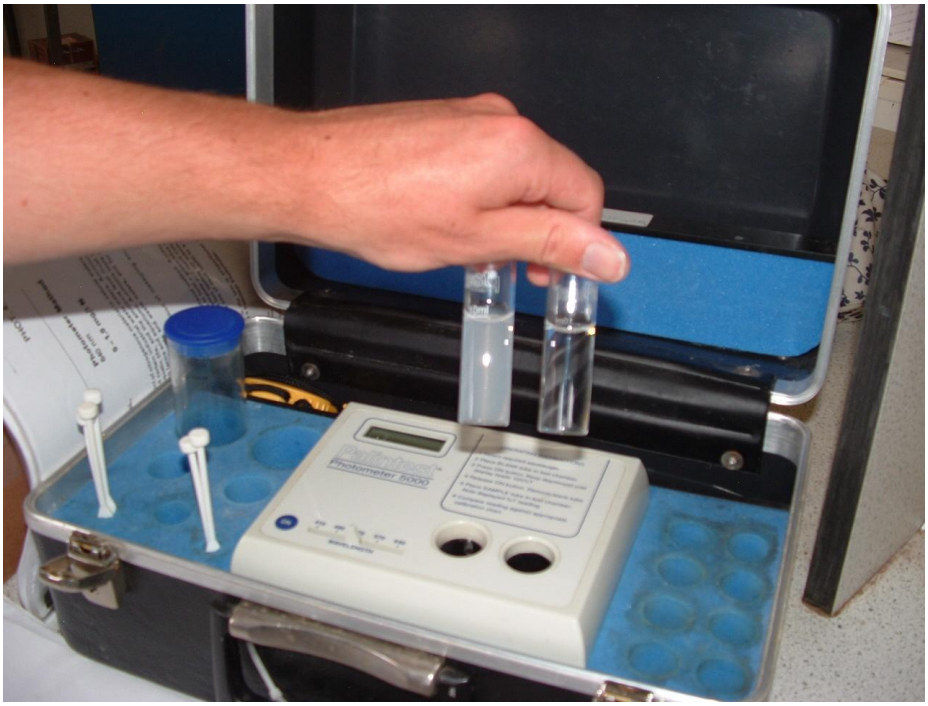


## 4.14 Fluorescence Analysis

The fluorescent properties of collected samples were analysed using the Perkin-Elmer LS-50B luminescence spectrometer, (Figure 4.14.1). The Rayman intensity (excitation 348nm, emission ~396 nm, 5 nm slit width) of distilled water in a sealed water cell was used as standard, which allowed testing of machine stability. Samples were subjected to a range of excitation wavelengths between 200-400nm and the intensity of emitted radiation and wavelength of

emitted radiation as well as excitation radiation was recorded. The data could be output in graphical and excel format for analysis.

Figure 4.14.1, Perkin-Elmer LS-50B luminescence spectrometer

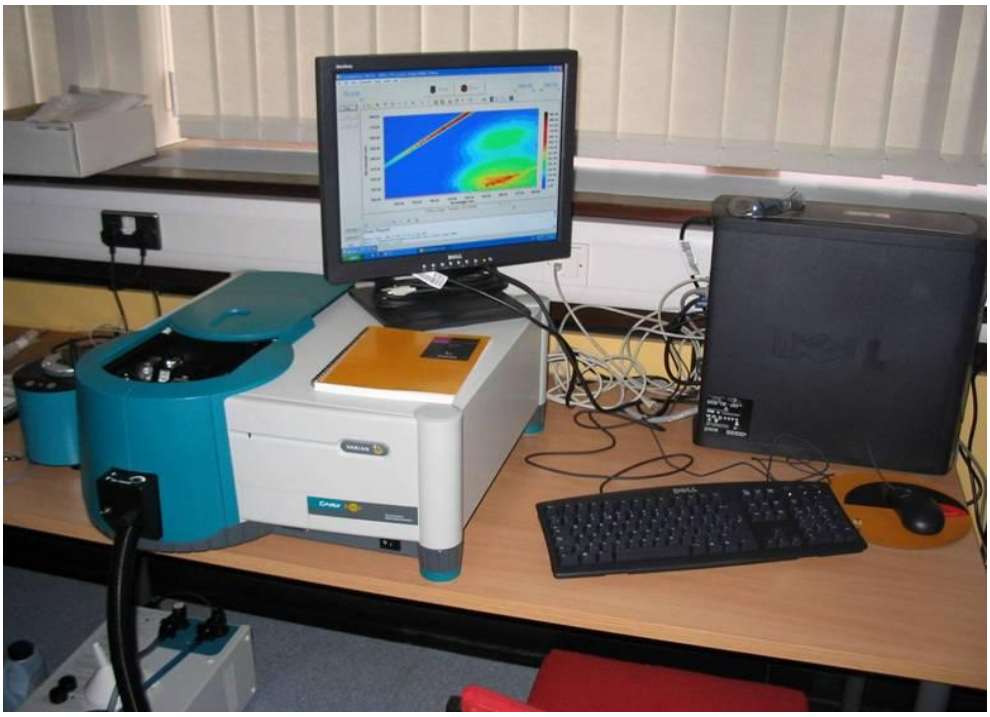

# Chapter 5 River and River Bed Sediment Characterisation

The following chapter presents the initial physical findings along the study reach. The physical characteristics of the river channel and river bed are first presented followed by hydraulic conductivity distribution within the bed sediments

## 5.1 Site Leveling and Sediment survey

The objective of the leveling survey carried out was to characterise the river channel of the initial full study section in terms of river width, bank elevation, river bed shape and gradient between profiles. The data gathered could then be used to identify the more suitable river gradients sites in which the refined site could be located. In all 12 profiles surveyed, one of the steeper river bed gradients was observed between profile 8 and 9. Table 5.1 illustrates the observations made at each profile along the original river stretch and the river bed gradient between consecutive profiles. The latter is represented graphically in (Figure 5.1) where it can be seen that between profile 8 and 11, the river bed is dropping in elevation and the steepest sub-section is between profile 8 and 9. The river stage varies dramatically over the whole section, however it must be noted that at some profiles (markedly 1, 2 and 7) the river has been artificially deepened due to effluent pipe inlets and infrastructural stability works.

Table 5.1, Physical characteristics or a 550m stretch of river channel and gradients between consecutive profiles.

| Profile No. | River Width (m) | Average Elevation (maod) | Maximum River Stage (m) | Gradient between this and next profile down stream. |
|---|---|---|---|---|
| 1 | 8.1 | 90.921 | 1.25 | 0.003085455 |
| 2 | 7.6 | 90.76672727 | 1.3 | -0.003777955 |
| 3 | 8.93 | 90.955625 | 0.618 | 0.00179625 |
| 4 | 8.4 | 90.8658125 | 0.68 | 0.002122917 |
| 5 | 10.03 | 90.75966667 | 0.67 | -0.002777778 |
| 6 | 11 | 90.89855556 | 0.49 | 0.001589293 |
| 7 | 8.55 | 90.81909091 | 0.93 | 0.001275818 |
| 8 | 10.1 | 90.7553 | 0.38 | 0.002553273 |
| 9 | 11.2 | 90.62763636 | 0.4 | 0.001557172 |
| 10 | 9.4 | 90.54977778 | 0.56 | 0.001690101 |
| 11 | 11 | 90.46527273 | 0.48 | 0.001153788 |
| 12 | 10.1 | 90.40758333 | 0.67 | |

Figure 5.1, Graphical representation of river bed elevation along the study section.

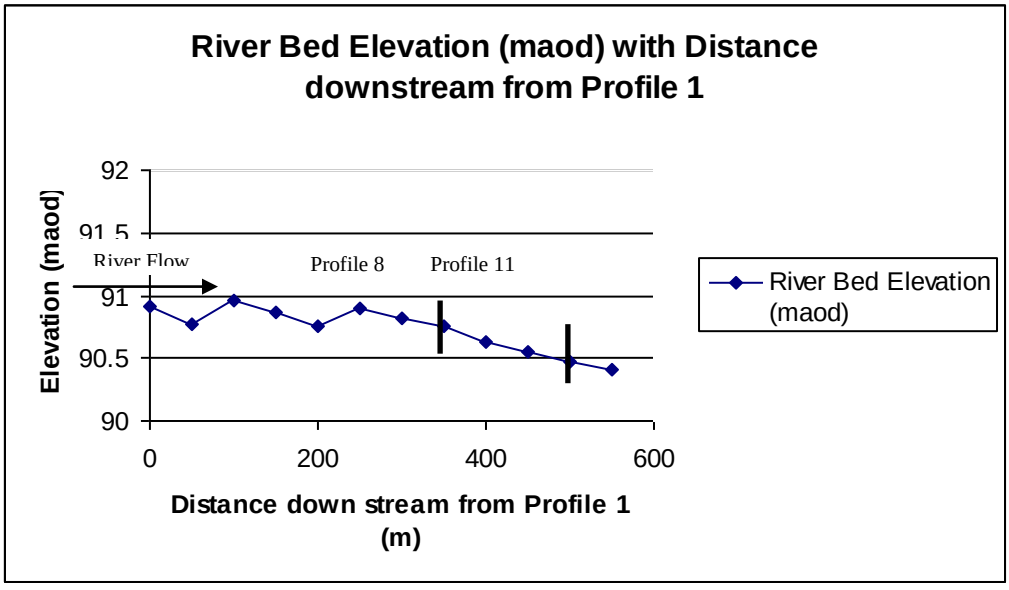

### 5.1.1 River Bed Sediment Survey

The initial sediment survey in which samples were retrieved from each profile revealed a wide variety of alluvial deposits in the top 0.4m of the river channel. Two samples were retrieved from each profile on which sieve analysis was carried out. However, due to samples not being representative of particular sediment horizons, a more general bulk sample was retrieved in most cases, hence grain-size distribution curves proved un-representable. More representable sediment samples were retrieved on a later date at selected profiles. The initial sediment survey, proved beneficial however in that it allowed for an overall assessment of sediment type throughout the initial longer site.

It was generally found that the upper reaches of the study area (Profile 1-7) consisted of mixtures of various proportions of sand, gravel and cobbles. Typical proportions can be seen in (Figure 5.1.1.1) in which a selection on samples are graphically represented in terms of sediment proportions and are representative of the inclusive sections. Profile 7 is located at the major bend in the study reach and consists mainly of fill material such as large boulders >0.2m.

Figure 5.1.1.1, Sediment proportions at profiles 1, 3, 5 and 6 in the upper western section of the study reach.

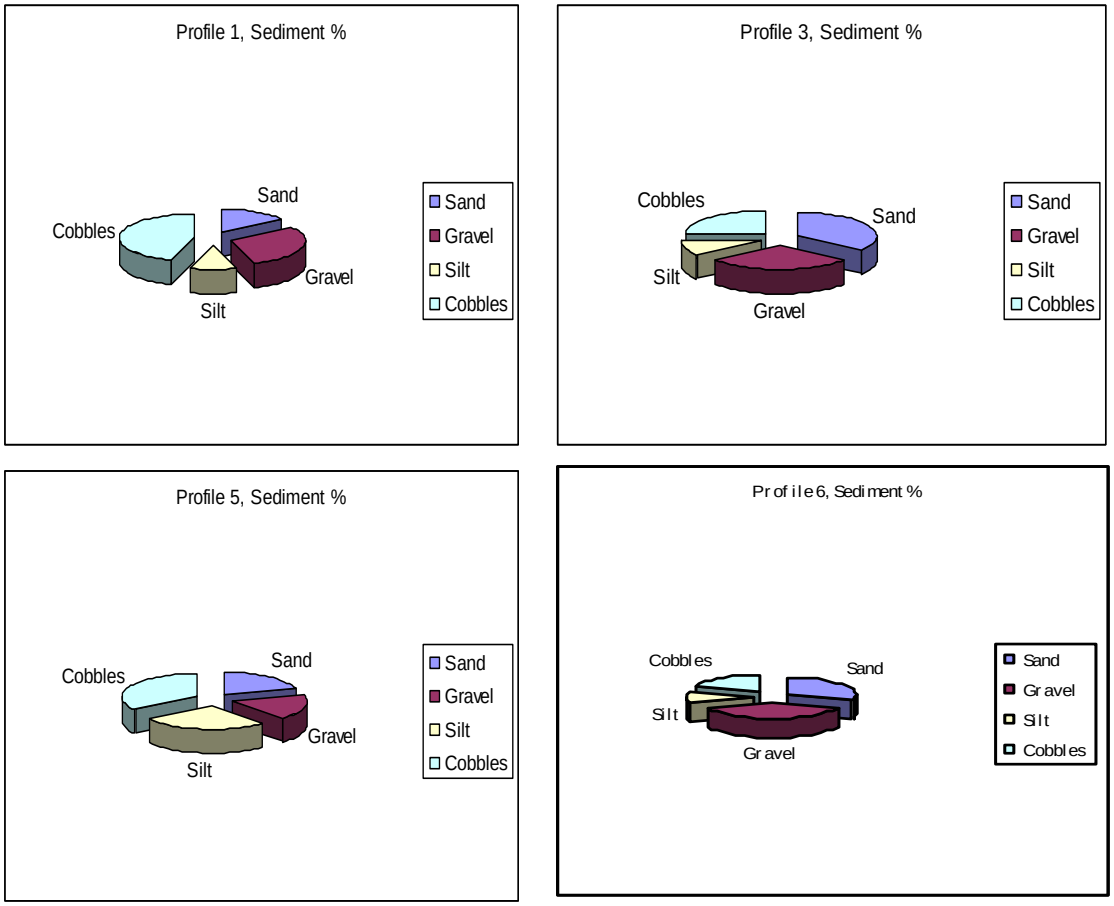


Sediment samples taken from profile 8 consisted of very high percentages of gravel and very little sand and cobbles. The surface was not armored and the river flow rate was relatively rapid. In contrast profiles 9-12 consisted of a much lower gravel content and higher silt and sand contents, (Figure 5.1.1.2).

Figure 5.1.1.2, Sediment proportions at profiles 8-11 in the lower eastern section of the study reach.

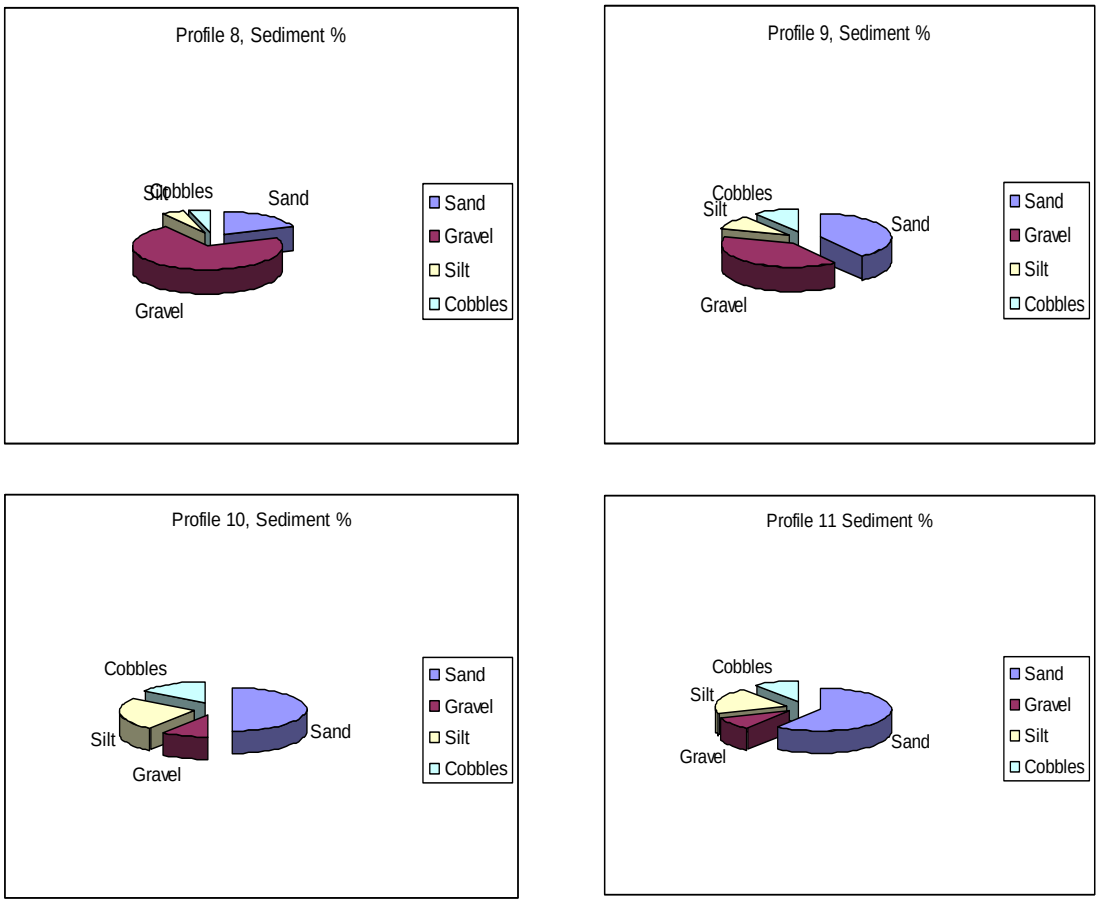


It can be seen that gravel percentage decreases steadily from profile 8 to 11, while sand content increases steadily in the same order. Generally there is a lightly armored surface which accounts for 10% of sediment type in the top 0.4m of the river bed. This is not the case at profile 8 which is comprised almost completely of gravel.

Because of the contrasting physical conditions observed between profile 8 and 11, it was decided to refine further physical investigations and all chemical sampling to this region of the study area. Sediment type, river bed gradient and river water velocities create distinctive environments

for a surface water groundwater mixing zone to form, and it is believed that the greatest contrast in hyporheic zone depth would be seen between these two profiles.

## 5.2 Refined Study Area Sediment Mapping

To generate a more detailed perception of the river bed sediments in the immediate vicinity of the profiles of interest, a detailed sediment mapping survey has been carried out to a distance of 13m up and downstream of profile 11 and 6m up and downstream of profile 8, (Figure 5.2.1 and 5.2.3).

Figure 5.2.1, River bed sediments 13m up and downstream of profile 11

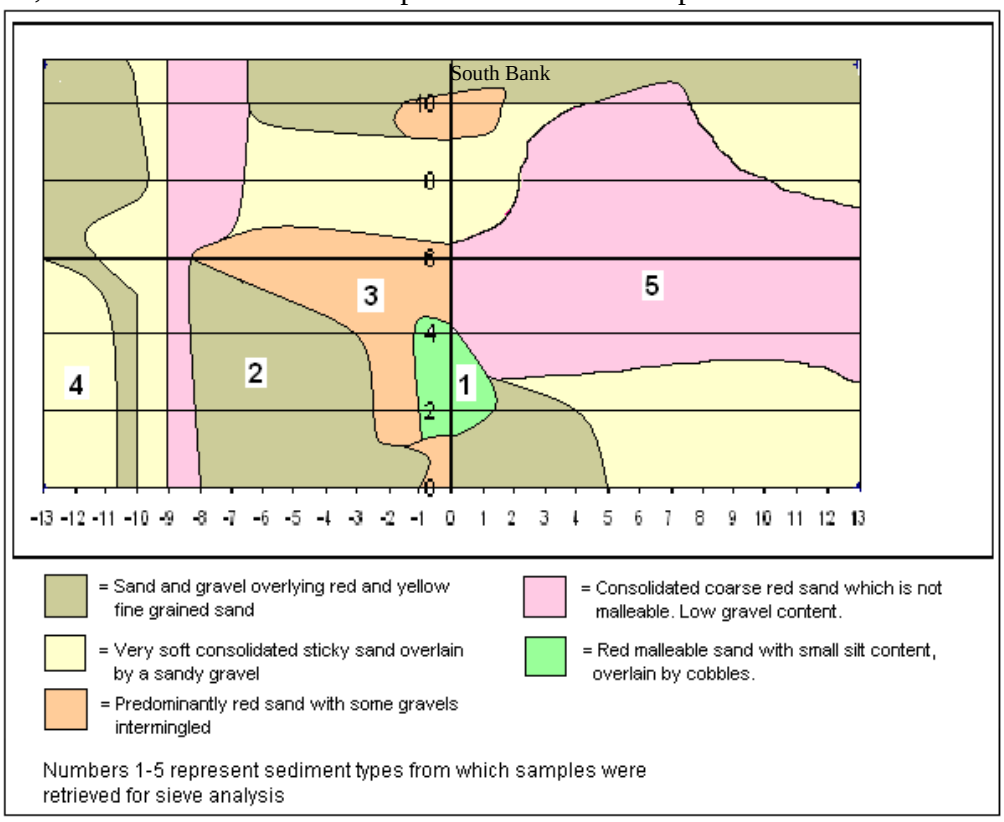


Sand is the predominant alluvial sediment within close proximity of profile 11. Different colorations can be seen at different locations of the mapped sediments which possibly reflects the

degree to which the sediment is being oxidised and highlights the likely heterogeneity of hydraulic conductivity within the bed sediments, (Figure 5.2.2). Some bed sediments permit surface water to penetrate the river bed faster than others, hence it is possible that the coloration contrasts are due to the varied degree of oxidation which can be seen spatially. Sand types varied in texture based on the amount to silt which they contained. Sands which contained silt had a more malleable property, and are more likely to have lower hydraulic conductivity values. The other most commonly encountered sand was consolidated red sand. This was fine grained and brittle when compressed. This sediment appeared to be well sorted and compact. The other sediments encountered consisted of mixed sands and gravels, the percentage of each is likely to affect their hydraulic properties. No obvious patter of river bed sediment type has been identified in relation to river hydraulics. This is likely explained by the relatively slow surface water velocity above the river bed. Grain size analysis has been carried out on the 5 sediment distinguishable sediment types shown in (Figure 5.2.1). Estimated hydraulic conductivity values are presented in Table 5.2.1

Figure 5.2.2, Typical sand river bed sample showing different colorations retrieved from profile 11.

Table 5.2.1, Grain size analysis results of sediment types close to profile 11

| Sample Number | D60/D10 (Cu) | K (m/d) |
|---|---|---|
| 1 | 2.484 | 16.46 |
| 2 | 2.125 | 24.19 |
| 3 | 1.910 | 47.41 |
| 4 | 2.153 | 22.99 |
| 5 | 2.194 | 21.83 |

As the uniformity coefficients (Cu) of all sediments are <4, all sediments are believed to be well sorted. Hydraulic conductivity values (K) do give a wide range with the highest value of 47.19$md^{-1}$ for the predominantly red sands with some gravel. Hydraulic conductivity estimates from grain size analysis techniques are one order of magnitude higher than those estimated using the Hvorslev analysis of slug tests.

Profile 8, seen in (Figure 5.2.3) comprised a number of sediments all of which have a relatively high proportion of gravel, (Figure 5.2.4). Along the south bank, a fine gravel of 0.01-0.05m grain size was found in which the smallest sand % was found. The center of the river bed consisted of a variety of sediments all with a higher sand than that encountered on the southern bank and at certain locations, organic rich matter and silts were found. The northern bank sediments, over which river velocities were highest, consisted of a more armored surface of cobbles underlain by a mix of sands and gravels before pure brittle red sand was encountered at depths of 0.6m below the river bed. The spatial sequence of the river bed sediments would appear to owe its existence to the major bend in the river which occurs upstream at profile 7. Surface water velocities are highest along the northern bank and the river is eroding the river bed sediments and depositing them further down stream. The elevation of the river bed at the southern bank is higher than that at the northern bank. This is likely due to the depositional properties of the lower velocity surface water at this location. However the velocity is moving sufficiently rapidly to carry finer

sands down stream. The centre of the channel is embedded with weed and hence velocities are lowest. Sediment type reflects this in that it is fine grained with dark organic matter and silt.

Figure 5.2.3, River bed sediments 6m up and down stream of Profile 8

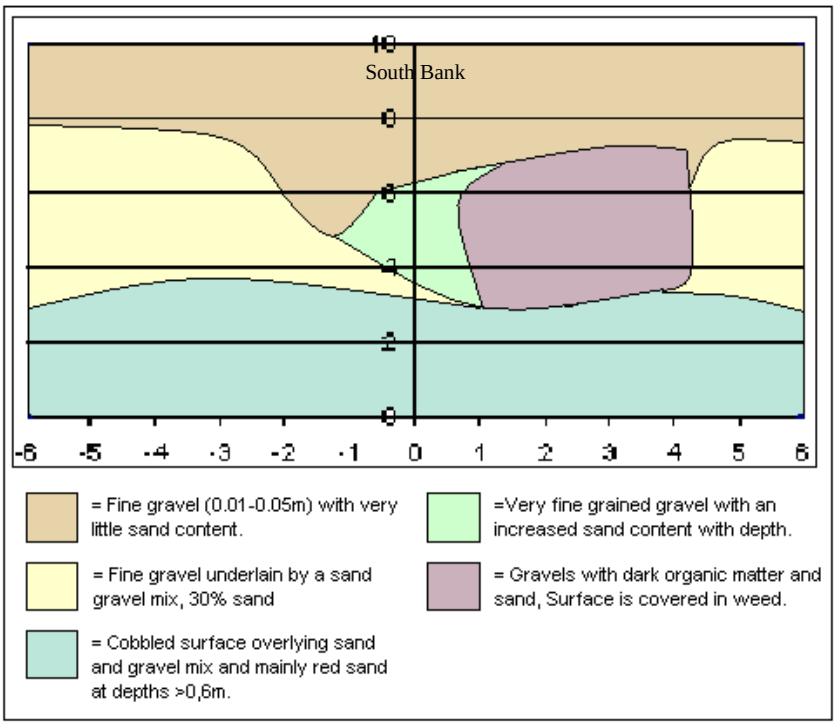


Figure 5.2.4 Sample retrieved from profile 8, 2m from southern bank

## 5.3 Sediment Cores

Two sediment cores were retrieved in the study section, both from profile 11, (Figure 5.3.1). As expected both cores consisted of a sand and gravel layer overlying red sands. Cores were not successfully retrieved from profile 8 and 10 which is likely due to the unconsolidated nature of the river bed sediments.

Figure 5.3.1, Core samples retrieved from Profile 11

Core Sample 4

Core Sample 5

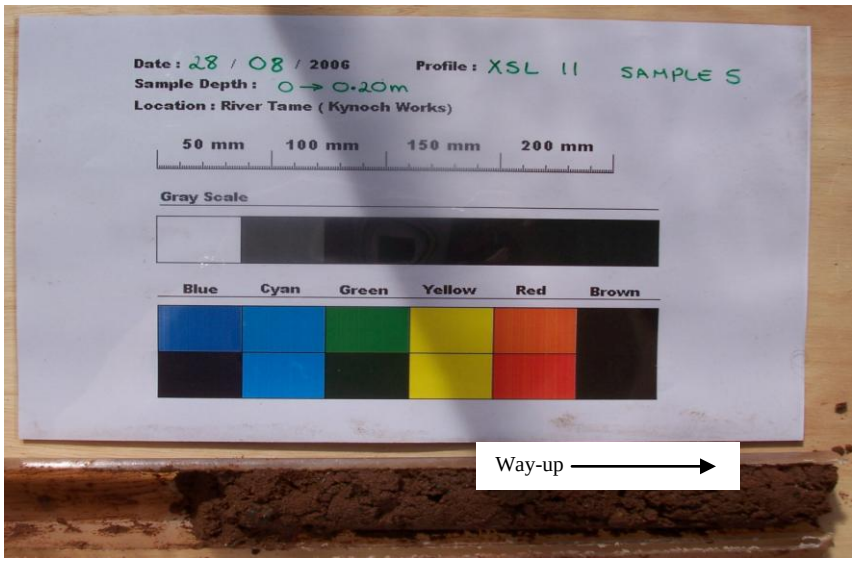


Core sample 4 was retrieved approximately 3 m from the southern bank, and sample 5 retrieved 3 m from the northern bank. Sample 4 extends to a depth of approximately 0.35 m below the river bed and consists entirely of red sand below 0.05m. The sediment is poorly consolidated and well sorted.

Core sample 5 represents sediments to a depth of 0.2 – 0.3 m below the river bed. The sample has a higher gravel content than that observed in core sample 4. Sediments are poorly sorted and poorly consolidated. Gravel composes approximately 20% of the core sample retrieved.

## 5.4 Hydraulic Properties of Bed Sediment

Hydraulic conductivity values were calculated at different depths at profiles between 7 and 11 inclusively, (Figure 5.4.1).

Figure 5.4.1, Positions and labeling strategy of MDP's and multi-level samplers along the study reach.

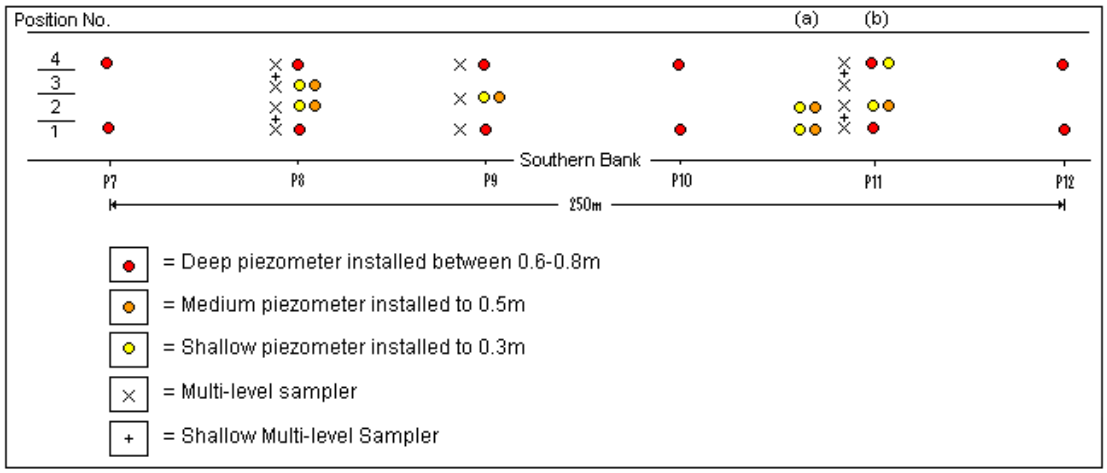


The sequence in which piezometers and multi-levels are referenced is as follows. First the profile number is listed, followed by installation type, piezometer (P), or multi-level (ML) and position number (1-4). Finally, in the case of MDP's, the depth to which it is installed will be noted as either, shallow, medium or deep, (Figure 5.4.1).

Prior to field measurements being made, the transducer was calibrated by plotting depth against average equivalent measured voltage. The following linear equation was obtained by fitting a trend line:

Depth of Water = 6.52404339 × Voltage – 2.88729653

During falling head tests, voltage readings were recorded every second. The results which were obtained using the Hvorslev method (Hvorslev 1951) are shown in Table 5.4.1 Profile 12 installed by (Ellis, 2003) was not suitable for falling head tests due to blockage by sand despite purge efforts. Two MDP's at profile 11 did not respond to a slug of water being added. This again is believed to be as a result of blockage by fine material.

Table 5.4.1, Hydraulic Conductivity values and installation depths of MDP's

| Piezometer Name | Exact Depth Of Installation (m) | Hydraulic Conductivity (m/d) |
|---|---|---|
| Profile 7 P1 Deep | 0.68 | 4.133 |
| Profile 7 P4 Deep | 0.35 | 0.851 |
| Profile 8 P1 Deep | 0.68 | 1.342 |
| Profile 8 P2 Shallow | 0.3 | 3.413 |
| Profile 8 P2 Medium | 0.5 | 1.36 |
| Profile 8 P3 Shallow | 0.3 | 2.012 |
| Profile 8 P3 Medium | 0.5 | 3.454 |
| Profile 9 P1 Deep | 0.299 | 3.262 |
| Profile 9 P3 Shallow | 0.3 | 7.861 |
| Profile 9 P3 Medium | 0.5 | 1.289 |
| Profile 9 P4 Deep | 0.545 | 1.047 |
| Profile 10 P1 Deep | 0.685 | 3.109 |
| Profile 10 P4 Deep | 0.51 | 2.089 |
| Profile 11 P1 Deep (b) | 0.655 | 1.32 |
| Profile 11 P1 Shallow (a) | 0.3 | 7.597 |
| Profile 11 P1 Medium (a) | 0.5 | 0.927 |
| Profile 11 P2 Shallow (a) | 0.3 | 9.129 |
| Profile 11 P2 Medium (a) | 0.5 | 0.332 |
| Profile 11 P2 Shallow (b) | 0.3 | non |
| Profile 11 P2 Medium (b) | 0.5 | 1.888 |
| Profile 11 P4 Deep (b) | 0.88 | 1.125 |
| Profile 11 P4 Shallow (b) | 0.4 | non |

## 5.5 Critique of Survey Method

The implementation of the river bed survey presented difficulties in that the retrieval of samples using a bucket and spade in high velocity waters disallowed for the full collection the finer material. Problems also arose with coarse upper river bed material falling back into river bed excavations in which it was hoped to retrieve samples at depths of up to 0.5m. However the rate at which this happened depended on the degree to which the sediments were consolidated, and representative samples were retrieved in most instances.

The retrieval of sediment cores proved difficult in some areas once again due to the unconsolidated nature of the river bad sediments at some locations, mainly at profile 8. This resulted in a complete lace of undisturbed sample retrieval from that profile.

## 5.6 Discussion

The sediment survey revealed contrasting river bed sediment types at profiles 8 and 11. The likely reason for contrasting sediment type is the velocity at which river water is passing over the sediments. Higher velocities at profile 8 tend to strip the river bed of the finer sand and silt material leaving a predominantly gravel sized river bed sediment type at profile 8. Further downstream, where river water velocities are slower, eroded sediment upstream is likely going to be deposited in the more stagnant water, leading to a more sand rich river bed. When slug test hydraulic conductivities are compared from piezometers which have been installed to depths of 0.5m at both profiles 8 and 11 (Table 5.6.1), the average K value at profile 8 at 0.5m below the river bed is 2.407 $md^{-1}$, while that at profile 11 is 1.049 $md^{-1}$.This data reinforces the claims made during the initial sediment visual survey that sediments at profile 8 are likely to have higher K values than those at profile 11.

Table 5.6.1, Comparison of hydraulic conductivity values from MDP's installed to 0.5m at profiles 8 and 11.

| | Profile 8 Hydraulic Conductivity m/d | Profile 11 Hydraulic Conductivity m/d |
|---|---|---|
| Depth (0.5m) | 1.36 | 0.927 |
| Depth (0.5m) | 3.454 | 0.332 |
| Depth (0.5m) | | 1.888 |
| Average Value | 2.407 | 1.049 |

Hydraulic conductivity values from sieve analysis and slug tests do not agree for profile 11. However, due to a higher degree of unreliability being associated with sieve analysis estimates, there values have been regarded as being less representative and thus slug test values are considered to be more accurate.

# Chapter 6 Hydraulic Conditions and Hyporheic Delineation

The temporal variation of hydraulic head in the aquifer and river can be seen to correlate with the depth to which chloride concentrations in the river penetrate the river bed. Multi-level sampling of chloride concentrations were taken on 4 occasions during the study. All sample rounds were carried out during times of contrasting rainfall occurrence and river flow rates. The temporal variation of chloride concentration with depth below the river bed is examined to establish how it is related to minor flood events and normal flow conditions.

## 6.1 River Flow, Rainfall and Aquifer Head

River Flow data obtained from Bescot flow station upstream of the study reach and Water Orton Flow Station downstream of the reach for dates between 1st June- 24th August have been obtained. The flow rates observed at the stations can be seen to fluctuate on two scales. On a diurnal scale a peak can be seen due to the discharge from sewage treatment works. This is a relatively small scale fluctuation that continued periodically throughout the field work stage of the project and is assumed not to affect surface water groundwater interactions significantly. The more significant peaks in the hydrographs (Appendix 6) are a cause of specific rainfall events (Appendix 7). The intensity and duration of rainfall events is directly related to the hydrograph patterns observed.

A typical minor rainfall event such as that which occurred on the 23rd July can be seen to impact the river flow rate for a duration of less than 1 day. However, more prolonged rainfall events can be seen to cause a smaller increase in flow rate in the river for a longer time period. Such an event has occurred on the 2nd August. The highest rainfall that occurred during the field work

period was 6.11mm in one day which occurred on the 23rd July. No significant rainfall fell in the 11 days prior to this relatively high event.

## 6.2 Temporal Variation in Aquifer Head

Temporal variations in aquifer head and river stage elevation correlate with rainfall data. (Figure 6.2.1 and 6.2.2) graphically represent the river stage and aquifer head fluctuation measured in two MDP's at profiles 8 and 11 respectfully.

Figure 6.2.1, Aquifer head and river stage elevation with time, Profile 8

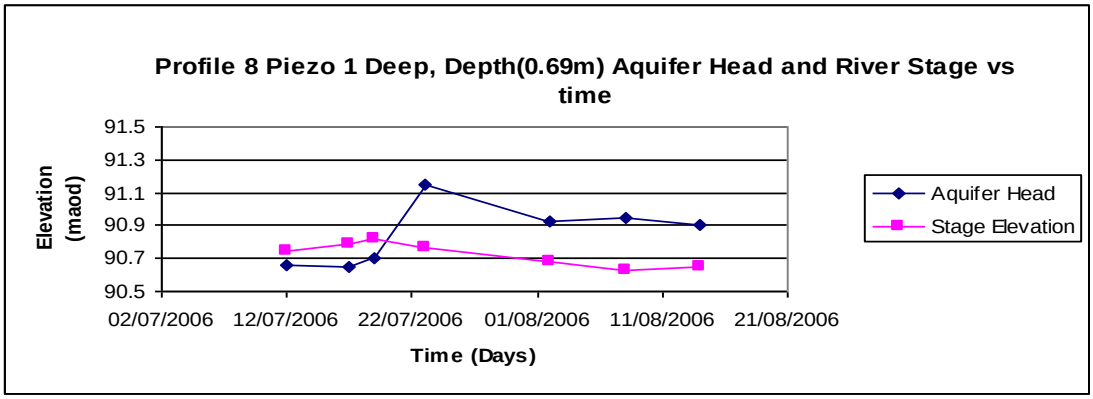


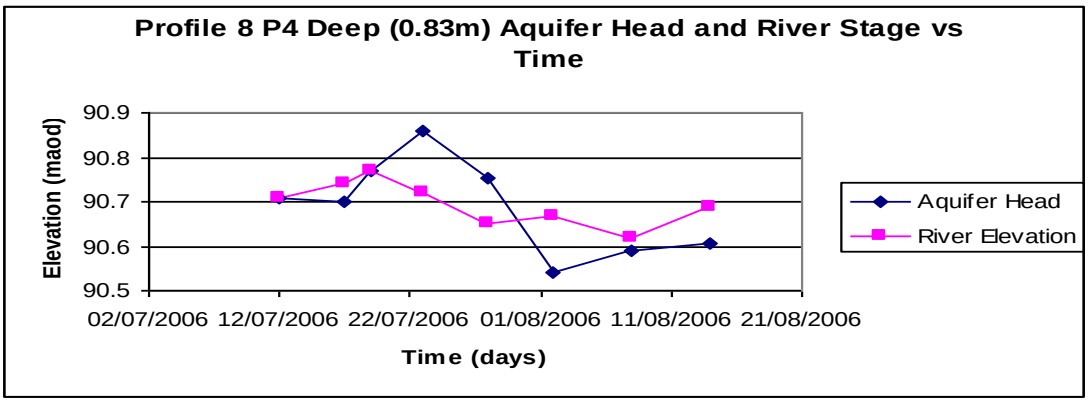

Figure 6.2.2, Aquifer head and river stage elevation with time, Profile 11

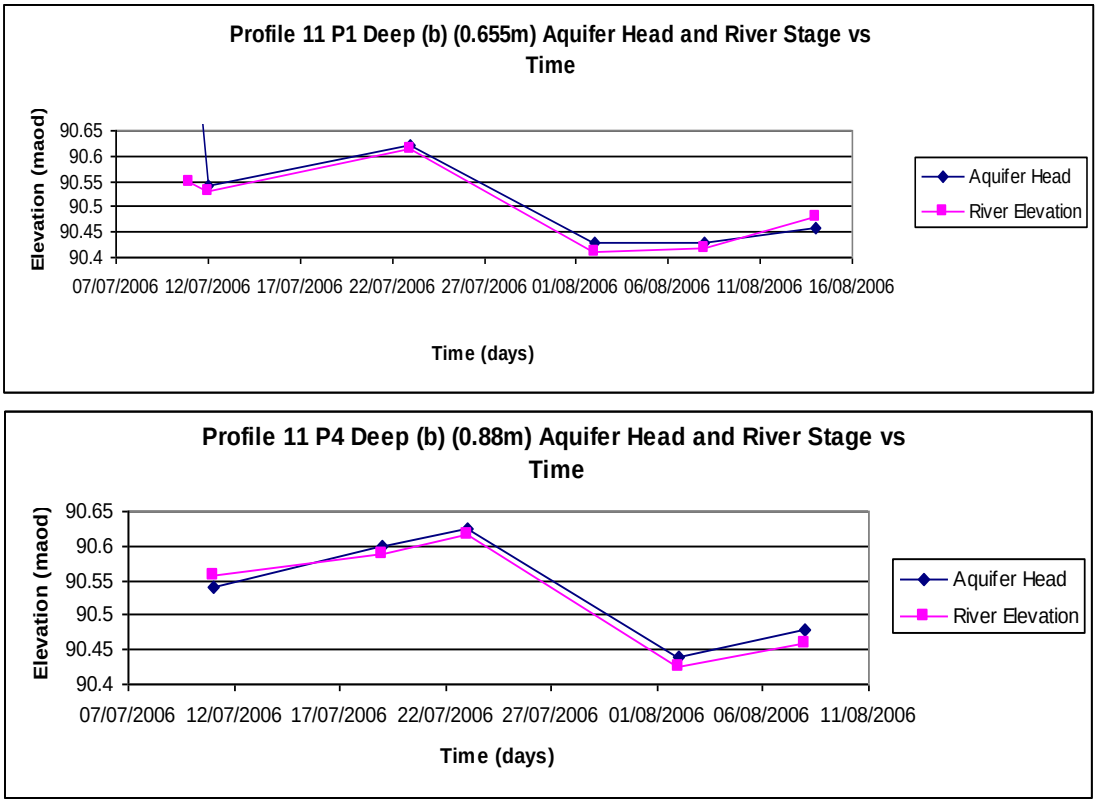


The peak aquifer head in all four MDP's, as well as the highest river stage occurs on the 23rd July directly after the peak rainfall event on 22/23rd July. Both piezometers at profile 8 indicated a lower head than in the river for the first portion of the monitoring session with P1 Deep registering a gaining system for the rest of the study. Profile 8 P4 Deep indicates a loosing river system close to the northern bank at profile 8 for 58% of the monitoring time. Temporal monitoring of piezometers at profile 11 indicate the river is gaining through out the study, except for the very end of the study where P1 Deep (b) indicates a loosing system.

Aquifer response times to minor flood events appear rapid in both MDP's at profile 11, however due to the continuously high heads observed at profile 8 after the first main rainfall event, it may be possible to assume a slow rebound from recharge in that particular area. This might be due to

a steep hydraulic gradient towards profile 8. (Figure 6.2.3) shows the temporal variation in hydraulic gradient beneath the river bed at profiles 8 and 11. The positive gradients indicate higher head in the aquifer and thus a gaining river system.

Figure 6.2.3, Temporal variation of hydraulic gradient at Profiles 8 and 11.

| | Temporal Variation in Hydraulic Gradient | | | |
|---|---|---|---|---|
| Date | Profile 8 P1 Deep | Profile 8 P4 Deep | Profile 11 P1 Deep (b) | Profile 11 P4 Deep(b) |
| 11/07/2006 | | | 0.603007519 | -0.019318182 |
| 12/07/2006 | -0.122058824 | 0.001212121 | 0.019548872 | |
| 17/07/2006 | -0.191176471 | -0.048484848 | | |
| 19/07/2006 | -0.183823529 | 0 | | 0.013636364 |
| 23/07/2006 | 0.561764706 | 0.16969697 | 0.010526316 | 0.011363636 |
| 28/07/2006 | | 0.127272727 | | |
| 02/08/2006 | 0.360294118 | -0.157575758 | 0.02406015 | 0.015909091 |
| 08/08/2006 | 0.458823529 | -0.036363636 | 0.016541353 | |
| 14/08/2006 | 0.373529412 | -0.098181818 | -0.033082707 | 0.023863636 |

## 6.3 Hyporheic Delineation

The extent to which the surface water enters the river bed and thickness of hyporheic zone in the river bed sediments varies temporally. In this study the base of the hyporheic zone has been defined hydrologically as the depth at which any surface water exists. The occurrence of varying chloride concentration with depth below the river bed appears to correlate to a certain degree to river flow data and rainfall data in that at high river flow, chloride concentrations penetrate the river bed to the highest degree. Although, this statement is somewhat dubious in that river water penetration rates is also dependent on base flow rates and hence the rate at which the aquifer responds to a recharge event. A correlation can be seen in this study reach between rainfall and increased penetration which may suggest a slower aquifer response time to rainfall than response times of the river. (Figures 6.3.1, 6.3.2, 6.3.3 and 6.3.4) illustrate the temporal variation in

chloride concentration with depth below the river bed at multi-level piezometers at profile 8 and 11. Table 6.3.1 highlights the correlation between specific sampling round, date and the rainfall occurrence which occurred on that day and on the day prior to sampling.

Table 6.3, Correlation of sample round number, date and rainfall occurrence on sampling day and on day prior.

| Sample Round Number | Date Conducted | Rainfall on that day and day previous |
|---|---|---|
| 1 | 23/07/2006 | 6.11mm over 1 day prior |
| 2 | 02/08/2006 | 2.95mm over 2 days |
| 3 | 08/08/2006 | 0.27mm over 2 days |
| 4 | 14/08/2006 | 10.3mm over 2 days |

Figures 6.3.1 and 6.3.2, Temporal variation of chloride concentration with depth below the River Bed

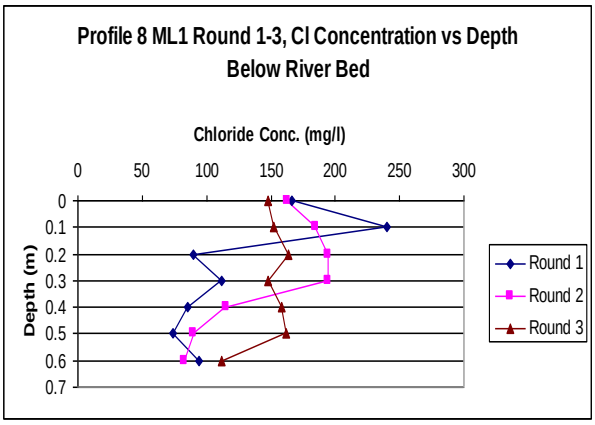


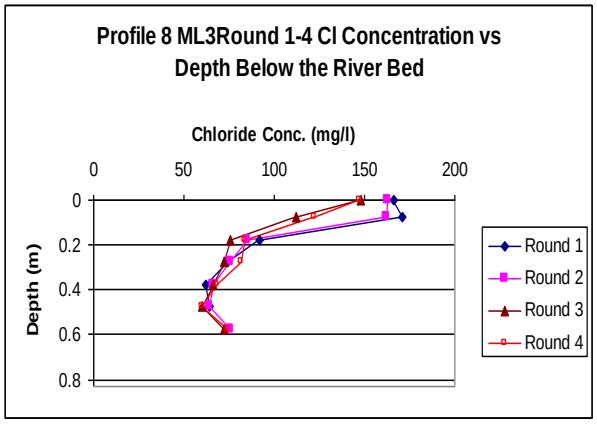


Figures 6.3.3 and 6.3.4, Temporal variation of chloride concentration with depth below the River Bed at Profile 11

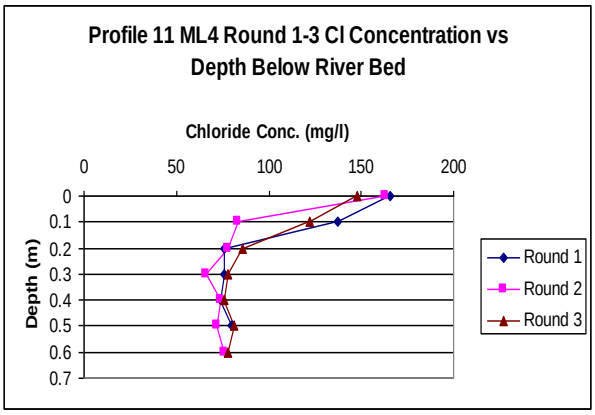


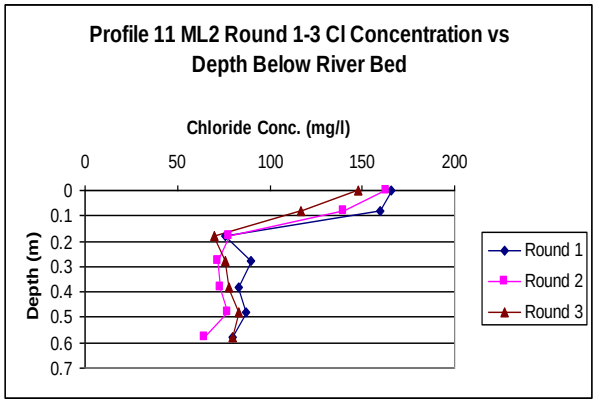


The temporal variability of chloride concentration under different flow conditions is seen on a variety of scales. The most pronounced is Profile 8 ML1, (Figure 6.3.1). At this location 100% river water can be seen to enter a distance of between 0.15-0.50m in the river bed during sampling rounds 1 and 3 respectfully. Profile 8 ML1 shows a high degree of fluctuation in river water presence in the river bed with time and it is the only multi-level in the profile which does so.

At Profile 8 ML3, the depth to which river water chloride concentrations enter the river bed is somewhat less variable with time although the surface water quality chloride concentration can be seen to enter the river bed to the greatest extent on the 23rd July when the greatest rainfall event occurred on the 22/23rd July. Profile 8 ML3 shows that the deepest river water chloride concentrations are seen during the first round of sampling where it has been calculated that river water composes 24% of all water present at 0.175m during round 1, in comparison to the second and third round in which only 16% and 5% respectfully of water present is of river water quality, (Figure6.3.5). It is also important to recognise the occurrence of a higher $Cl^{-1}$ concentration during round 1 at 0.75m below the river bed than that observed in the river on the same day. This pattern has also been identified at ML1 where the chloride concentration at 0.1m is 240 mg/l and that in the river is 166 mg/l, (Figure 6.3.1).

Figure 6.3.5, Chloride concentrations in top 0.2m of river bed at Profile 8 ML 3

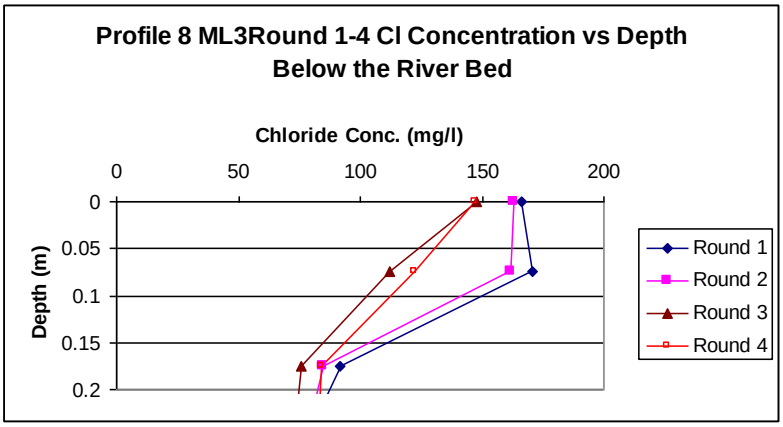


Sampling round 2 was carried out during a period at which 2.95 mm of rainfall occurred over 48 hours. The shallow chloride patterns observed at profile 8 again vary substantially. ML1 shows the greatest temporal contrast, with river water chloride concentrations penetration to a depth of 0.3m. ML's 2, 3 or 4 do not show such a substantial variation, however higher chloride

concentrations have been identified at a depth of 0.75m when compared to sample rounds 3 and 4.

Spatially the river water Cl concentration can be seen to penetrate the river bed on a variety of scales, Appendix 1. This reinforces the claim that the hydraulic properties in the river bed sediments are highly heterogeneous over a small area (cross-profile).

Shallow multi-level piezometers were sampled during round 4 during which 10.3 mm of rainfall fell over 48 hours, (Figure 6.3.6). These ML chloride gradients have shown the high degree of spatial variability of surface water penetration even in the upper 0.25cm of the river bed on a cross channel profile. No temporal observations can be made at this scale due to only one round of sampling being carried out

Figure 6.3.6, Shallow multi-level piezometer chloride concentrations with depth at profiles 8 and 11 observed during round 4.

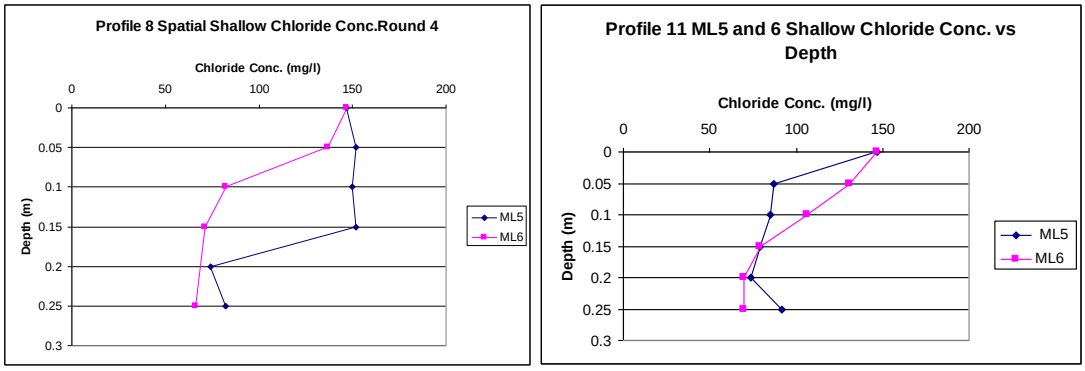


The frequency distribution of all chloride values measured throughout the quality monitoring stage of the project are shown in (Figure 6.3.7). The concentration bands in which the highest number of samples retrieved were between 60-80 mg/l, 81-100 mg/l and between 141-160 mg/l chloride. 83 samples fell into the 60-80 mg/l bracket of which the majority were retrieved from the deepest sampling horizons below the river bed. 23 samples were retrieved which fell into the 80-100 mg/l bracket, which again are representative of the deeper samples. The next high

frequency peak is seen at the 141-160 mg/l bracket in which 21 sample concentrations were found. This concentration is typically representable of river water chloride concentrations. 13 samples were retrieved in which chloride concentrations were higher than 160 mg/l, with the highest recorded concentration being 240mg/l which was found at profile 8 ML1 at a distance of 0.1m below the river bed during sample round 1, (Figure 6.3.1).

Figure, 6.3.7, Frequency of chloride sample concentrations within particular concentration brackets

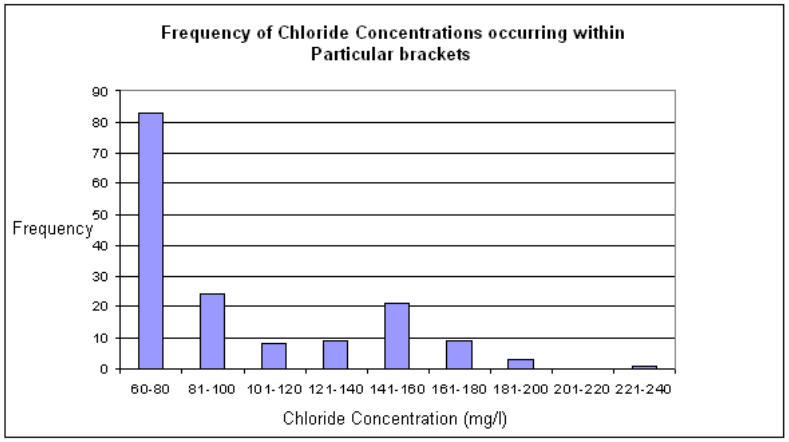


To interpret temporal and spatial chloride concentration variability, concentrations of river water and aquifer water have been obtained and the percentage of river water present at different depths has been calculated. To obtain an estimate for absolute chloride concentrations for 100% river water and 100% aquifer water, the geometric mean of all the deepest sampling point concentrations was calculated for absolute aquifer Cl concentration and the arithmetic mean used for all river sample concentrations retrieved.

| | River Cl. Concentration (mg/l) | Aquifer Cl. Concentration (mg/l) |
|---|---|---|
| Geometric Mean | 155.793158 | 71.8251363 |
| Average | 156.1111111 | 72.29166667 |

Based on values calculated above, any value greater than the average chloride concentration is assumed to be 100% river water, any value lower than the geometric mean of aquifer chloride concentration is assumed to be 100% aquifer water and any value in between is assumed to be a mixture of both.

Patterns of chloride concentration in river bed sediments varied both temporally and spatially, however in most scenarios, a relatively sharp transition could be seen between surface water Cl concentrations and groundwater Cl concentrations below the river bed. River water Cl concentrations were commonly seen at depths of 0.1m below the river bed however in many instances river water concentrations were seen at depths of 0.2-0.3m below the river bed. (Figure 6.3.8) illustrates the spatial variability of surface water penetration depths at Profile 8 during round 1 of sampling.

Figure 6.3.8, Observations of spatial river water penetration at Profile 8 during Round 1 of sampling

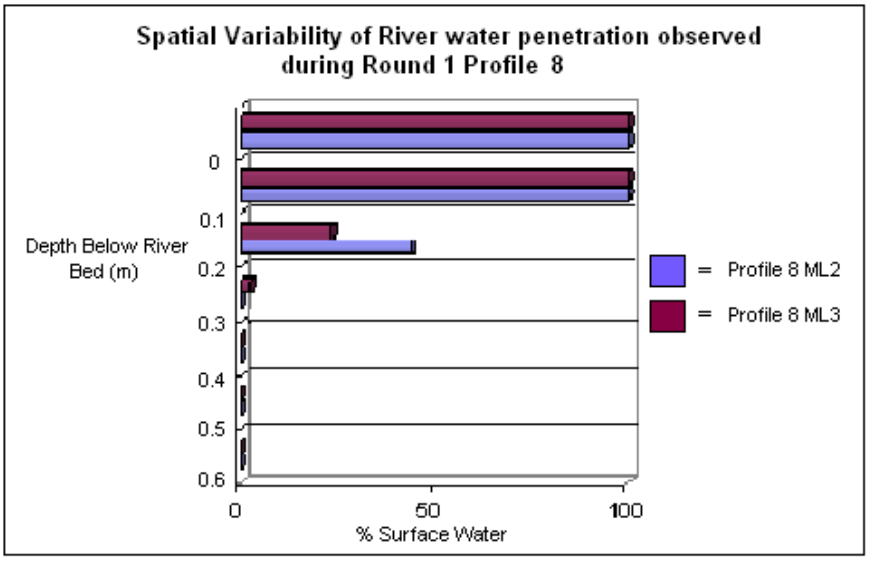


At multi-levels 2 and 3, river water can be seen to occupy the upper 0.1m of the river bed, and at 0.2m the river water occupies less than 50% of the overall pore space. Little or no river water can be seen to exist below 0.3m in the river bed. In stark contrast to this Chloride pattern, ML1 has a

deep distribution of river water within the river bed, (Figure 6.3.9). At this location, river water has been calculated to occupy 26% of the water volume at 0.6m below the river bed, hence a mixing zone of at least 0.5m is likely present given that 100% surface water occupied the upper 0.1m of the river bed.

Figure 6.3.9, Percentage of river water present at different depths below the river bed

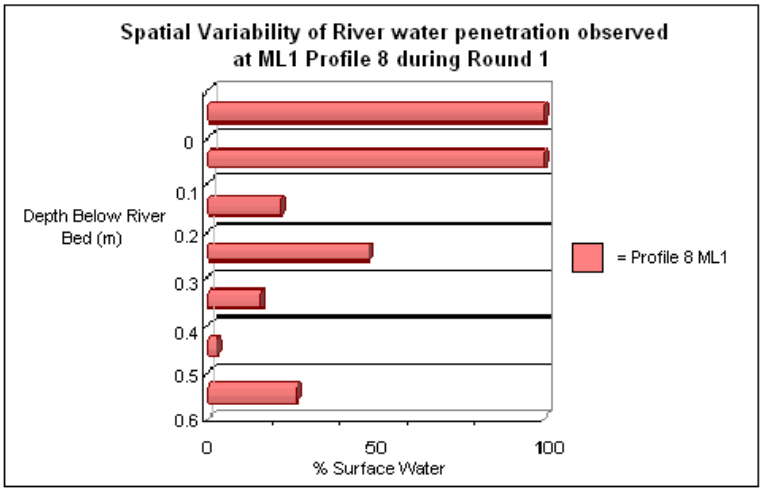


The spatial variability of river water % present at different depths in the river bed at Profile 11 indicates a somewhat larger mixing zone. (Figure 6.3.10) illustrates the calculated % of river water present at different depth horizons below the river bed. No samples retrieved below the river bed at profile 11 indicate the presence of 100% river water as was the case at all sampling sites at profile 8. This indicates a much shallower hyporheic zone directly below the river bed. In almost all instances, some proportion of river water was found to be present at depths of 0.5m below the riverbed which would suggest a different hydraulic environment exists in comparison to that seen at profile 8.

Figure 6.3.10, Percentage river water present at different depths below the river bed, Profile 11.

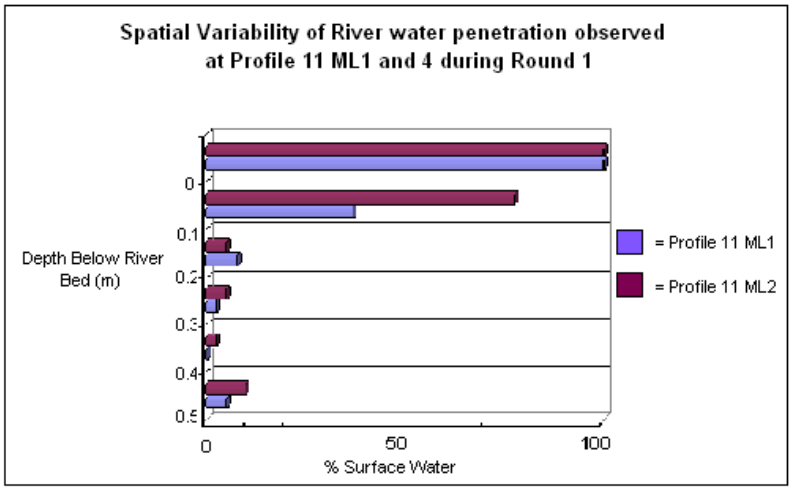


The frequency of different hyporheic zone thickness which have been identified throughout the water monitoring stage of the field work are presented in (Figure 6.3.11). It can be seen that 50% of all water quality measurements indicate a hyporheic thickness of between 0.4-0.5m in extent. However the variability of hyporheic thickness is high with the other 50% of measurements indicating a range of hyporheic thicknesses of between 0-0.4m. The second larges hyporheic thickness encountered was within the 0-0.1m range.

Figure 6.3.11, Frequency of hyporheic zone thickness based on chloride data.

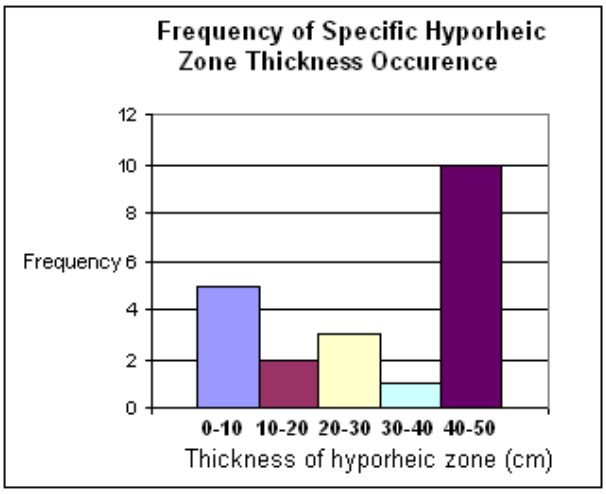

The spatial distribution of these hyporheic zone thicknesses is presented in (Figure 6.3.12). It can be seen that the distribution is relatively straight forward in that the majority of observed zones at profile 8 are in the 0-0.1m bracket while the majority of hyporheic zones at profile 11 are in the 0.4-0.5m thickness bracket.

Figure 6.3.12, Spatial distribution of observed hyporheic zone thicknesses at profiles 8 and 11.

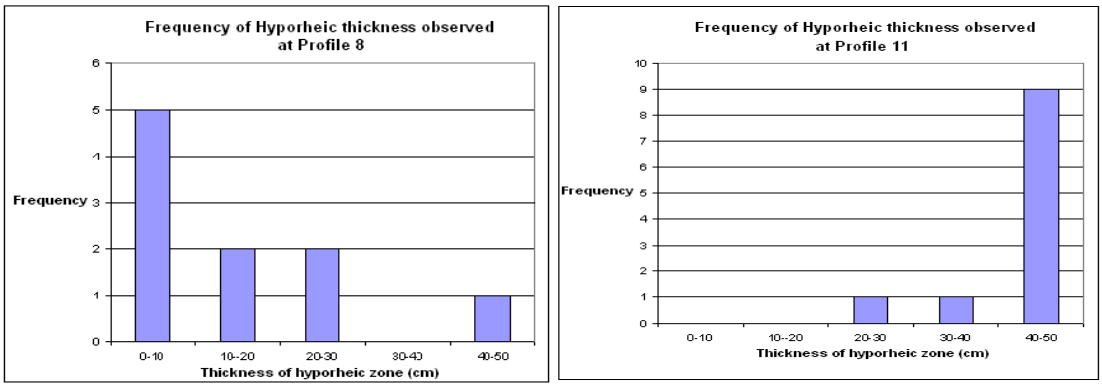


## 6.4 Critique of survey Technique

Survey techniques have been carried out as accurately as possible, however as with all methodology, some degree of uncertainty exists in results obtained. The reliability of the results obtained is dependent on the technique and reliability of the methodology of field work completion.

### 6.4.1 River Flow, Rainfall and Aquifer Head

Rainfall data has been collected from 2 weather stations in the Birmingham area over the study period. Although main rainfall events register on similar dates at both weather stations, there is a slight contrast between the stations with regards to absolute rainfall levels on those days, (Figure 6.4.1.1). This is likely due to the patchy nature in which precipitation occurred in the

Birmingham area throughout the summer. Neither rainfall station is in the immediate vicinity of the study site. Selly Oak weather station which is the closest, is situated approximately 9.5km in a south-westerly direction from the study site and Sollihull weather station is situated approximately 16.5km in a south-easterly direction from the study site.

To estimate rainfall intensity close to the site, the weighted mean has been calculated for the two stations. Weights are represented by the distances from the study site to the respective weather stations.

Figure 6.4.1.1, Contrast Temporal Rainfall measurements at Sollihull and Selly Oak Weather Stations for relevant sampling dates and calculated weighted means.

| | Rainfall at Particular Station (mm) | | Weighted Mean |
|---|---|---|---|
| Date | Selly Oak | Sollihul | (mm) |
| 22/08/2006 | 0.2 | 0 | 0.073076923 |
| 23/07/2006 | 5 | 6.75 | 6.110576923 |
| 01/08/2006 | 1.5 | 3 | 2.451923077 |
| 02/08/2006 | 0.7 | 0.35 | 0.477884615 |
| 03/08/2006 | 0.5 | 3 | 2.086538462 |
| 07/08/2006 | 0.2 | 0 | 0.073076923 |
| 08/08/2006 | na | 0.2 | 0.2 |
| 13/08/2006 | na | 6.1 | 6.1 |
| 14/08/2006 | 8.5 | 1.85 | 4.279807692 |

The reliability of such a method for estimating actual rainfall in the study reach is somewhat questionable in that it may not represent the intensity of rainfall occurrence accurately. However, due to the consistent correlation of date of rainfall event between the two weather stations, it is believed that temporal rainfall event occurrence is represented accurately and intensity it reasonably accurate for the purpose it serves.

The reliability of measurement of aquifer head in the installed MDP's depends on the hydraulic properties of the river bed sediments within which the MDP's were installed. It has commonly been found that water levels within the MDP's could take up to 10-15 minutes to re-equilibrate to aquifer conditions once the rubber bung had been removed. In some MDP's, the rate of response was particularly slow or non-occurring possibly due to blockage of MDP open section with silt or clay. Nevertheless, all MDP's register a relative temporal change in water level across the study reach The short scale response times in some of the river bed sediments may be misleading, as low hydraulic conductivity sediments will take longer to re-equilibrate to the general hydraulic conditions seen in the aquifer.

### 6.4.2 Hyporheic Delineation Critique

The use of chloride as a tracer to delineated the likely depth to which river water enters the river bed and the extent of the mixing zone is reliable in that $Cl^-$ is a conservative ion and is not going to be altered in the river bed system, however the following issues have been highlighted as possible source of ambiguity in the use of chloride for this purpose and the possible causes for misinterpretation.

1. Chloride analysis by optical photometry has been found to give a standard deviation of 1.5 mg/l and a range of 3 mg/l on 4 repeat analyses on one sample.
2. Variation of sample volume extraction produces a range of chloride concentration with a max. value of 77 mg/l, min. value of 68 mg/l and a standard deviation of 2.79mg/l.
3. The use of geometric mean of deep water samples and average of all surface water samples may not accurately represent true concentrations.

4. The temporal variability of chloride concentrations in the river due to sewage treatment works discharges undermines the assumptions made for calculations of % river water at different depths below the river bed.
5. The possible variation of groundwater chloride concentration due to the presence of groundwater plumes of chloride in the study reach.

## 6.5 Discussion

The effect of rainfall and increased river flow in the study area substantially affects the extent to which river water enters the river bed sediments. This can clearly be seen in the temporal chloride concentration gradient patterns observed at both profile 8 and 11.At profile 8 (ML1), the temporal variation is significantly greater than the variation observed at all other sites. The reason for this is somewhat unclear, however a possible explanation is that there is greater inflow from the river at this location due to the gravely nature of the river bed sediments and the velocity at which river water is passing over the sediments, although, if this was the case, it would be reasonable to expect to see a similar pattern in the multi-level positioned 2m further out in the river channel (ML2), which clearly is not seen.

The occurrence of 6.11mm of rainfall on the day prior to sample round 1 produced a somewhat turbent flow environment. River flow rates rose substantially and peaked at approximately $10.5ms^{-1}$ (Water Orton flow station). With average dry weather flow rates of $2.5\text{-}3ms^{-1}$ at Water Orton, rainfall increased river flow by approximately 400%. The highly irregular chloride pattern observed at profile 8 ML1 (Figure 6.3.1) could somewhat be expected if rapid through flow of river water is indeed occurring. A peak concentration of 240 mg/l chloride is observes at 0.1m below the river bed. The occurrence of this peak (which is 74 mg/l higher in concentration that river water on that day) is likely due to the increased chloride concentrations which are often

seen during rainfall when urban surface water runoff enters the river. (Ellis, 2003) correlated conductivity of river with flow rates and found that conductivities did indeed increase with river flow rates. Rainfall events are sometimes seen to produce a rapid initial peak in EC reaching values of over 1,500 $\mu Scm^{-1}$ associated with the first flush of urban run-off and overflow discharges from combined sewer overflows. Levels of EC then fall due to dilution by the subsequent drainage of less contaminated run-of, (Ellis, 2003). As Chloride concentration is proportional to EC, (Figure 6.5.1), chloride concentration observations at ML1 suggest that increased flow rates in the river prior to sampling round 1 possibly caused a influx on river water to the high k bed sediments at profile 8 ML1. Once the flood water had dissipated, chloride concentrations returned to average values (during round 1), however the higher than average concentration river water remained in the river bed for some time.

Figure 6.5.1, Correlation of Chloride Concentration with EC for river water samples.

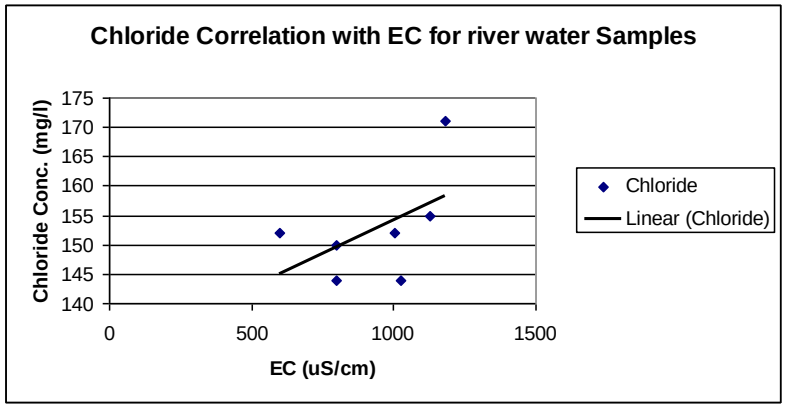


This peak is somewhat less obvious in the 3 other ML's located at profile 8, however is seen to a certain degree in ML's 3 and 4. The general lack of correlation of these ML's is likely due to the

short duration of the flood event and the lower hydraulic conductivity sediments restricting the access of the river water.

The use of shallow multi-level piezometers at profiles 8 and 11 proved advantageous in that they allowed for a more detailed identification of the boundary between 100% surface water and hyporheic water, however due to a late installation date, only one round of sampling was carried out and temporal fluctuations could not be assessed.

From rainfall data, it has been assumed that round 3 chloride concentration gradient data represents the normal flow environment. In this flow environment river water penetrates 0.5m into the river bed at ML1 profile 8. Again, in stark contrast to river water penetration patterns seen at other multi-levels at profile 8 with average penetration depths in all three ML's of less than 0.1m. This provides further evidence for the likely high inflow of river water to river bed sediments at ML 1.

Profile 11 presents a somewhat different set of surface water penetration patterns, in that some proportion of river water appears to be present at depths of up to 0.4m at all sample points based on absolute chloride concentrations, (Figures 6.3.3 and 6.3.4). No significantly high chloride concentration was seen immediately below the river bed surface during round 1 of sampling which suggests that the river water concentrations observed at Profile 8 ML1 were not present in the river long enough to enter the river bed at Profile 11. This in turn suggests a more stable flow routine in which equilibration times are longer than those at Profile 8 ML1 and that river water resident times in the river bed is likely longer than upstream. However higher chloride concentrations have still been identified at 0.1m below the river bed during round 1 of sampling when compared to concentrations at the same depths during round 2 and 3. Thus, the bed sediments still respond to rainfall events, though not to the same degree as those at profile 8.

In the four deep multi-levels at profile 11, chloride concentrations drop steadily in the top 0.2m of the river bed and chloride gradients can be seen to become more stable thereafter. River water does not appear to solely occupy any portion of the river bed at profile 11, (Figure 6.3.10) which implies the existence of a hyporheic zone immediately below the channel. When using the same absolute groundwater and surface water values as those used at Profile 8. A small proportion of surface water can be seen to be present at depths of up to 0.6m below the river bed. From the defining boundaries of the hyporheic zone used in this study, this implies that the mixing zone is at least 0.5m thick and up to 0.6m thick in some multi-levels at Profile 11.

One possible reason for the difference in hyporheic thicknesses seen at profile 8 and 11 is that the surface water resident times are different, in that there are longer resident times at Profile 11 than Profile 8. This creates a greater potential for diffusion and dispersion of the surface water in within the bed sediments at Profile 11. In contrast, low resident times of surface water at Profile 8 do not allow for significant dispersion processes, thus resulting in a sharper interface between surface and groundwater and consequently a narrow hyporheic zone.

# Chapter 7 Geochemical Analysis

## 7.1 Geochemical Conditions

Concentrations of $NO_3$, D.O. and $SO_4$ in the river bed environment varied significantly between profile 8 and 11 during July and August. Groundwater nitrate concentrations vary significantly with mean concentrations of 21.15 mg/l $NO_3$ at profile 8 and mean concentrations of 55.76 mg/l at profile 11, with average river water values at 28.94 mg/l.

Sulphate concentrations in deep piezometers show the opposite trend in that higher concentrations are seen at profile 8 (Geometric Mean 277.66mg/l) than at profile 11 (geometric mean 157.74). Average river water concentrations of sulphate for the months in question being slightly lower than concentrations observed at profile 11 (average river water concentration 143.14 mg/l).

At both profiles, D.O. concentrations decrease with depth below the river bed however there is a higher concentration at depth at profile 11 than profile 8 with geometric mean concentrations at profile 8 and 11 being 0.47 mg/l and 2.63 mg/l respectfully. Average river water concentrations were relatively higher at 6.11 mg/l. (Figure 7.1.1)

Figure 7.1.1 Statistical analysis of Nitrate, Sulphate and D.O. at Profiles 8 and 11

| **Nitrate (mg/l)** | Profile 8 Deep | Profile 11 Deep | River Water |
|---|---|---|---|
| Average | 22.39 | 57.98 | 28.94 |
| Geometric Mean | 21.15 | 55.76 | 27.76 |
| Std. Dev | 7.36 | 15.13 | 8.34 |

| **Sulphate (mg/l)** | Profile 8 Deep | Profile 11 Deep | River Water |
|---|---|---|---|
| Average | 279.25 | 158 | 143.14 |
| Geometric Mean | 277.66 | 157.74 | 142.70 |
| Std. Dev | 30.55 | 9.72 | 12.37 |

| **D.O. (ppm)** | Profile 8 Deep | Profile 11 Deep | River Water |
|---|---|---|---|
| Average | 0.73 | 2.88 | 6.11 |
| Geometric Mean | 0.47 | 2.63 | 5.24 |
| Std. Dev | 0.72 | 1.23 | 3.44 |

From this spatial distribution of geochemistry, it can be seen that the river bed environment at profile 8 is relatively anaerobic in comparison to profile 11. Thus reduction is likely occurring in which $O_2$ is being reduced by organic species present as this reaction is thermodynamically preferred. This has produced an anaerobic environment at profile 8. Evidence in support of this can be seen in the contrasting nitrate concentrations observed at both profiles. As expected from monitored D.O. concentrations, nitrate has a lower concentration at profile 8 than profile 11, thus suggesting that anaerobic reduction of nitrate is occurring at profile 8 but not to such a degree at profile 11.

When the redox potentials of both profiles are compared (Figure 7.1.2) it can be seen that a much higher $E_H$ of over 200mV has been identified at deep sampling points at profile 11, which is indicative of aerobic reduction of $O_2$ as well as other redox reactions including nitrate reduction. Similar Eh values were identified in the river again suggesting $O_2$ reduction. In contrast a much broader range of Eh values can be seen with depth at profile 8 which are indicative of $O_2$ reduction, denitrification, and $NO_3^-$ reduction. As $NO_3^-$ reduction is thermodynamically less

preferably (Eh ≈> -150mV), it only occurs post $O_2$ reduction, thus observations at profile 8, of an almost anaerobic environment and much lower $E_H$ values (lowest observed was -145mV during round 1) do suggest that nitrate is being reduced. Eh values suggest that $S0_4$ reduction is not occurring at either profile.

Figure 7.1.2, Redox potentials of multi-level samplers at profile 8 and 11 taken during round 1 of sampling

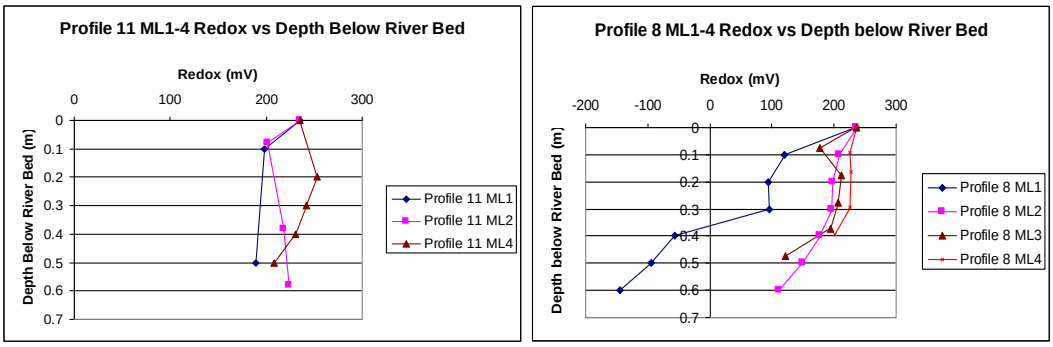


The contrasting mean sulphate concentrations of 277.66 mg/l and 157.74mg/l at profiles 8 and 11 respectfully do suggest sulphate reduction is occurring and are somewhat in disagreement with D.O. and $NO_3/NO_2$ concentrations. The river bed environment is at the most under nitrate reducing conditions, and is likely under aerobic reducing conditions at profile 11, hence sulphate concentrations should be similar across the study reach as no sulphate reduction should be occurring. One possible explanation for the high sulphate concentrations at profile 8 is the presence of a contaminant sulphate plume entering the river bed environment at this location. Localised plumes are commonly seen in shallow urban groundwaters of urban aquifers (Ellis, 2003).

## 7.2 Nitrate

The temporal variation of nitrate concentrations seen at profile 8 are graphically represented in (Figures 7.2.1 and 7.2.2). At ML1, a large drop in concentration to approximately 15 mg/l $NO_3$ can be seen between depths of 0.2-0.3 m below the river bed during round 1 and 2. This is a significant drop when compared to observer values directly above and below the 0.3m sampling horizon of 22 mg/l and 24.64 mg/l and 17.6mg/l and 30.8mg/l during round 1 and 2 respectfully. Nitrate concentrations observed during round 3 at ML1 show a similar pattern however, concentration drops are not as pronounced as those seen during the two rounds previous. At ML3 large scale drops in concentration occur during rounds 2 and 4 at 0.175m below the river bed. These drops in concentration are of a similar magnitude to those seen at ML1 with concentrations dropping to 11.88 mg/l, 12.32 mg/l and 6.16 mg/l $NO_3/NO_2$ during rounds 1, 2 and 3 respectfully. These concentrations and concentrations 0.1m above and below are highlighted in table 7.2.1.

Figure 7.2.1 and 7.2.2, Temporal variation in Nitrate concentration with depth below the river bed at multi-levels 1 and 3 profile 8.

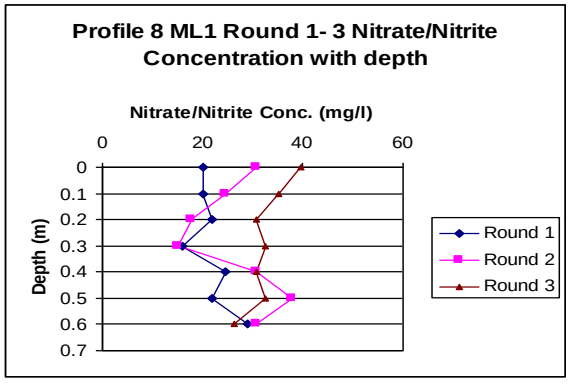


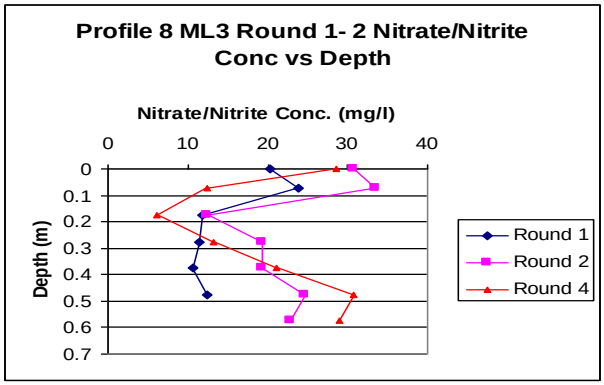

Table 7.2.1, $NO_3$ concentration gradients observed during rounds 1, 2 and 3 of sampling between depths of 0.075-0.275 m below the river bed at Profile 8 ML3.

| Depth (m) | Round 1 | Round 2 | Round 3 |
|---|---|---|---|
| 0.075 | 23.76 mg/l | 33.44 mg/l | 12.32 mg/l |
| 0.175 | 11.88 mg/l | 12.32 mg/l | 6.16 mg/l |
| 0.275 | 11.44 mg/l | 19.36 mg/l | 13.2 mg/l |

Nitrate reducing conditions are unlikely to be as prevalent at Profile 11 as the river bed environment did not appear to be anaerobic over the sampling period with mean aquifer D.O. concentrations of 2.63 (ppm). However large drops in $NO_3$ concentration are still seen at particular depth horizons within the river bed, (Figure 7.2.3). The occurrence of these concentration drops at 2 horizons (0.1m and 0.3-0.4m below the river bed) in multi-levels from profile 11 suggests that nitrate reduction may be occurring to a certain degree despite the slightly higher concentrations of D.O. observed. These concentrations drops are particularly apparent in rounds 2 and 3 at ML2 and in rounds 1 and 2 at ML4. During round 1 ML4 registered the largest drop in concentration at 0.3m below the river bed of 17.6 mg/l $NO_3$ to 52.8mg/l. Average value from horizons above and below this horizon during round 1 were 70.4 mg/l. At Profile 11 ML2, a similar drop in concentration was seen during all sample rounds. The most pronounced of these is at a depth of 0.38m below the river bed during round 3 of sampling. Concentrations fell from average values above and below the 0.38m sampling horizon of 70.4 mg/l to 57.2 mg/l $NO_3$ at horizon 0.38m. This represents an average drop in concentration of 13.2 mg/l $NO_3$ at that point which is difficult to dismiss as being purely because of flow heterogeneities within the river bed.

Figures 7.2.3 and 7.2.4, Temporal variation in Nitrate concentration with depth below the river bed at multi-levels 2 and 4 profile 11.

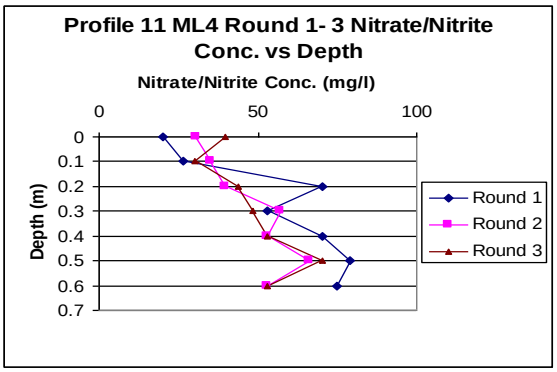


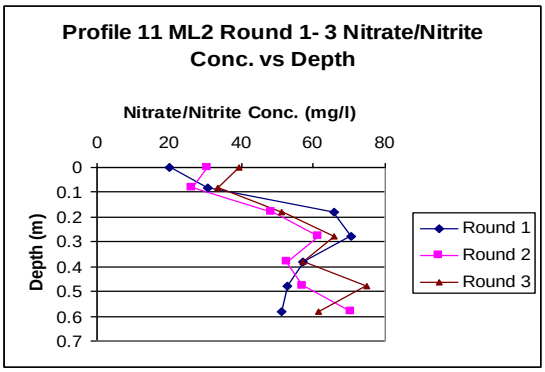


Because of the high degree of variability of concentration of supposedly groundwater samples (Standard Deviation of 7.36 mg/l), and the small contrast in $NO_3$ concentration between groundwater and river water of 21.15 mg/l and 27.76 mg/l respectfully at profile 8, calculated percentage river water from chloride data at each sample horizon could not be compared to calculated nitrate concentrations if no attenuation was occurring. At profile 11, although the contrast between groundwater and surface water $NO_3$ concentrations were much higher, with geometric mean concentrations of groundwater and surface water of 57.98 mg/l and 28.94 mg/l respectfully, the standard deviation of all groundwater samples was 15.13 mg/l which again disallowed the use of comparative studies between calculated river water proportions, concentration of NO3 if no attenuation was occurring and actual concentrations observed. Although this would have allowed for a quantification of the degree of NO3 attenuation to be calculated, results would not be reliable because of the high degree of heterogeneity of concentrations in the river and groundwater.

## 7.3 Dissolved Oxygen and Sulphate

D.O. concentrations in river bed sediments at Profile 8 generally followed a pattern in which concentrations were high in the river water and low or non-existent in the groundwater. Surface water penetration into the upper 0.1m of the river bed during round 1 of sampling is apparent at two locations in the cross-channel profile. D.O. measurements do not give any indication of microbial aerobic degredation of organic matter as the environment is anaerobic below 0.1m in the river bed. (Figure 7.3.1).

Figure 7.3.1, Temporal variation in D.O. concentration with depth below the river bed at multi-levels 2 and 3 profile 8.

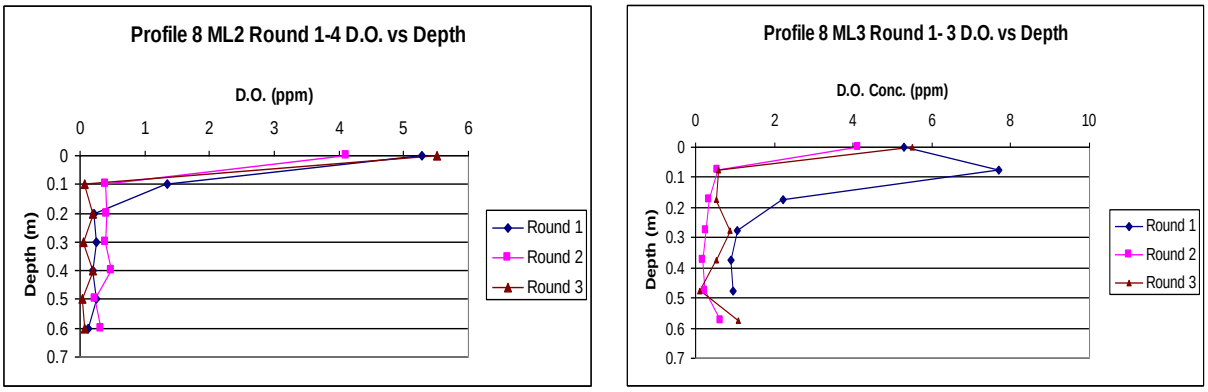


Groundwater D.O. concentrations from profile 11 are higher with geometric mean of all samples taken below 0.5m of 2.63 ppm which is almost 6 times greater than the concentrations observed at profile 8 (0.47 ppm). D.O. concentration patterns in the riverbed sediments at profile 11 do reveal pronounced areas of low concentration where reduction of $O_2$ is likely taking place (Figure 7.3.2). This drop in concentration is seen at ML2 during round 2 and 3 of sampling at a depth of 0.18m and during round 1 at a depth of 0.38m. At ML4 one significant drop in concentration is seen at a depth of 0.1m below the river bed during the second round of sampling. Another relative drop in D.O. concentration is seen at a depth of 0.4m which is

apparent during all sampling rounds. Although these sharp drops in concentration may be indicative of $O_2$ reduction, it is also possible that the sample point is located within a relatively low hydraulic conductivity layer of sediment which would effectively act as a barrier to groundwater with higher K values entering the sample tube.

Figure 7.3.2, Temporal variation in D.O. concentration with depth below the river bed at multi-levels 2 and 4 profile 11.

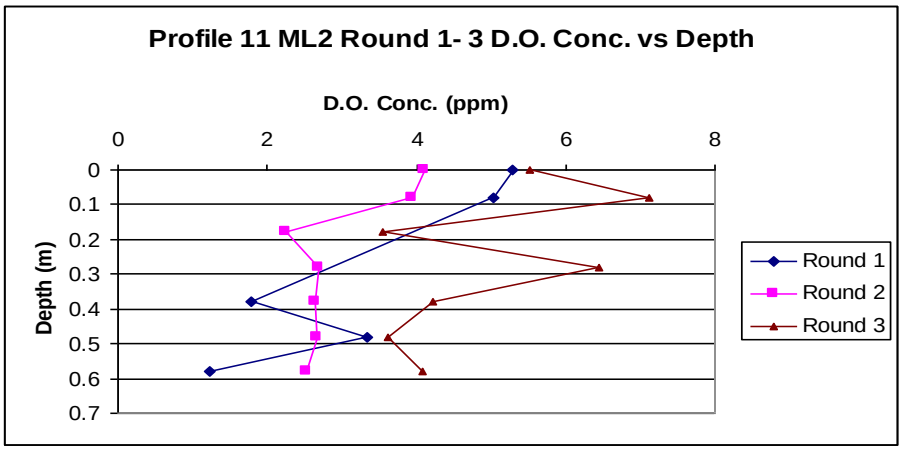


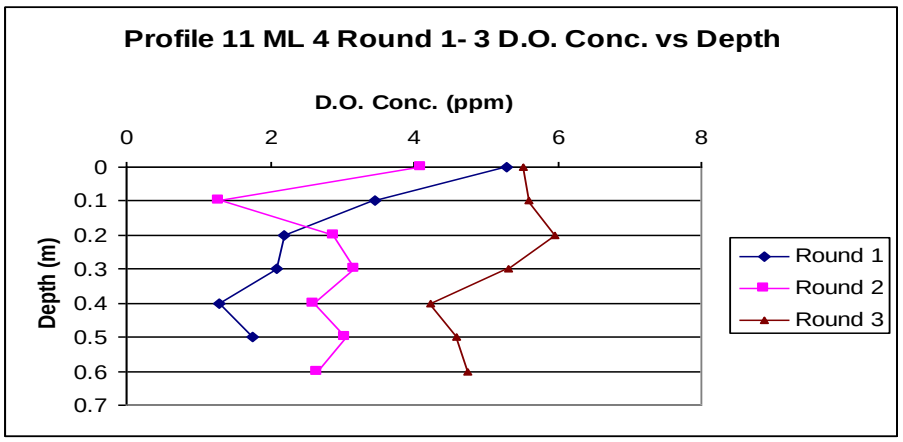


Sulphate concentrations gradients in the river bed are not indicative of attenuation as sulphate reduction is highly unlikely to be occurring. Highly contrasting signatures of $SO_4$ are seen between river water and groundwater at profile 8, and concentration gradients are comparable to

those seen with chloride which suggests that $SO_4$ is relatively stable in the river bed environment, (Figure 7.3.3).

Figure 7.3.3, Comparison of concentration gradients of chloride and sulphate at Profile 8 ML 1-4 round 1.

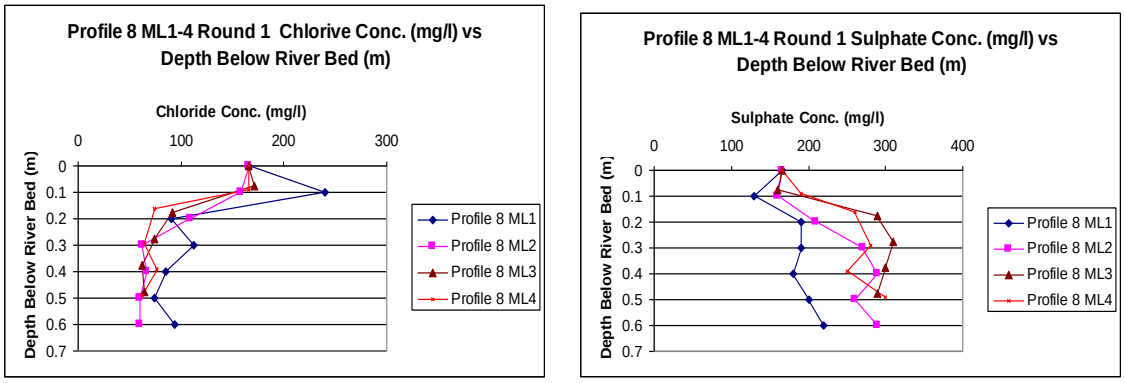


(Figure 7.3.4) graphically represents the range of sulphate concentration values seen at profiles 8 and 11. The contrast in groundwater concentrations is easily identified from the graphs which support the theory that a sulphate plume is possibly to be entering the river at profile 8.

Figure 7.3.4, All temporal and spatial distributions of $SO_4$ concentrations observed below the river bed at profiles 8 and 11.

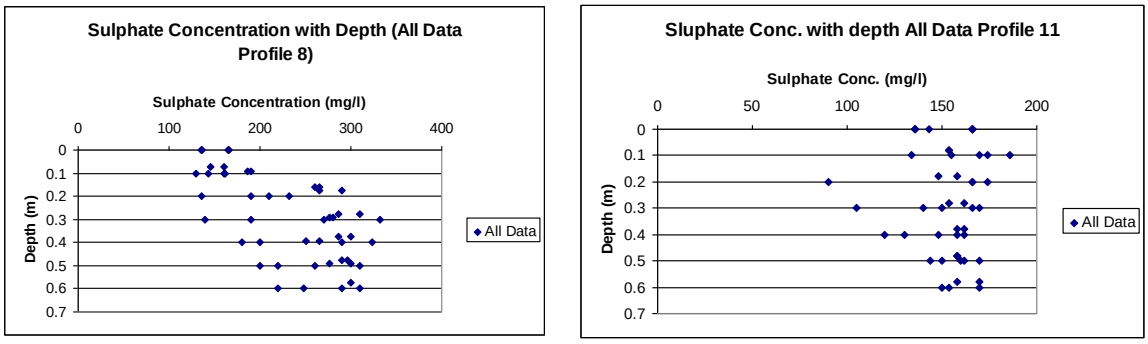

The rate at which sulphate concentrations are dropping with decreasing depth below the river bed at profile 8 is due to the increasing percentage of river water present in the bed sediments. Comparable to chloride, a sharp drop in concentration is seen between 0.1m and 0.2m below the river bed at profile 8 again suggesting the sharp drop in % river water present in the pore space below 0.1m.

## 7.4 Critique of Methodology

The variation in extraction times of water samples from the river bed results in concentration variations of D.O., $SO_4$ and $NO_3$. With increasing sampling time of any one ML sampling horizon the radius from which the sample is retrieved increases exponentially, thus the greater the sample volume retrieved, the less likely the sample is going to be representable of the depth horizon at which the HDPE tube is installed. From time series experiments carried out at profiles 8 and 11, it has been found that after 6 minutes of sample extraction at an average pump rate of 1.01 l/hr, the spherical sample horizon radius has expanded by 0.05m, thus any sample extracted after 2.5 minutes will be partly composed of pore water from sample horizons above and below the horizon from which the sample is intended to be extracted. (Figure 7.4.1) illustrates the growth of sample radius with increased pump times and the maximum radius at which samples can be considered representable of the sample horizon of interest.

Figure 7.4.1, Sample radius growth with increased pumping time.

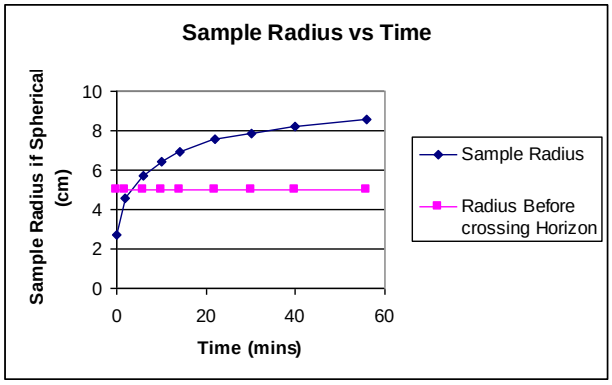


Assuming the sample horizon growth is spherical, after 6 minutes the sample sphere will have grown to 0.057m, thus is not truly representable of the horizon of interest as multi-level sample points are located 0.1m apart on the installation.

The variation in of determinands concentration during time series carried out at profile 8 and 11 is presented in Table 7.4.1 and 7.4.2 along with concentration variations observed during sample analysis.

Table 7.4.1 and 7.4.2, Variation in determinand concentration during time series at profile 8 and comparison to concentration variation observed during sample analysis.

| Profile 8 | Mean Conc. (mg/l) (ppm) | Std. Deviation TS* | Std. Deviation SA* |
|---|---|---|---|
| Nitrate/Nitrite | 24.47667357 | 3.005772225 | 6.48160474 |
| D.O. | 0.668167048 | 1.625759896 | na |
| Sulphate | na | na | 8.640987598 |
| Chloride | 62.82191194 | 2.267786838 | 1.5 |

| Profile 11 | Mean Conc.(mg/l) (ppm) | Std. Deviation TS* | Std. Deviation SA* |
|---|---|---|---|
| Nitrate/Nitrite | 56.33905343 | 5.968450385 | 6.48160474 |
| D.O. | 3.462678634 | 0.332453004 | na |
| Sulphate | 158.9132402 | 8.491826135 | 8.640987598 |
| Chloride | 74.39635857 | 2.788866755 | 1.5 |

TS* = Standard Deviation obtained from varying time-series concentrations
SA* = Standard Deviation obtained from varying sample analysis concentrations.

The standard deviation (SD) of sample concentration variation seen during the time-series are lower than SD's seen during lab sample analysis for all but one of the determinands. SD was not calculated for D.O. concentrations during lab sample analysis as it was conducted in the field using a D.O. probe. This result suggests that the margin of error produced by optical photometric lab techniques is larger than that seen when sample horizons are over pumped, hence duration of sample extraction is not as critical as one might expect. Chloride is the only determinand which shows a greater SD for time series concentration variations, which is likely due to the more reliable optical spectrometric technique used for chloride than the other determinands. Hence, chloride is the only determinand in which concentration variations due to prolonged pumping at a particular horizon are of concern.

## 7.5 Discussion

Geochemical sampling of pore water and surface water in the study reach has revealed the likely locations at which aerobic and anaerobic degradation of organic substances is occurring. At almost all multi-level locations, the highest degree of degredation of inorganics appears to be occurring at depth horizons at which river water and groundwater co-exist, thus supporting the claim that natural attenuation and oxidation of organic contaminants is greatest in pore space which contains both river water and surface-water, the hyporheic zone.

Deep D.O. concentrations are substantially lower and almost neglible at profile 8 compared to profile 11. This suggests an anaerobic environment at profile 8. A direct correlation between % river water and D.0. concentration at different depths at profile 11 cannot be seen hence it is assumed that $O_2$ is being consumed at preferential horizons by aerobic microbiological

processes. Degradation of $O_2$ at profile 11 predominantly occurs at depth horizons in which river water and groundwater co-exist. (Figure 7.5.1) compares the temporal variation in calculated % surface water present and observed concentration drops in D.O. It can be seen that during rounds 2 and 3 the main drops in D.O. concentration occur at 0.1m and 0.5m respectfully. A these times, percentage river water calculated to be present at 0.1m and 0.5m below the river bed is 13% and 11% respectfully. However a correlation of % river water present and rate of D.O. consumption cannot be used to identify the most ideal percentages of surface and groundwater because a drop in concentration of a similar magnitude occurs during round 2 at 0.5m below the river bed where it has been calculated that only 0.2% of the water present is river water. As well as this, other depth horizons with similar percentages of river water present as those showing preferential consumption of D.O. actually show an increase in D.O. concentration (0.2m, Round 3). This re-emphasises the fact that D.O. consumption is not directly related to the % river water present, however is predominantly occurring at horizons in which surface water and groundwater coexist.

Figure 7.5.1, Comparison of temporal variation in calculated % surface water present and observed concentration drops in D.O.

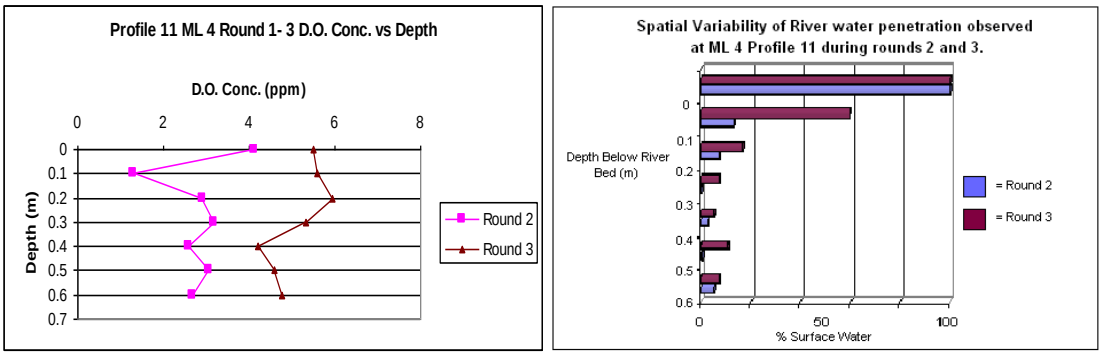


Nitrate concentration gradients show similar patterns to those seen with D.O. concentrations with significant drops in concentration at depth horizons in which surface water and groundwater

coexist. (Figure 7.5.2) illustrates the temporal variation of % river water present at different depths below the river bed and the observed concentration drops in nitrate seen during rounds 2 and 4 at profile 8 ML3. A sharp drop in concentration occurs at between 0m-0.4m below the river bed which reaches its lowest concentration at 0.175m of 6.16 mg/l $NO_3$ during round 4. Mean groundwater and surface concentrations at profile 8 are 21.15 and 27.76 mg/l respectfully. Nitrate concentration does not correlate directly to % surface water present (calculated using conservative chloride concentrations) hence it can be assumed that nitrate is being attenuated in the system.

At a depth of 0.075m, a large contrast is seen between $NO_3$ concentrations during round 2 and 4. This is likely due to the fact that there was 100% river water present at that depth during round 2 and only 60 % river water present at that depth during round 4. Although direct quantification of the degree of nitrate attenuation which has possibly occurred at this depth during round 4 by comparison to conservative chloride concentrations is not possible due to reasons explained in section 7.2, attenuation is likely to be occurring because of the complete lack of correlation which can be seen between decreasing % river water present with depth and decreasing, and then increasing concentrations of nitrate with depth (Figure 7.5.3).

The attenuation peak of nitrate occurs at 0.175m below the river bed during both sampling rounds when % groundwater present has been calculated to be 16 and 14 % during rounds 2 and 4 respectfully. Below this depth, concentrations rise steadily in pore sediments which are considered to contain 100% groundwater.

Figure 7.5.2, Temporal variation of % river water present at different depths below the river bed and the observed concentration drops in nitrate seen during rounds 2 and 4 at profile 8 ML3

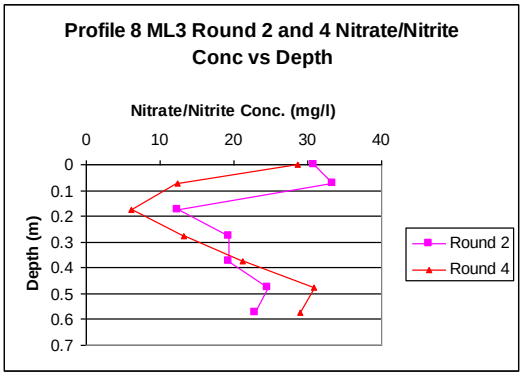


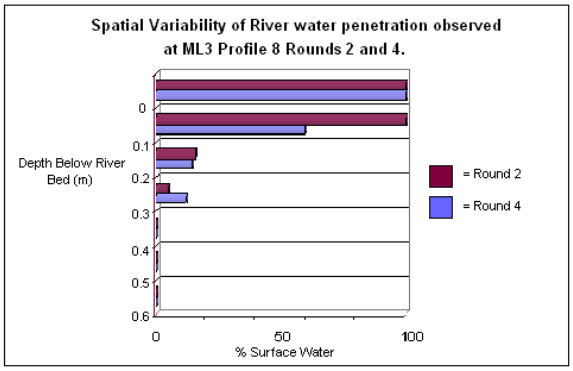


Figure 7.5.3, Correlation of % river water present in pore water and % total nitrate concentration with depth below the river bed.

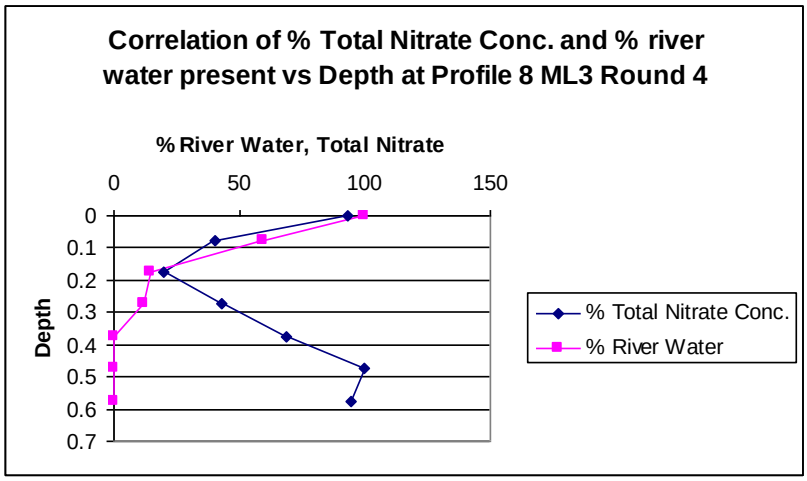


The evidence presented in (Figure 7.5.3) leaves no doubt that nitrate attenuation is occurring and predominantly so in pore space where groundwater and surface water coexist. The optimal % river water present for attenuation to be highest is in the range of 14-16 %. This % is comparable to optimal % river water (11-13 %) present in river bed pore space for the highest rates of D.O. consumption seen at profile 11.

The highly contrasting aquifer sulphate concentrations seen at profiles 8 and 11 are not believed to be due to the occurrence of sulphate reduction at profile 11, but rather the presence of a sulphate plume at profile 8.When sulphate concentrations are compared to % river water present in the pore sediments at Profile 8 ML 3 during round 2, (Figure 7.5.4), a high degree of correlation can be seen. Concentrations and % river water present are almost equal in the top 0.1m of the river bed and then concentrations increase substantially and proportionately to decreasing % river water present with depth. This strengthens the assumption that sulphate is relatively stable in the river bed environment and concentrations at different depth horizons are proportional to % river water present, hence sulphate reduction is not occurring.

Figure 7.5.4, Correlation of calculated % river water in pore space and % of total sulphate present with depth below the river bed.

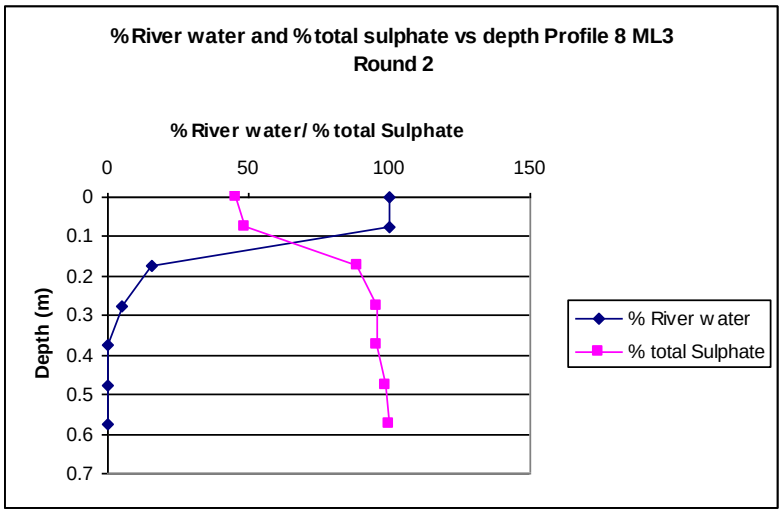

# Chapter 8 Fluorescence

The use of optical fluorescence has provided another tool to distinguish groundwater and surface water as well as identify the rates at which microbial activity is occurring. By identifying the intensities of humic-like peaks (A and C) and tryptophan and tyrosine-like fluorescent material peaks (T and B respectfully), a delineation of surface water and groundwater quality can be made (Figure 8.1). As tryptophan (Peak T) can be directly related to the growth stage of a bacterial community, its intensity can be seen to be high in all river water samples due to sewage effluent discharge and associated degredation. As tryptophan and tyrosine-like peaks are absent in supposed purely groundwater samples, it is proposed that a correlation between % river water present at different depths below the river bed and the corresponding ratio of tryptophan fluorescent intensity/ humic fluorescent intensity in pore waters at these depths will allow for the identification of specific hyporheic degredation of organic material as oppose to that seen solely in river water.

Figure 8.1, EEM showing the positions of peaks, C, A, T and B

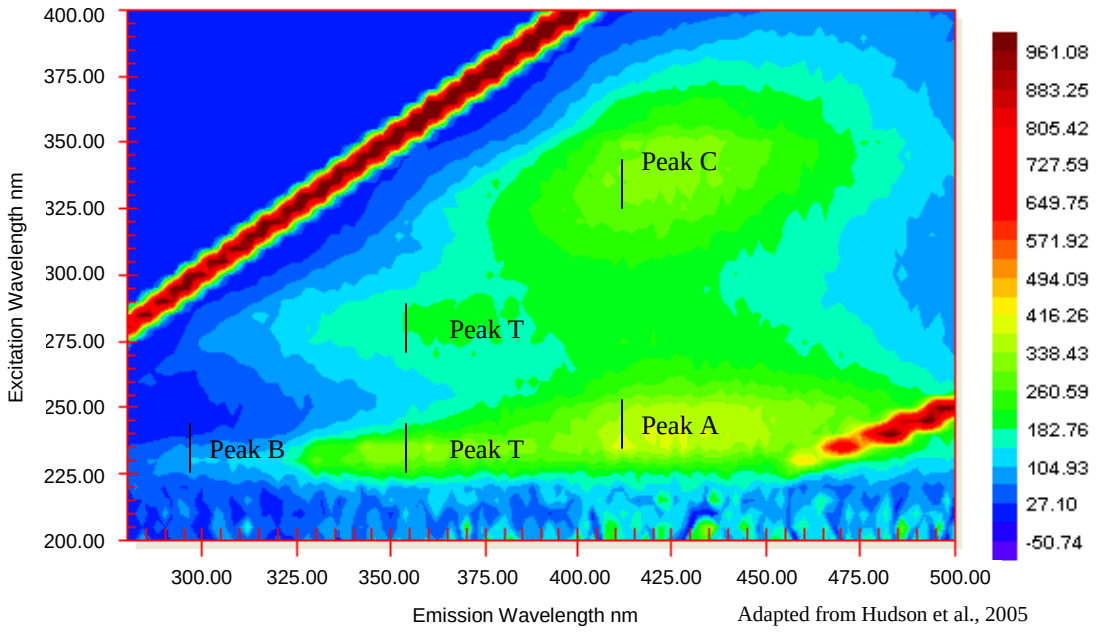


Adapted from Hudson et al., 2005

## 8.1 Groundwater and River water fluorescence

The analysis of fluorescent properties of water samples taken from all deep sample horizons at profiles 8 and 11 revealed that varying quantities of organic matter exist in the groundwater. (Figure 8.1.1) illustrates a typical groundwater EEM from the study site. The sample was retrieved from profile 8 ML 2 during round 2. Peak intensity excitation an emission (Ex/Em) wavelengths can be seen to occur at 397nm and 334 nm respectfully with intensity of 182. The position of this peak indicates the presence of humic substances, however the relative intensities indicate that concentrations are relatively low. A second less intense peak is seen at (Ex/Em) wavelengths of 399 and 334 nm respectfully and with intensity of 89. This corresponds with the position of the C Peak (Figure 8.1.1) and again is indicative of humic-like substances. The presence of a minor T Peak at Ex/Em of 353 and 234 nm may indicates the minor presence of tryptophan ( intensity 134 nm) in the sample which indicates possible minor amounts of microbial activity at this depth, however the relatively low intensity suggests minimal activity.

Figure 8.1.1, EEM of deep sample water taken during round 2 at profile 8 ML2

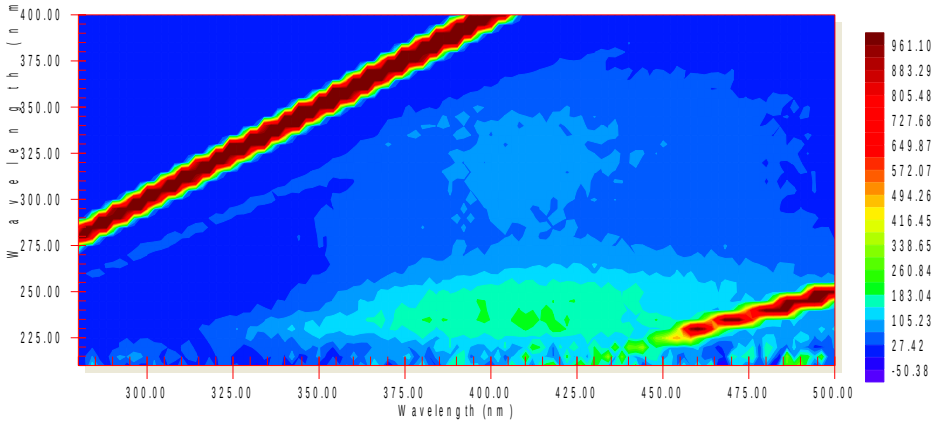


EEM's of groundwater samples taken from profile 11 ML2 during round 2 indicate a much lower concentration of total organic carbon such as humic material, (Figure 8.1.2). Peak A

intensity of 68 at Ex/Em 401/247 nm does suggest the presence of humic-like organic matter at this depth and the occurrence of a Peak T of intensity 59 at Ex/Em 352/239 nm implies the presence of tryptophan hence microbial activity. However the occurrence of humic material and microbial activity is not as high as that seen at profile 8 during the same sampling round. During round 2, chloride mixing equation calculations suggest that there is 0% river water present at the deepest sample points of profiles 8 and 11 ML2, hence EEM's should be representable of total organic carbon groundwater composition at those depths.

Figure 8.1.2, EEM of deep sample water taken from Profile 11 ML2 during round 2

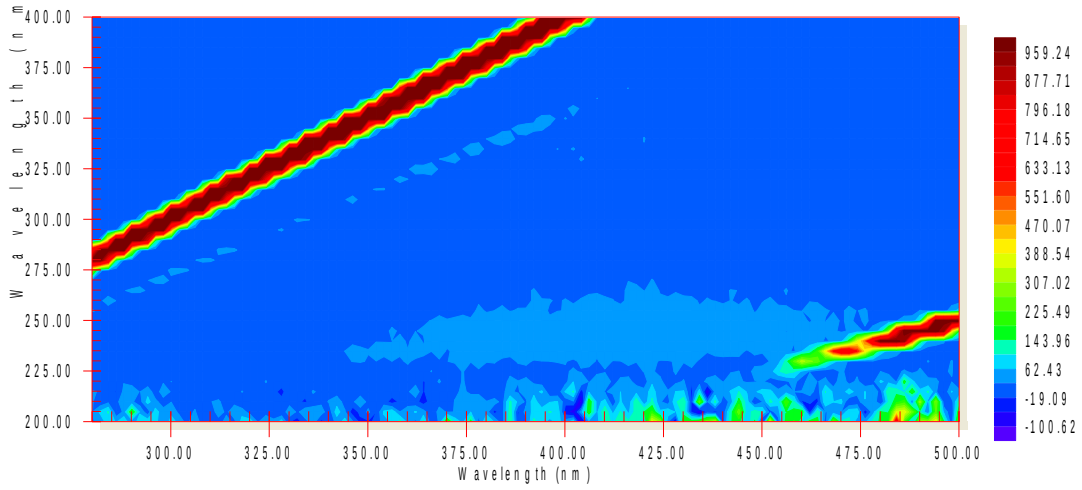


Surface water EEM's illustrate the highly contrasting organic chemical signatures when compared to groundwater samples. (Figure 8.1.3) represents a typical river water sample which was retrieved during round 2. Peaks C, A, T and B all show higher intensities when compared to groundwater sampled which indicated a much higher TOC in the river water. Humic Peaks A and C register intensities of 640 and 301 respectfully and amino acid peaks T and B have intensities of 572/216 and 93 respectfully. Such high intensities of peaks T and B are characteristic of untreated waste waters and sewage effluent and increased anthropogenic origin.

The contrasting Peak T intensities between surface and ground water provides a useful instrument for delineating the depths to which river water extends and the degree of microbial activity within the hyporheic zone.

Figure 8.1.3, EEM of river water taken during round 2

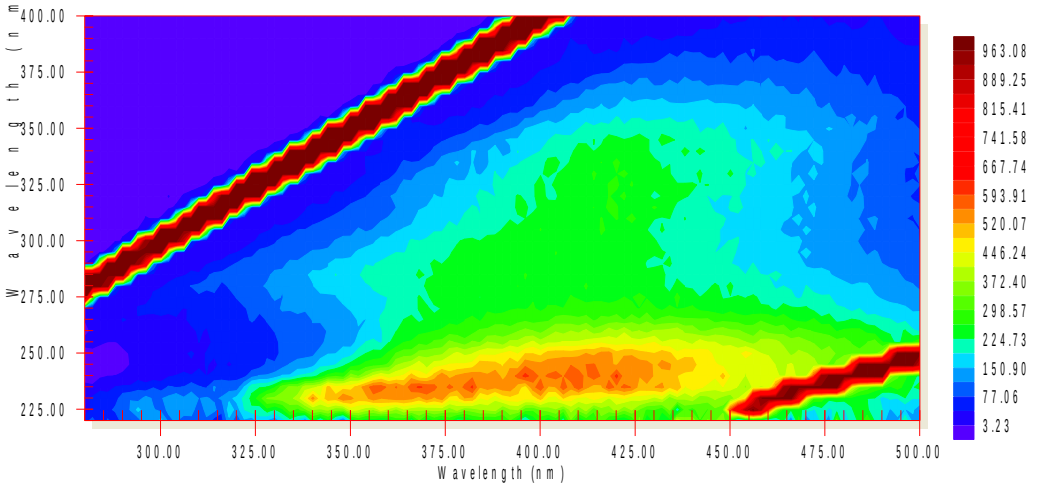


## 8.2 Hyporheic Zone Fluorescence

A general decrease of intensity of humic and amino acid peaks is seen with increasing depth blow the river bed. At profile 8 ML1, high intensity peaks of humic material can be seen to be present at 0.3m below the river bed. During round 2, humic peak (A) intensities at 0.2m and 0.3m below the river bed at profile 8 ML1 are close to that seen in river water, with 88 and 83% of surface water humic intensity present at depths of 0.2 and 0.3m. This intensity drops significantly to 29% of its river water value at a depth of 0.6m below the river bed which suggests the predominant presence of surface water. When the intensity of humic peak A (percentage of river water value) with depth is correlated with % river water present with depth, (Figure 8.2.1), the proportion of humic material present at different depths correlates to a certain

degree to the % surface water present. Although attenuation of the organic material is occurring in the river bed and there is a source of humic material in the groundwater, the most prominent source can be seen to be river water.

Figure 8.2.1 Correlation of % River Water and % total humic intensity with depth below the river bed at profile 8 ML3 during round 2.

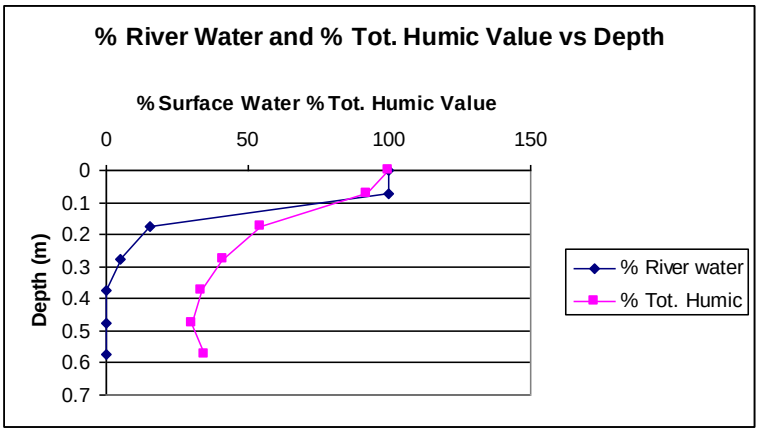


To qualitatively estimate the degree of microbial activity occurring beneath the river bed, the intensities of Amino acid (tryptophan) can be divided by the intensity of the humic-like matter (Peak A) at any depth. The higher the ratio, the higher the microbial activity at any particular horizon and thus the more active the redox environment. As nitrate is the more active inorganic determinand in the river bed in relation to microbial catalyzed redox reactions (oxidation of the organic substance and reduction of the inorganic), the correlation of nitrate degredation and microbial activity strengthens the theory that nitrate reduction is occurring in the river bed and is oxidising organic contaminants. To correlate the microbial activity with the drop in nitrate concentration, it is convenient to convert microbial activity fractions to % of total activity and nitrate concentrations to % total nitrate. This allows for a unified scale assessment of microbial activity and nitrate degredation.

(Figure 8.2.2) illustrates the variation in % total nitrate and % total microbial activity at profile 8 ML1 during round 1. It can generally be seen that with increased microbial activity, a drop in nitrate concentrations occurs and vica-versa.

Figure 8.2.2, Variation in % total nitrate and % total microbial activity with depth at profile 8 ML1 during round 1

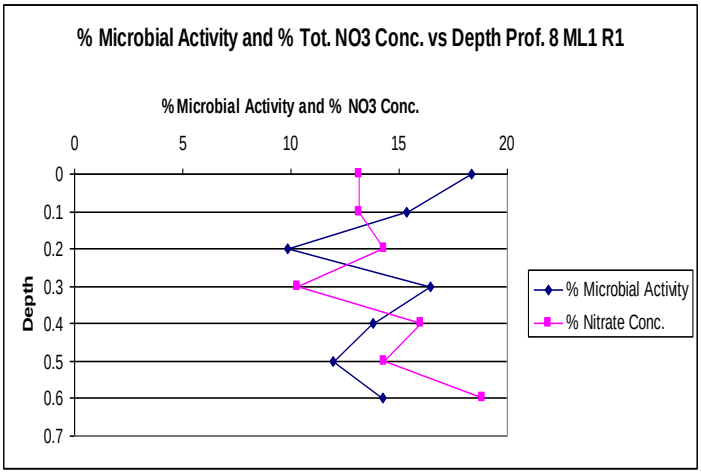


The more pronounced of these correlations can be seen between depths of 0.2 and 0.3m where % microbial activity rises from 9.84% to 16.45% (0.56 to 0.63) of its total cumulative activity over a space of 0.1m. Over the same distance, the % total nitrate concentration drops from 14.26% to 10.29% (22 mg/l to 15.84 mg/l). The zigzag pattern of the graph above does suggest a highly varied microbial active environment in which nitrate consumption only occurs at particular depth horizons.

A similar pattern is seen at profile 8 ML3 during round 2 of sampling (Figure 8.2.3). Relatively high microbial activity in the top 0.175m of the river bed can be correlated with a large drop in nitrate concentration from 33.4 mg/l to 12.3mg/l. Between depths of 0.175 and 0.475m microbial activity declines steadily with increasing concentrations of nitrate. At the deepest sample point, microbial activity is seen to increase with a decrease in nitrate concentration.

Figure 8.2.3, Variation in % total nitrate and % total microbial activity with depth at profile 8 ML3 during round 2

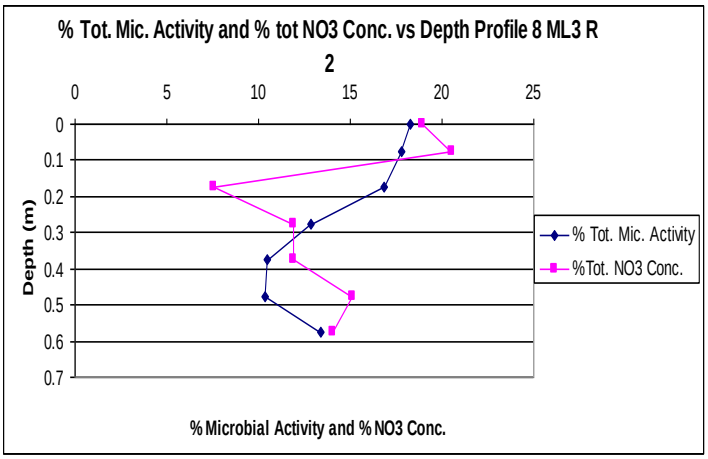


Similar patterns can be seen at profile 11, (Figure 8.2.4), however, below depths of 0.3m, rising microbial activity is not causing a decrease in nitrate concentration except at depths between 0.5 and 0.6m. This is likely because of the relatively low activity ratios (Peak T intensity / Peak A intensity) between depths of 0.4 and 0.5m which have activity ratios of 0.53 and 0.67 respectfully. It has generally been found in all ML's in the study reach, that significant decreased in nitrate concentrations can only be seen at points where activity ratios are >0.65-0.70. Lower ratios generally reflect a greater relative presence of humic material and hence, produced protein and amino acids being a by-product of humic material oxidation rather than organic groundwater contaminants.

Figure 8.2.4, Variation in % total nitrate and % total microbial activity with depth at profile 11 ML4 during round 1

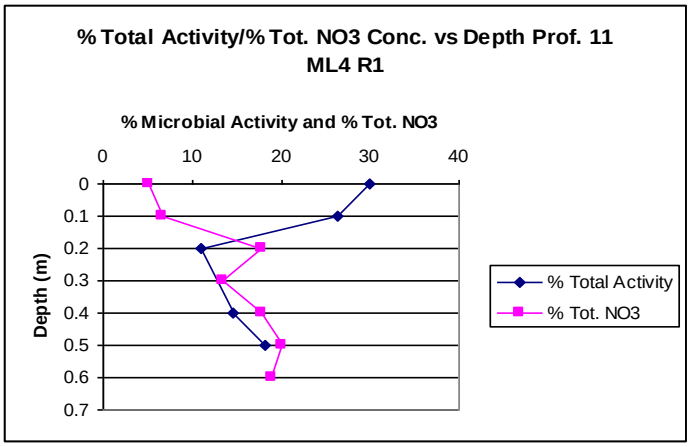


## 8.3 Critique of Technique

The reliability of the use of fluorescence to qualitatively assess the fraction of dissolved organic matter in the water within the river bed is good however, the inability to correlate tryptophan fluorescence intensity with particular redox reactions occurring within the river bed proved somewhat inconvenient. Nevertheless, fluorescence spectroscopy does allow for a qualitative separation of surface water and groundwater, an assessment of the likely origin of the organic matter and a quantification of microbial activity occurring.

## 8.4 Discussion

The identification of organic fluorescent fingerprints for both surface water and groundwater has provided another tool to identify the likely position of the boundary between 100% river water and pore water which contains some groundwater. This is possible because of the relatively high humic-like organic matter concentrations in the river water when compared to groundwater

quantities. This high humic content is associated directly with treated and untreated sewage discharges, (Figure 2.5.2). The high concentrations of humic matter in the river shows similar patterns of intensity decline to chloride concentration drops with depth below the river. (Figure 8.4.1) illustrates the percentage of total Peak A intensity and % total Cl concentration variation with depth. The patterns are similar shape but show different scale drops in % over the full depth of monitoring. The larger scale drop is seen in % total humic intensity where values in the river water and at 0.475m below are 25.94, 8.24% respectfully which corresponds to a total drop of 17.7%. Total % chloride concentration drops are from 23.55% to 9.25% in the river water and at 0.475m below the river bed respectfully which corresponds to a total drop of 14.3%. This larger drop of humic peak A intensity is likely due to the unstable nature of the organic matter, hence the attenuation of the matter in the river bed environment. Nevertheless, the separation of groundwater and surface water is still easily identified and can be seen to occur at depths between 0.075m and 0.175m at profile 8 ML3 during round 2, (Figure 8.4.1), which is in agreement with conservative chloride boundary estimates.

Figure 8.4.1, Percentage of total Peak A intensity and percentage of tot. Cl concentration variation with depth below the river bed at profile 8 ML3 during round 2.

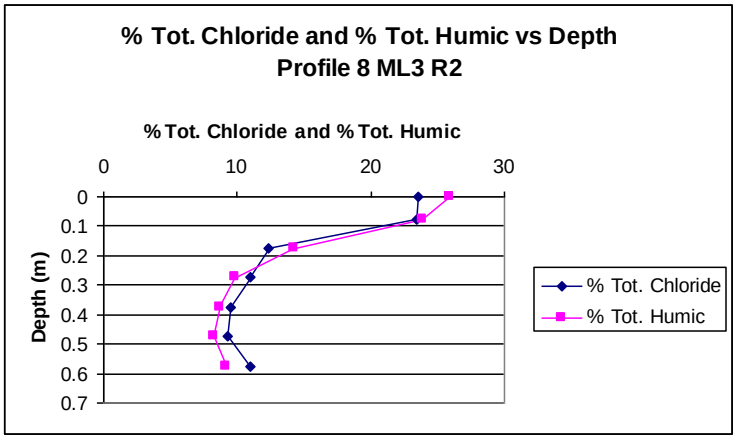

The analysis of tryptophan/humic-like matter ratios (T/A) has allowed for an assessment to be made of the likely microbial activity which may be associated with nitrate reduction and organic contaminant oxidation in the river bed environment. It has generally been found that when activity ratios are >0.65-0.7, nitrate concentrations fall significantly which is likely due to the increased rates of microbial activity at those particular horizons.

The occurrence of increasing Peak T/Peak A ratios at different depths below the river bed does seem to correlate well with decreasing nitrate concentrations, however due to a lack ability to correlate tryptophan intensities with any specific microbial community activity and thus with specific redox reactions, it is not possible to conclude that the increased microbial activity is causing the decrease in nitrate concentration and thus oxidation of organic contaminants. Nevertheless, the strong correlation between T/A ratios and nitrate concentration does suggest some degree of connection between the two. It is possible to conclude however that increased microbial activity over 0.56-0.7 is occurring at preferential horizons below the river bed, most of which have been calculated to contain a mixture of surface water and groundwater.

# Chapter 9 Base flow Quantification

Base-flow estimates over a 5m stretch of river at profiles 8 and 11 have been calculated for all sampling rounds using hydraulic conductivity (K) values and temporally varying head gradients. Hydraulic conductivity data has been calculated for three depths horizons (0.3m. 0.5m and 0.6-0.8m) below the river bed at profiles 8 and 11 which allows for a more accurate estimation of effective hydraulic conductivity. Head gradients have been calculated using the two deeper MDP's installed at both profiles, and assigned throughout the area which they are assumed to best represent. Calculated hydraulic conductivity values give a 3 layered river bed system. At each profile, the river has been divided in two, based solely on hydraulic gradients observed in the two deep MDP's. Average hydraulic conductivity values for each layer were then calculated based on MDP's installation location, and the weighted harmonic mean of K values of the 3 layers was found and assigned as the effective vertical hydraulic conductivity ($K_v$ eff) for that section of river bed. Thicknesses of the layers were used as weights for the harmonic mean. These thicknesses were calculated based on the assumption that layer boundaries lie halfway between the actual measurement points or depths of the open section of MDP's.

## 9.1 Results

(Figure 9.1.1 and 9.1.2) illustrate the locations of MDP's at profiles 8 and 11 respectfully.

Figure 9.1.1, Area of river bed which hydraulic properties calculated from 6 MDP's have been assigned at profile 8

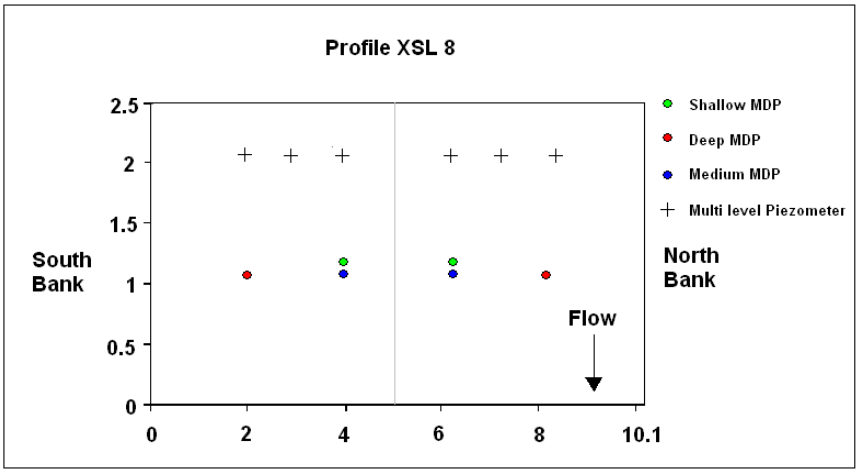


Figure 9.1.2, Area of river bed which hydraulic properties calculated from 6 MDP's have been assigned at profile 11

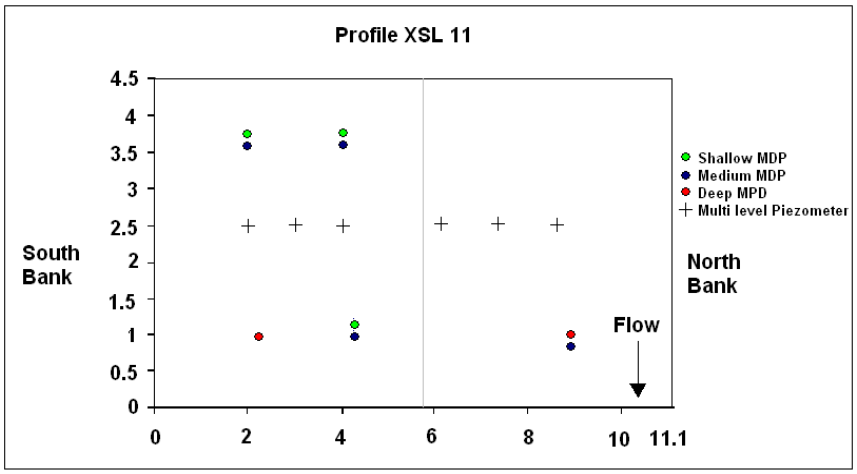


Calculated temporal variations in base-flow rates are shown in table 9.1. During some sampling rounds, hydraulic gradients appeared to be negative, in that heads in the aquifer were lower than stage in the river. Total flow rates were calculated by adding those calculated for the southern half of the river and northern half of river.

Table 9.1 Temporal and spatial variation in head gradients, effective vertical hydraulic conductivity values, specific discharges and discharges for a 5m stretch of river at both profiles 8 and 11 during rounds 1,2,3 and 4 of sampling.

| Profile | Round No. | Location | dh/dx | $K_v$ eff (m/d) | q (m/d) | Applicable Length | Q (m3/d) unit length | Q 5M of river | Total Q (m3/d) |
|---|---|---|---|---|---|---|---|---|---|
| 8 | 1 | South | 0.561765 | 1.96 | 1.1061 | 5.05 | 5.586 | 27.931 | |
| | | North | 0.169697 | 2.33 | 0.3966 | 5.05 | 2.002 | 10.014 | 37.946 |
| | | | | | | | | | |
| 8 | 2 | South | 0.360294 | 1.96 | 0.7094 | 5.05 | 3.582 | 17.914 | |
| | | North | -0.15758 | 2.33 | -0.3683 | 5.05 | -1.85 | -9.2994 | 8.6146 |
| | | | | | | | | | |
| 8 | 3 | South | 0.458824 | 1.96 | 0.9034 | 5.05 | 4.562 | 22.813 | |
| | | North | -0.03636 | 2.33 | -0.0849 | 5.05 | -0.429 | -2.1460 | 20.667 |
| | | | | | | | | | |
| 8 | 4 | South | 0.373529 | 1.96 | 0.7355 | 5.05 | 3.714 | 18.572 | |
| | | North | -0.09818 | 2.33 | -0.229 | 5.05 | -1.158 | -5.7942 | 12.777 |
| | | | | | | | | | |
| | | | | | | | | | |
| 11 | 1 | South | 0.010526 | 2.19 | 0.0230 | 5.325 | 0.122 | 0.6137 | |
| | | North | 0.011364 | 1.12 | 0.0127 | 5.775 | 0.073 | 0.3691 | 0.9829 |
| | | | | | | | | | |
| 11 | 2 | South | 0.02406 | 2.19 | 0.0526 | 5.325 | 0.280 | 1.4029 | |
| | | North | 0.015909 | 1.125 | 0.0178 | 5.775 | 0.103 | 0.5167 | 1.9197 |
| | | | | | | | | | |
| 11 | 3 | South | 0.016541 | 2.19 | 0.0362 | 5.325 | 0.192 | 0.9645 | |
| | | North | 0.023864 | 1.125 | 0.0268 | 5.775 | 0.155 | 0.7751 | 1.7397 |
| | | | | | | | | | |
| 11 | 4 | South | -0.03308 | 2.19 | -0.0724 | 5.325 | -0.385 | -1.9290 | |
| | | North | na | 1.125 | na | 5.775 | na | na | -1.9290 |

## 9.2 Critique of methodology

The reliability of monitoring aquifer head variation using MDP's has been discussed in detail in section 6.4.1 in which it was concluded that all head measurements may not be entirely accurate. Thus the extent of hydraulic gradient estimates obtained from some MDP's may be questionable. However general trends are similar in MDP's which does suggest a certain degree of accuracy, (Figure 6.2.1 and 6.2.1)

The calculation of effective vertical hydraulic conductivity at profiles 8 and 11 is only accurate to the scale of homogeneity of the river bed sediments. Hence due to typically heterogeneous nature of alluvial sediments K value estimates are likely to be inaccurate when applied to the southern and northern halves of the river. However, for the purpose of this study, precise

quantification of base-flow is not necessary. If the method is repeated in a similar manner for all sample rounds a relative temporal base-flow flux has been obtained which will allow for the aims of the exercise to be met.

## 9.3 Discussion

The temporal variation of base-flow magnitude at profiles 8 and 11 does not correlate when dates of the greatest and lowest base-flows are looked at, (Table 9.1). Base-flow was greatest during round 1 at profile 8 and was the second smallest during round 1 at profile 11. Base-flows were greatest during round 2 at profile 11 while they were the smallest at profile 8 during that round. The reasons behind this lack of correlation is somewhat unclear. Possible scenarios include:

1. The river stage at profiles 8 and 11 react differently to rainfall events. Because profile 11 is located in pool like, slow velocity, shallow gradient section of the river, it may be more susceptible to greater variation in river stage elevation when compared to the steeper river bed gradient at profile 8 which would require a larger scale flood event to affect river stage elevations to a similar magnitude. (Figure 9.3.1) illustrates a conceptual model of the high velocity river at profile 8 and low velocity at profile 11. The river stage depth is dependent upon river velocity and thus river bed gradient. Higher river stage leads to lower hydraulic gradients and thus base-flow calculations.
2. Different hydraulic environments exist below the river bed at profiles 8 and 11 generating different response times of shallow groundwater levels and thus different relative calculations of base-flow during particular rain fall events.

Figure 9.3.1, Conceptual model of the spatial variation of river stage depth during no rainfall conditions (Time 1) and a minor flood event (Time 2) at profile 8 and 11, high velocity and low velocity river sections respectfully.

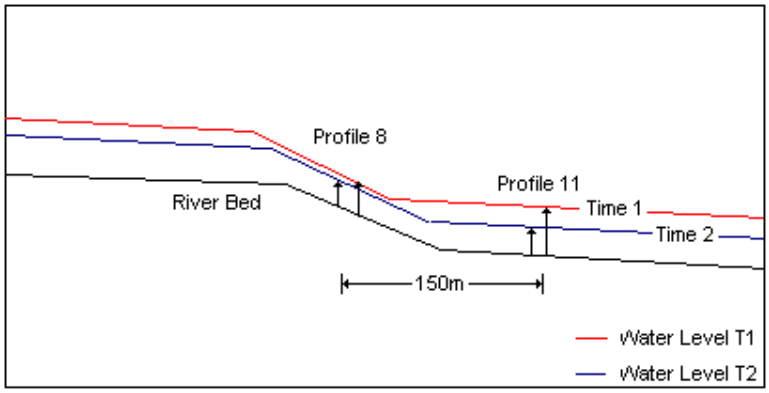


Figure 9.3.2, Temporal variation in river stage at profiles 8 and 11.

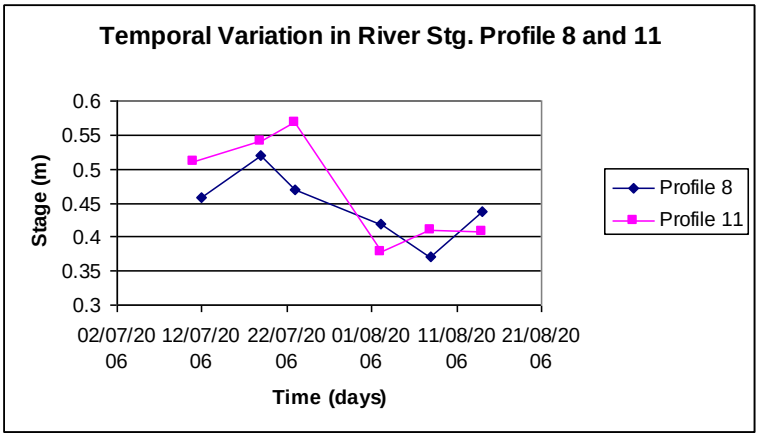


(Figure 9.3.2) does suggest that there has been a greater temporal deviation of river stage level seen at profile 11, however this is not likely of the magnitude that could generate such contrasting base-flow temporal correlations such as those seen in Table 9.1. Thus, the reasons for the temporal lack of correlation is likely owed to a number of scenarios with high dependence of the hypothesis mentioned above.

When base flow magnitude estimates are compared to calculated hyporheic zone thicknesses and surface water penetration depths, it has been found that at some multi-levels, surface water calculations correlate well with temporally varying base flow estimates while at others, surface

water penetration depths and hyporheic water percentages appear to act completely independently of base flow rates.

At profile 8 ML1 it can be seen that during round 1 when base-flow was highest ($38m^3d^{-1}$ over a 5m stretch of river) 100% river water can be seen to only enter the top 0.1 m of the river bed as oppose to round 2 when base-flow has been calculated to be the lowest ( $8.6\ m^3d^{-1}$ over a 5m stretch of river), 100% surface water can be seen at depths of 0.3m below the river bed (Figure 9.3.3). This suggests a strong correlation between river water entering the river bed and groundwater discharges restricting this process.

Figure 9.3.3, Temporal variation in base flow magnitude correlated with % river water present below the river bed, profile 8.

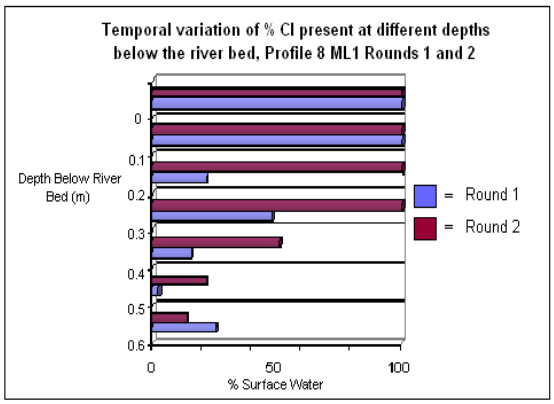


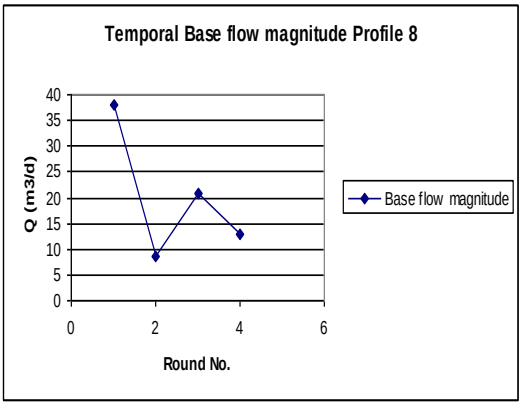


During both sample rounds, some % of surface water has been calculated to be present at all depths below the river bed, however during sample round 2, a higher % of surface water can be seen at 0.3 and 0.4m below the river bed (51 and 22% respectively) as oppose to round 1 where % surface water at 0.3 and 0.4m are only 16% and 3%. This shows some degree of agreement of increased base-flow and lower penetration of surface water.

A temporal variation in hyporheic zone thickness can be seen at profile 8 ML1 during rounds 1 and 2. During round 1, the hyporheic zone can be seen to occupy a depth of 0.4m between 0.2-0.6m below the river bed. A smaller hyporheic zone thickness has been encountered during round 2, with a thickness of 0.2m between 0.4-0.6m below the river bed. Hence it can be seen that with increased base-flow at profile 8 hyporheic zone thickness also increases but depth to which 100% surface water penetrates deceases.

Correlations of base flow and % surface water present at different depths below the river bed at profile 11 do show a similar pattern to those seen at profile 8. At profile 11, round 4 shows the a negative discharge of -1.93 $m^3d^{-1}$ which represents an overall loosing river system at that location, unfortunately no deep chemical samples were taken during this round. The second lowest recorded base-flow was during round 1 (0.98 $m^3d^{-1}$over a 5m stretch of river). This is the only round in which 100% river water has been calculated to occupy total pore space at 0.1m below the river bed and it is also the round in which the highest % surface water occupies 5 out of 6 of the sampling horizons, (Figure 9.3.4). Base-flow calculations for sample round 2 and 3 (1.92 and 1.74 $m^3d^{-1}$ respectfully) are relatively similar however large differences in river water penetration depths and % river water in hyporheic waters can be seen. Although during round 3 which has the 3$^{rd}$ lowest base-flow rate, the second highest percentages of river water can be seen at all sample horizons below 0.2m, the correlation is somewhat unconvincing because during round 2, which is representing highest base-flow rates, higher quantities of river water can be seen to enter the river bed at 0.1 and 0.2m than in round 3. This once again, somewhat detracts from any conclusion that river water penetration depths and % river water in hyporheic waters can be directly related to base-flow rates.

Figure 9.3.4, Temporal variation in base flow magnitude correlated with % river water present below the river bed, profile 11.

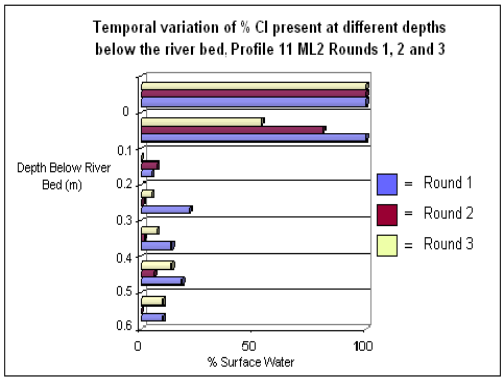


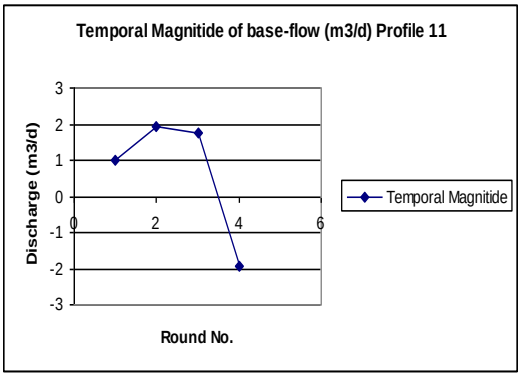


Temporal variations in hyporheic zone thickness can also be seen at profile 11 ML2 (Figure 9.3.4). During round 1, when base flow is smallest a hyporheic zone can be seen to exist between 0.1-0.6m below the river bed. Round 2 gives a hyporheic zone of similar magnitude, but shifted vertically upwards by 0.1m and round 3 which represents more normal flow conditions (no rainfall over 48 hours) and has a base-flow between the two extremes, shows the greatest hyporheic thickness of 0.6m between 0-0.6m below the river bed.

In conclusion, increased river water penetration depths and increased % river water in hyporheic waters does correlate to decreased base-flow rates in many of the ML locations along the study reach but not in all. Thus, it is possible to conclude that under appropriate hydraulic conditions the above variables do correlate with base flow rates, however under heterogeneous and anisotropic hydraulic conditions (K), varying resident times of both groundwater and river water are seen on a vertical scale in the river bed sediments and rapid and equal responses of all river bed pore water to varying base-flow rates is not always seen.

Hyporheic zone thickness can be seen to vary under different base flow conditions and seems to depend on normal flow 100% groundwater penetration depth, and normal flow base-flow rates.

At profile 8 increased base flows causes increased hyporheic zone thickness. With increased base flow rates sediments which initially contained 100% river water receives increased inflows of groundwater which displaces portions of the surface water to generate a greater hyporheic zone thickness. The temporal stability of such a hyporheic environment is likely to be low. At profile 11 the opposite occurs in that with increased base-flow, the hyporheic zone diminishes. This is likely because of the small proportion of river water which occupies the river bed pore space under normal flow conditions. With increased base-flow this river water is forced out of the deeper horizons resulting in a reduction in hyporheic zone thickness and under very low base-flow rates river water entirely occupies the upper sections of the river bed which also results in a decrease in hyporheic thickness. Maximum hyporheic thicknesses are seen at profile 11 under ideal base-flow conditions. Extremes base-flow rates result in hyporheic diminishment.

Hyporheic thickness hence depends on the rate at which river water velocity advanced diffusive forces cause surface water penetration in the upper river bed. Temporal variation of base-flow merely readjusts river water proportions of river bed pore space under ideal hydraulic conditions.

# Chapter 10 Conclusions and Further Work

The characterisation of a 600m stretch of the River Tame in North Birmingham has led to the identification of 2 sites of contrasting hydraulic conditions including base-flow rates, sediment type, hydraulic conductivities, river bed gradients and hydrologic river properties. Through a detailed field study, these sites have been used successfully to identify temporal and spatial variations in river water inflow to the river bed and a delineation of hyporheic zone thickness based on the conservative chloride mixing equation. Following this, the degree of inorganic determinand degredation was looked at within the hyporheic zone, pure groundwater and surface water to determine the chemical environments present at both sites and to determine the degree of inorganic determinand reduction occurring within the hyporheic zone as well as above and below. Fluorescent EEM scans were taken to qualitatively identify fractions of organic matter at different depths below the river bed and the use of fluorescence as a tool to delineate the hyporheic zone was assessed. Inorganic concentration gradients were compared to qualitative fluorescent EEM's to attempt to correlate areas of enhanced microbial activity with inorganic determinand degredation. This allowed for a possible explanation for inorganic concentration drops at preferential depth horizons to be made, and an assessment of the likely occurrence of urban organic contaminant degredation in the river bed environment. Finally the dependence of hyporheic zone thickness on temporally varying base-flow rates has been assessed to identify reasons for the temporal and spatial variability of hyporheic thickness and to assess whether increased base-flows and increased contaminant fluxes to the hyporheic zone would be attenuated to a greater or lesser extent by the modified hyporheic zone thickness.

## 10.1 Conclusions

The aim of this research was to examine the relationship between physical hydraulic properties, base flow rates and observed chemical gradients to delineate the mixing zone and explain the reasons for its temporal and spatial variability in thickness. Discussion has been presented in chapters 6, 7, 8 and 9 remarking on the relevant conclusions from individual works. This section concludes generically on the aims and objectives of the study.

The extent of the hyporheic zone has been delineated based on a simple definition that it contains a mixture of groundwater and surface water. A chloride mixing equation has been used to identify different proportions of surface water in the river bed sediments at two river profiles. From this, two distinctive hyporheic zone symmetries have been identified. The hyporheic zone at profile 8 shows distinct variability in symmetry in a cross-channel scale. On the southern bank of the river a relatively small hyporheic zone has been identified in which pure river water appears to penetrate depths of up to 0.5m into the river bed, and as hyporheic water are by definition a “mixture of surface water and groundwater”, this zone has not been classes as hyporheic. As well as showing penetration depths of river water of this magnitude, the bed sediments at this location also show the highest degree of river water penetration variability, all in all suggesting a higher than usual degree of through flow in the area possibly due the high river velocity and high conductivity values of bed sediments. Else where at profile 8, the hyporheic zone is very thin (0.1-0.2m) at depths of 0.1-0.3m. Profile 11 generally has a much wider hyporheic zone with some percentage of river water present at 0.6m below the river bed on most occasions and a general lack of occurrence of 100% river water at any depth below the river bed. These contrasting hyporheic symmetries are believed to be owed to lower river flow rates, lower hydraulic conductivity values and lower base-flow rates at profile 11.

The geochemical environment at profile 8 is anaerobic in which drops in nitrate concentration can be seen to be occurring at preferential depth horizons within the river bed. All concentration drops occur at horizons in which it has been calculated that a fraction of the pore space contains surface water. A quantification of the concentration drop which has occurred has not been possible by comparisons to river water % presence due to high variability of absolute surface water concentration and absolute groundwater concentration, however due to a lack of correlation between decreasing water content with depth and decreasing nitrate concentration it can be stated that nitrate is being attenuated in the system. Higher D.O. concentrations have been identified at profile 11 which suggests a more aerobic environment and consumption of $O_2$ is occurring at a broader range of depths below the river bed when compared to depths at which nitrate concentration drops occurred at profile 8. Generally pure groundwater nitrate concentrations are higher at profile 11 that at profile 8 which may be due to the more aerobic environment at profile 11 of may be due to the occurrence of a nitrate plume. Despite higher D.O. concentrations at profile 11, nitrate attenuation does still appear to be occurring and furthermore, appears to be occurring over a broader range of depths. This somewhat reinforces the … that inorganic attenuation is occurring at preferential depth horizons in which surface water and groundwater co-exist and is possibly occurring on a larger scale at profile 11 where hyporheic zone thicknesses are greater.

Temporally the depths at which these concentration drops occur varied and the preferential concentration drops appear to occur not only in areas in where river water and groundwater co-exist, but also appear to be occurring in areas which contain particular percentages of each water type. However, more geochemical survey data would be required to support such a claim.

To assess whether inorganic determinand attenuation can be linked to inorganic reduction, organic matter oxidation and possible organic contamination oxidation, the fluorescent properties of river and river bed water samples were examined. By looking at fluorescent intensities of humic matter and amino acids, it can be seen that high relative rates of microbial activity correspond to drops in inorganic nitrate concentrations in hyporheic waters. Although this increased microbial activity could possibly be due to the oxidation of natural humic organic matter, the increased ratio of tryptophan/humic-like matter suggests that oxidation of organic contaminants is occurring, particularly so at depth horizons where the ratio exceeds 0.65-0.7. These depths again correlate to areas in which surface water and groundwater co-exist. However due to a lack of ability to correlate tryptophan presence to oxidation of any particular organic fraction, it is not possible to conclude that organic contaminant degredation is occurring even though ratios do suggest so.

The use of fluorescence analysis as a hyporheic delineation tool has also been examined and it is clear that the presence of 100% surface water can be mapped at any depth below the river bed relatively easily due to highly contrasting organic signatures. However, due to the unstable nature of the DOM hyporheic zone delineation is some what more complicated and is not as accurate of conservative chloride techniques used.

At profiles 8 and 11 different hyporheic zone thicknesses can be correlated to different base-flow regimes. Profile 8 generally has a thin hyporheic zone with a zone of 100% surface water directly below the river bed. Base flow rates at profile 8 were on some occasions calculated to be 2 orders of magnitude greater than those at profile 11 and on all occasions were higher. Profile 11 has no zone of 100% river water below the river bed and had a much wider hyporheic zone. Temporally with increased base flow at profile 11, hyporheic thicknesses tends to decrease due

to the expulsion of the small proportions of river water present. This is in contrast to profile 11 where increased base-flow causes the pore space which had previously been occupied by 100% surface water to be injected with a proportion of groundwater, thus generating a much larger hyporheic zone thickness. However the temporal stability of such an altered zone has not been assessed.

## 10.2 Further Work

In light of the occurrence of a temporally varying hyporheic zone thickness, it may be advantageous to explore in a more meaningful manner the temporal variation in thickness of the mixed water zone under different rainfall events. If a more continuous sampling strategy was adopted with the possible use of a chloride probe, the short term temporal stability of an altered hyporheic zone thickness could be assessed. If a situation occurs in which the hyporheic zone increases in size due to adjusted hydraulic conditions, the potential for greater pollution oxidation may be assessed in a quantitative manner using specific organic contaminant monitoring techniques. Thus the potential of the adjusted hyporheic zone to attenuate the likely increased contamination fluxes to the river can be examined.

The potential to generate a numerical model to explore a number if different hypothesis in which river water enters the river bed environment would be of particular use in assessing the long-term behavior of a hyporheic zone environment. To numerically represent the localised forces which generate hyporheic zones in gaining river systems is somewhat obscure, the advanced diffusion effects of river flow velocity would likely be of particular interest when modeling such a system. However, other more common numerical representations could be explored to represent hypothetical hydraulic occurrences which are just as likely to be the cause of observed hyporheic

conditions. Such a hypothesis would be a loosing river in close proximity to the observed gaining river system observed, thus allowing inflow of river water upstream and expulsion of the river water in the monitored gaining river system. This hypothesis was numerically explored in a preliminary sense during this research and is presented in Appendix 3

As a spatially varied response time of hyporheic zone thickness to rainfall events was observed during this study, a stream tracer test using a conservative tracer other than chloride would prove advantageous. By using the pulse tracer injection method and by monitoring the concentration breakthrough curve down stream, the river water resident times in the river bed can be assessed. Although not very indicative of local scale heterogeneity, it will identify the overall retention capacity of the system and thus indicate likely hyporheic response times to different precipitation events.

# References


Acworth, R.I. and Dasey, G.R., 2003. Mapping of the hyporheic zone around a tidal creek using a combination of borehole logging, borehole electrical tomography and cross-creek electrical imaging, New South Wales, Australia. Hydrogeological Journal, 11, 368-377.

Baker, A., and Inverarity, R.., 2004. Protein-like fluorescence intensity as a possible tool for determining river water quality. Hydrological Processes, 18, 2927-2945.

Conant, B. 2000 Ground-water Plume behavior Near the Ground-water/Surface Water Interface of a River. . Proceedings of the Ground Water/Surface-Water Interactions Workshop. USEPA

Ellis, P.A., 2003. The impact of urban groundwater upon surface water quality: Birmingham-River Tame study, UK. Unpublished PhD thesis, School of Earth Sciences, University of Birmingham.

Ellis, P.A., Rivett, M.O. and Mackay, R., 2004. Estimation of groundwater contaminant fluxes to urban rivers. Hydrology: Science and Practice for the 21st Century. Volume 2.

Environment Agency (UK), 2005. Groundwater-surface water interactions in the hyporheic zone. Report July 2005.

Fetter, C.W., 2004. Applied Hydrogeology, Third edition. Published by Prentice-Hall.

Ford, M. & Tellam, J.H., 1994. Source, type and extent of inorganic groundwater contamination within the Birmingham urban aquifer system, UK. Journal of Hydrology 156, pp 101-135.

Greswell, R., 1992. The modeling of groundwater rise in the Birmingham area. Unpublished Msc thesis, School of Earth Sciences, University of Birmingham.

Harvey, J.W., Wagner, B.J., & Bencala, K.E., 1996. Evaluating the reliability of the stream tracer approach to characterise stream-subsurface exchange. Water Resources Research 32, pp 2441-2451.

Hill, A.R. and Lymburner, D.J., 1998. Hyporheic zone chemistry and stream-subsurface exchange in two groundwater-fed streams. Canadian Journal of Fisheries Aquatic Science, 55(2), 495-506.

Hudson, N., Baker, A., Reynolds, D., 2005. Fluorescence analysis of dissolved organic matter in natural, waste and polluted waters – a review. Background research report, unpublished, School of Geography, University of Birmingham.

Knipe C.V., Lloyd, J.W., Lerner, D.N. & Greswell, R.B., 1993. Rising groundwater levels in Birmingham and the engineering implications. CIRIA Special Publication 92, Construction Industry Research and Information Association, London.

Malard, F., Galassi, D., Lafont, M., Doledec, S. and Ward, J.V., 2003. Longitudinal patterns of invertebrates in the hyporheic zone of a glacial river. Freshwater Biology, 48, 1709-1735.

Mc Lanachan, P., 2004. Urban groundwater/surface water interactions: Spatial variability at the reach scale. Unpublished Msc thesis, School of Earth Sciences, University of Birmingham.

Powell, J.H, Glover, B.W. & Waters, C.N., 2000. Geology of the Birmingham area. Memoir of the British Geolgical Survey, Sheet 168 (England and Wales).

Shepherd, K.A., Ellis, P.A and Rivett, M.O., 2005. Integrated understanding of urban land, groundwater, baseflow and surface-water quality-The City of Birmingham, UK.

Wilcox, T., 2005. Attenuation of Chlorinated plumes in the shallow hyporheic zone. Unpublished Msc thesis, School of Earth Sciences, University of Birmingham.

Woessner, W.W., 2000. Stream and fluvial plain ground water interactions: Rescaling hydrogeologic thought. Ground Water 2000, 38 (3) pp 423-429.

Reed, C. and Clinton, S., 2004. Delineation of the hyporheic zone. The Water Centre, University of Washington.